UNIVERSITY OF NAPLES FEDERICO II
SCHOOL OF MEDICINE AND SURGERY

DEPARTMENT OF PHARMACY

Ph.D. Thesis

XXXVI cycle

PALMITOYLETHANOLAMIDE (PEA) IN PRECLINICAL EXPERIMENTAL MODELS OF INTESTINAL DISORDERS

Maria Francesca Nanì

TUTOR: PROF. BARBARA ROMANO
TUTOR AZIENDALE: DOTT.SSA STEFANIA PETROSINO
COORDINATOR: PROF. ANGELO ANTONIO IZZO

Ph.D. program in Nutraceuticals, Functional Foods, and Human Health

A.Y. 2020-2024

UNIONE EUROPEA
Fondo Sociale Europeo

Ministero dell'Istruzione, dell'Università e della Ricerca

PON RICERCA E INNOVAZIONE

Abstract

Background and Aim

Intestinal diseases considered in this PhD project (i.e., gut fibrosis associated with Crohn's disease- and colorectal cancer) are a heterogeneous worldwide group of disorders that impact the global healthcare system and reduce the quality of life due to various characteristic symptoms. Despite considerable advancements in managing pathological conditions, colorectal cancer (CRC) remains a challenge. On the other hand, for CD patients with intestinal fibrosis, surgical resection remains the only therapeutic option for alleviating intestinal strictures, and a little headway has been made in the development of efficient pharmacological treatments.

Palmitoylethanolamide (PEA) is a fatty acid belonging to the family of Acylethanolamides (AEs) produced both endogenously that present in nature in many food sources (i.e., egg yolk, soy lecithin, milk, and peanuts). Moreover, PEA is already commercially available and sold as food supplements and/or foods for medical purposes. PEA actions are preferentially terminated by its hydrolytic enzyme N-acylethanolamine acid amidase (NAAA), a lysosomal enzyme whose inhibition determines an increase of endogenous PEA levels.

NAAA inhibitors have opened new promise for developing new and effective therapies for various diseases, including those affecting the gut. Evidence suggests that by interacting with multiple targets, PEA reduces inflammation in murine and human colon tissues, suggesting a possible involvement in CRC and intestinal fibrosis. Concurrently, NAAA pharmacological inhibition by using a selective pharmacological inhibitor (i.e., AM9053) is reported to exert beneficial effects in inflammatory conditions, with no shreds of evidence in CRC and intestinal fibrosis. Here, we investigate the functional role of PEA and its primary degradative enzyme inhibitor, NAAA, in preclinical experimental CRC and intestinal fibrosis models.

Design
The functional roles of PEA and NAAA were assessed using multiple approaches, including in vivo, ex-vivo and in vitro analysis. Human intestinal tissues were analyzed, too. Specifically, we aimed to explore:
1) The role of exogenous PEA in colon carcinogenesis, elucidating its effects and related mechanism of action in CRC cell proliferation, migration, and cell cycle.
2) The functional role of NAAA in vivo by using two different models of CRC. NAAA inhibition was also evaluated in vitro on CRC cell lines (and for comparison on a CRC cell line with a transient NAAA deletion) for cell proliferation and migration behaviour changes. Human biopsies from surgically resected CRC patients were used to evaluate NAAA expression and its substrate levels.
3) The role of NAAA and its pharmacological inhibition effects in vivo model of Crohn's disease gut fibrosis and in vitro on bone-marrow-derived macrophages for the study of IL-23 pathway involvement. Human clinically diagnosed CD samples were also characterised by their fibrotic features, NAAA expression, and AEs levels.

Results
1) Exogenous PEA showed beneficial effects in vitro by i) reducing colon cancer cell proliferation (without affecting the proliferation of healthy colonic epithelial cells) *via* PPAR-α and GPR55; ii) inducing cell cycle arrest in the G2/M phase by promoting DNA damage through upregulation of the cyclin B1-CDK1 complex, and iii) negatively influencing tumor cell migration through downregulation of MMP2 and TIMP1 expression.
2) AM9053, a selective and reversible NAAA inhibitor, reduced CRC xenograft tumor growth and impacted tumor development in the sporadic model of CRC induced by azoxymethane

administration. In vitro, NAAA inhibition: i) reduced CRC cell proliferation *via* PPAR-α and TRPV-1; ii) induced cell cycle arrest in the S phase by promoting cyclin A2/CDK2 down-regulation. NAAA transient knockdown mirrored the effects of NAAA inhibition with AM9053. In human CRC specimens, NAAA expression resulted in down-regulation with a joint up-regulation in AEs levels.
3) *In vivo* NAAA pharmacological inhibition with AM9053 determined a rescue of gut fibrosis by reducing inflammatory parameters, collagen deposition, fibrosis genes, and immune response related to IL-23 signalling. In vitro, on BMDM, AM9053 was able to significantly reduce the production of IL-23 and some of the actors involved in its signalling, including pSTAT3. NAAA expression was downregulated in fibrotic CD patients, coincidentally decreasing its substrates OEA and PEA.

Conclusions
Overall, these results provide new promises into the beneficial effects of targeting PEA levels (through its exogenous administration and/or the pharmacological inhibition of its degradative enzyme NAAA) in gut disorders.

Abbreviation list

2-AG	2-Arachidonoylglycerol
5-FU	5-fluorouracil
ACF	Aberrant crypt foci
AEs	Acylethanolamides
AEA	Anandamide
AM9053	10-isothiocyanatodecyl benzene
AOM	Azoxymethane
BMDM	Bone-marrow-derived-macrophages
Ca-NAT	Calcium-dependent N-acyltransferase
JNK	c-Jun N-terminal kinase
CRC	Colorectal cancer
CD	Crohn's disease
CDK2	Cyclin-dependent kinase 2
CDK1	Cyclin-dependent kinase 1
COX-2	Cyclooxygenase 2
COL2A1	Collagen Type II Alpha 1 Chain
COL3A1	Collagen Type III Alpha 1 Chain
CTLA4	Cytotoxic-T-lymphocyte associated protein 4
DAI	Disease activity index
DMEM	Dulbecco's modified Eagle's medium.
dMMR	Mismatch repair deficient tumors
DMSO	Dimethyl sulfoxide
DSS	Dextran Sulfate Sodium
EMEM	Eagle's Minimum Essential Medium
EndMT	Endothelial-mesenchymal transition
ELISA	Enzyme-linked immunosorbent assay
EGF	Epidermal growth factor
EMT	Epithelial-to-mesenchymal transition
ECM	Extracellular matrix
ERK	Extracellular signal-regulated kinases
FAP	Familial adenomatous polyposis
FAAH	Fatty acid amide hydrolase
FBS	Fetal bovine serum
FACS	Flow cytometry analysis
GENT	Gene expression across Normal and Tumor tissue
GPR55	G protein-coupled receptor 55
GRP119	G protein-coupled receptor 119
HCEC	Healthy colonic epithelial cells
HNPCC	Hereditary non-polyposis colon cancer
HPLC	High performance liquid chromatography
iNOS	Inducible nitric oxide synthase
IBD	Inflammatory bowel disease
IGF-I	Insulin-like growth factor
ILCs	Innate lymphoid cells

IL-1β	Interleukin-
IL-4	Interleukin-4
IL-6	Interleukin-6
IL-13	Interleukin-13
IL-17	Interleukin—17
IL-23	Interleukin-23
IF	Intestinal fibrosis
IR	Irinotecan
LPS	Lipopolysaccharide
LC-APCI-MS	Liquid chromatography–atmospheric pressure chemical ionization–mass spectrometry
M-CSF	Macrophages colony-stimulating factor
MMP	Matrix metalloproteinases
MMP2	Matrix metalloproteinases 2
MMP3	Matrix metalloproteinases 3
MMP8	Matrix metalloproteinases 8
MMP9	Matrix metalloproteinases 9
MLNs	Mesenteric lymph nodes
MAPK	Mitogen-activated protein kinase
MEICS	Murine endoscopic index of colitis severity
MSI	Microsatellite instability
MTT	3-(4,5-dimethylthiazol-2-yl)-2,5-diphenyltetrazolium bromide
NAAA	N-acylethanolamide acid amidase
NAPEs	N-acylphosphatidylethanolamines
NR	Neutral red
OEA	Oleoylethanolamide
PBS	phosphate buffer saline
PDGF	Platelet-Derived Growth Factor
PEA	Palmitoylethanolamide
PPAR-α	Peroxisome proliferator-activated receptor α
ROR-γt	Retinoic acid receptor-related orphan receptor γt
RT-PCR	Reverse transcription-polymerase chain reaction.
SIM	Selected ion-monitoring
Th1	T helper 1 cells
Th2	T helper 2 cells
Th17	T helper 17 cells
TIMP 1	Tissue inhibitor matrix metalloproteinases 1
TIMPs	Tissue inhibitor of metalloproteinases
TGF- β	Transforming growth factor-beta
TNBS	2,4,6-trinitrobenzen sulfonic acid
TNF-α	Tumor necrosis factor-alpha
TNM	Tumor-node-metastasis
TRPV1	Transient receptor potential vanilloid type 1
UC	Ulcerative colitis
um-PEA	Ultra micronized PEA
ZOs	Zonulae Occludentes
αSMA	α-Smooth muscle actin

Introduction

1.1 Colorectal cancer (CRC)

Colorectal cancer (CRC) is a heterogeneous disease that poses a global health challenge and is the third most common malignancy (Figure 1) (Gupta et al., 2020; Siegel, Miller, Fuchs, & Jemal, 2022; Testa, Pelosi, & Castelli, 2018; Xi & Xu, 2021). Moreover, CRC is the second most common cause of cancer-related deaths, carrying a lifetime risk of around 4% to 5% (O'Sullivan et al., 2022; Patel, Karlitz, Yen, Lieu, & Boland, 2022; Xi & Xu, 2021). A noteworthy aspect is that CRC affects both men and women equally and is a multi-stage pathology marked by an interaction of acquired genetic and epigenetic alterations, responsible for the transformation of normal colonic epithelial cells into invasive carcinoma, with aberrant crypt foci (ACF) as the earliest premalignant lesions and adenomatous polyps serving as transitional stages within this progression (Abotchie, Vernon, & Du, 2012; Luebeck & Moolgavkar, 2002) (Figure 2). It is well established that CRC is highly influenced by a large number of factors encompassing lifestyle routine, a diet rich in fat, physical inactivity, alterations in gut microbiota, additional pathologies, and notably, conditions like diabetes and obesity, and hereditary genetic component (i.e., familial adenomatous polyposis, FAP, and non-polyposis syndromes, such as Lynch syndrome, also known as hereditary non-polyposis colon cancer, HNPCC), and a history of inflammatory bowel disease (IBD) (Figure 3) (Borrelli et al., 2015; Morgan et al., 2023; Vipperla & O'Keefe, 2016). The incidence increases dramatically after the age of 50 years, and the prognosis is closely related to the stage of the neoplasm (Simon, 2016). Recently, the worldwide early-onset incidence of CRC under the age of 50 has notably risen, and it is estimated that colorectal tumors found in young adults are related to hereditary syndromes (Cho et al., 2022; Medina Pabon & Babiker, 2024; Patel et al., 2022).

Due to its gradual development, which generally takes 10 to 15 years, screening average individuals is the most effective approach to prevent CRC, detect the early on-set and reduce CRC-related deaths in average-risk individuals (Edwards et al., 2010) (Hossain et al., 2022). Despite the increase in early screening, almost 25% of CRC cases are diagnosed at an advanced stage when the cancer has already metastasised, leading to a 10% 5-year survival rate in such cases (Hossain et al., 2022). Generally, the surgery approach and chemotherapy or radiotherapy before or after surgery are the cornerstones of metastatic CRC treatment (Benson et al., 2021). A current medical approach to treatment is influenced by several factors (i.e., the tumor treatment goal and mutational characteristics). It encompasses both single-agent therapies, like 5-fluorouracil 5-FU), and multi-agent regimens, like FOLFOX (Fluorouracil/Leucovorin and

Oxaliplatin) and FOLFIRI [Fluorouracil/Leucovorin and Irinotecan (IR)] (Hossain et al., 2022) (Gustavsson et al., 2015; Xie, Chen, & Fang, 2020). Nonetheless, conventional chemotherapy has several limitations (i.e., overall body toxicity, unsatisfactory response rates, variable resistance (both innate and acquired), and lack of specificity for tumor cells) (Hossain et al., 2022; Xie et al., 2020). Immunotherapy is considered a groundbreaking cancer treatment tool because it alters the host's immune system, which is useful when traditional treatments may have failed (Ling et al., 2022; O Dillmann, 2011). Immunotherapy efficacy has been demonstrated in various cancers, including CRC patients with high microsatellite instability (MSI) and mismatch repair deficient (dMMR) tumors (Weng et al., 2022). Immunotherapy offers several benefits, including fewer side effects, good combinability with other treatments, and long-term remission (Weng et al., 2022; Franke et al., 2019; Ganesh et al., 2019). Several immunotherapy drugs have been approved, including those checkpoint inhibitors targeting PD-1/PDL-1 [i.e., Pembrolizumab (Keytruda), Nivolumab (Opdivo), and Durvalumab (Imfinzi)] and targeting CTLA-4 [i.e., Ipilimumab (Yervoy)] (Weng et al., 2022). As a result, significant resources and funding have been dedicated to developing novel techniques to improve or potentially substitute traditional colorectal cancer chemotherapy (Hossain et al., 2022; Xie et al., 2020). Therefore, ongoing research focuses on developing more effective and non-invasive therapies for colorectal cancer treatment.

In this PhD work, we took advantage of two well-known in vivo models of CRC. First, to replicate human morphological characteristics and pathogenic features of sporadic CRC (i.e., localisation and pathogenic features) and to study the molecular mechanisms underlying carcinogenesis, we used the azoxymethane (AOM)-CRC model, a well-established 14-week-mouse model (Neufert, Becker, & Neurath, 2007). Second, we used the xenograft model of CRC by transplanting colorectal cancer cells into the back of immunodeficient mice, with the primary goal of evaluating the effect of NAAA inhibition on tumor formation. As reported in the literature, this model is suited for investigating tumor growth and drug discovery (X. Liu, Xin, & Wang, 2023; Wagner et al., 2021).

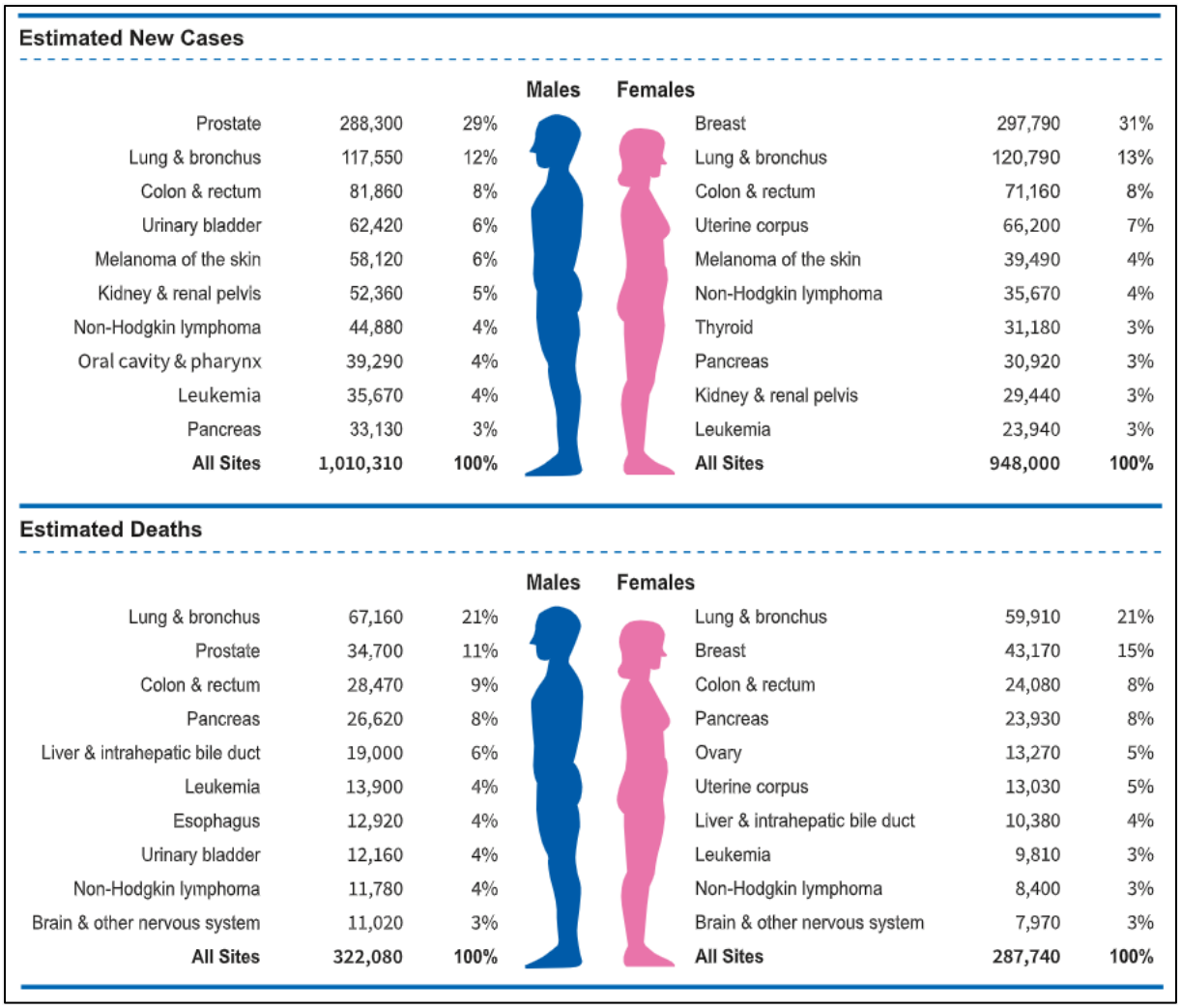

Estimated New Cases

			Males	Females			
Prostate	288,300	29%			Breast	297,790	31%
Lung & bronchus	117,550	12%			Lung & bronchus	120,790	13%
Colon & rectum	81,860	8%			Colon & rectum	71,160	8%
Urinary bladder	62,420	6%			Uterine corpus	66,200	7%
Melanoma of the skin	58,120	6%			Melanoma of the skin	39,490	4%
Kidney & renal pelvis	52,360	5%			Non-Hodgkin lymphoma	35,670	4%
Non-Hodgkin lymphoma	44,880	4%			Thyroid	31,180	3%
Oral cavity & pharynx	39,290	4%			Pancreas	30,920	3%
Leukemia	35,670	4%			Kidney & renal pelvis	29,440	3%
Pancreas	33,130	3%			Leukemia	23,940	3%
All Sites	**1,010,310**	**100%**			**All Sites**	**948,000**	**100%**

Estimated Deaths

			Males	Females			
Lung & bronchus	67,160	21%			Lung & bronchus	59,910	21%
Prostate	34,700	11%			Breast	43,170	15%
Colon & rectum	28,470	9%			Colon & rectum	24,080	8%
Pancreas	26,620	8%			Pancreas	23,930	8%
Liver & intrahepatic bile duct	19,000	6%			Ovary	13,270	5%
Leukemia	13,900	4%			Uterine corpus	13,030	5%
Esophagus	12,920	4%			Liver & intrahepatic bile duct	10,380	4%
Urinary bladder	12,160	4%			Leukemia	9,810	3%
Non-Hodgkin lymphoma	11,780	4%			Non-Hodgkin lymphoma	8,400	3%
Brain & other nervous system	11,020	3%			Brain & other nervous system	7,970	3%
All Sites	**322,080**	**100%**			**All Sites**	**287,740**	**100%**

Figure 1. The ten most prevalent types of cancer in terms of estimated new cases and deaths, categorised by sex, in the United States for 2023 (Siegel et al., CA Cancer J Clin. 2023).

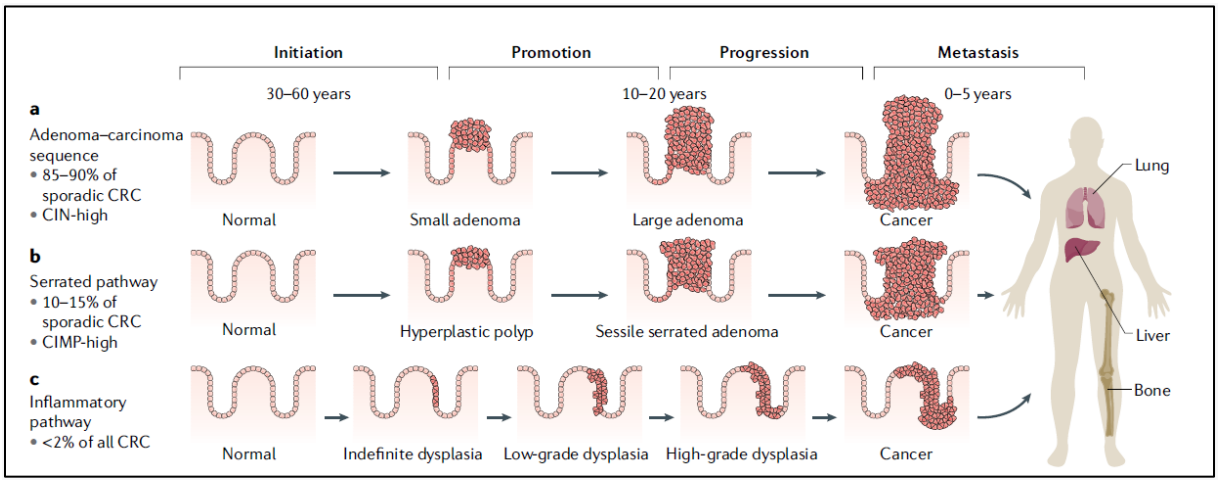

Figure 2. Pathways of colorectal carcinogenesis (Keum and Giovannucci. Nat Rev Gastroenterol Hepatol, 2019).

Table 1 | Risk and protective factors for colorectal cancer

Factor	Measurement	Level of evidence	Relative risk (95% CI)
Risk factors			
Smoking	Ever versus never	Convincing	1.18 (1.11–1.25)
Processed meat	50 g/day	Convincing	1.16 (1.08–1.26)
Alcohol use	10 g/day	Convincing	1.07 (1.05–1.08)
Obesity	5 kg/m^2	Convincing	1.05 (1.03–1.07)
Height in adulthood	Per 5 cm increase	Convincing	1.05 (1.02–1.07)
Inflammatory bowel disease	NA	Convincing	1.7 (1.2–2.2)[a]
Red meat	100 g/day	Probable	1.12 (1.00–1.25)
Protective factors			
Physical activity	High versus low	Convincing	0.80 (0.72–0.88)
Non-steroidal anti-inflammatory drugs	≥75 mg/day	Convincing	0.75 (0.56–0.97)
Whole grains	90 g/day	Probable	0.83 (0.78–0.89)
Dietary fibre	10 g/day	Probable	0.93 (0.87–1.00)
Dairy	400 g/day	Probable	0.87 (0.83–0.90)
Dietary calcium	200 mg/day	Probable	0.94 (0.93–0.96)
Postmenopausal hormone therapy	Ever versus never	Probable	0.80 (0.74–0.86) for colon cancer 0.81 (0.72–0.92) for rectal cancer

Data derived from ref. 32 unless otherwise noted. NA, not applicable. [a]Standardized incidence ratio, not relative risk.

Figure 3. Risk and protective factors for CRC (Murphy and Zaki. Nat Rev Gastroenterol Hepatol. 2024).

1.2 Inflammatory Bowel Disease (IBD)

Inflammatory bowel disease (IBD) is a public global health challenge, with the highest incidence in the Western world, with a dramatical rise in incidence in regions such as South America, Eastern Europe, Asia, and Africa due to environmental factors (Figure 4) (Desai & Dhoble, 2024; Frolkis et al., 2013; Kaplan & Ng, 2017; Molodecky et al., 2012; Ng et al., 2017; Y. Wang et al., 2022). IBD is characterised by an early onset of around 15 to 30 years, with a second peak occurring in 10% to 15% of individuals after 60 (McDowell, Farooq, & Haseeb, 2024; L. J. Su et al., 2019). Of relevance, IBD is an immune-based chronic condition affecting the gastrointestinal system, comprising two idiopathic subtypes, namely Crohn's disease (CD) and ulcerative colitis (UC) (Figure 5) (Neurath, 2019). IBD is a multifactorial and multistage disorder with unknown causes (Kofla-Dlubacz et al., 2022). However, mounting literature evidence suggests that IBD is influenced by an inadequate inflammatory reaction to intestinal microorganisms in a genetically vulnerable host and is characterised by an interplay between genetic, environmental, and immune factors (Figure 6) (Ananthakrishnan, Kaplan, & Ng, 2020; Khan et al., 2019; Kofla-Dlubacz et al., 2022). CD and UC share standard clinical and pathological features but involve gastrointestinal tracts differently (McDowell et al., 2024; Wijmenga, 2005). While a shallower colon mucosa inflammation characterises UC, CD is distinguished by the transmural small intestine and colon inflammation ((McDowell et al., 2024; Neurath, 2019). Moreover, IBD's common clinical symptoms are chronic diarrhoea, abdominal pain, weight loss, rectal bleeding, and compromising health-related quality of life (Glocker & Grimbacher, 2012; Knowles et al., 2018).

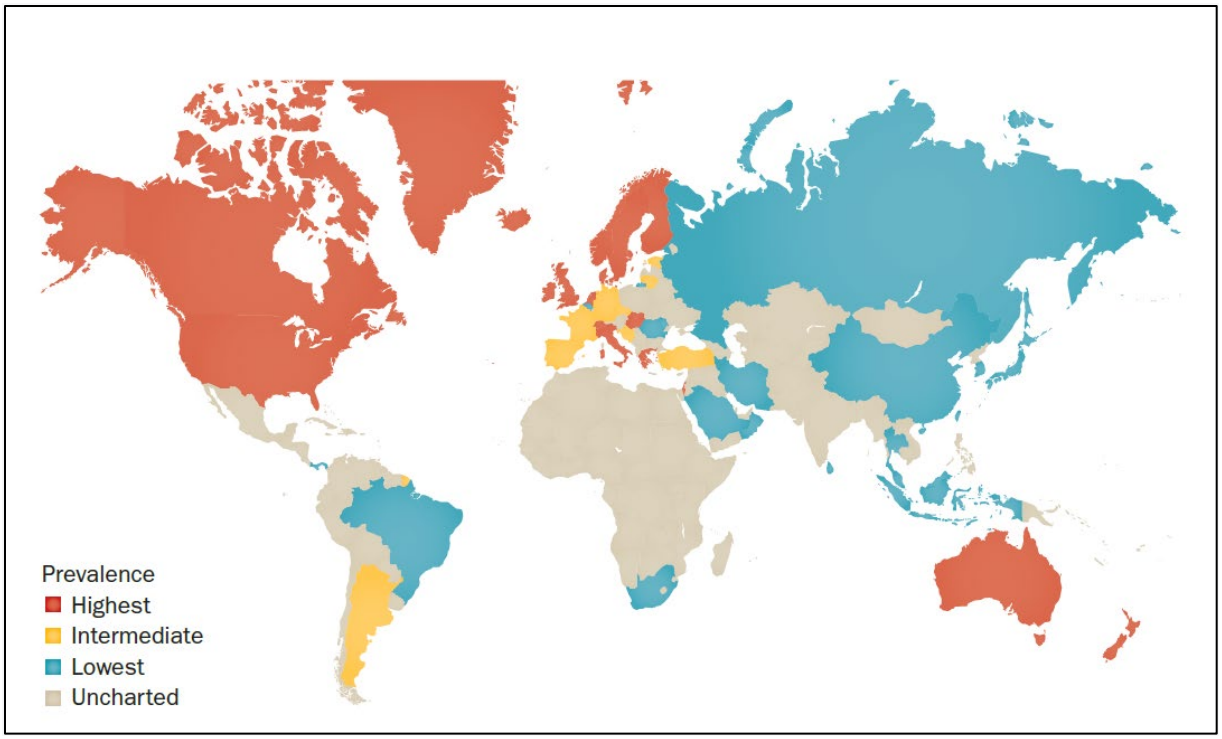

Figure 4. The global burden of IBD: from 2015 to 2025 (Kaplan. Nat Rev Gastroenterol Hepatol., 2015).

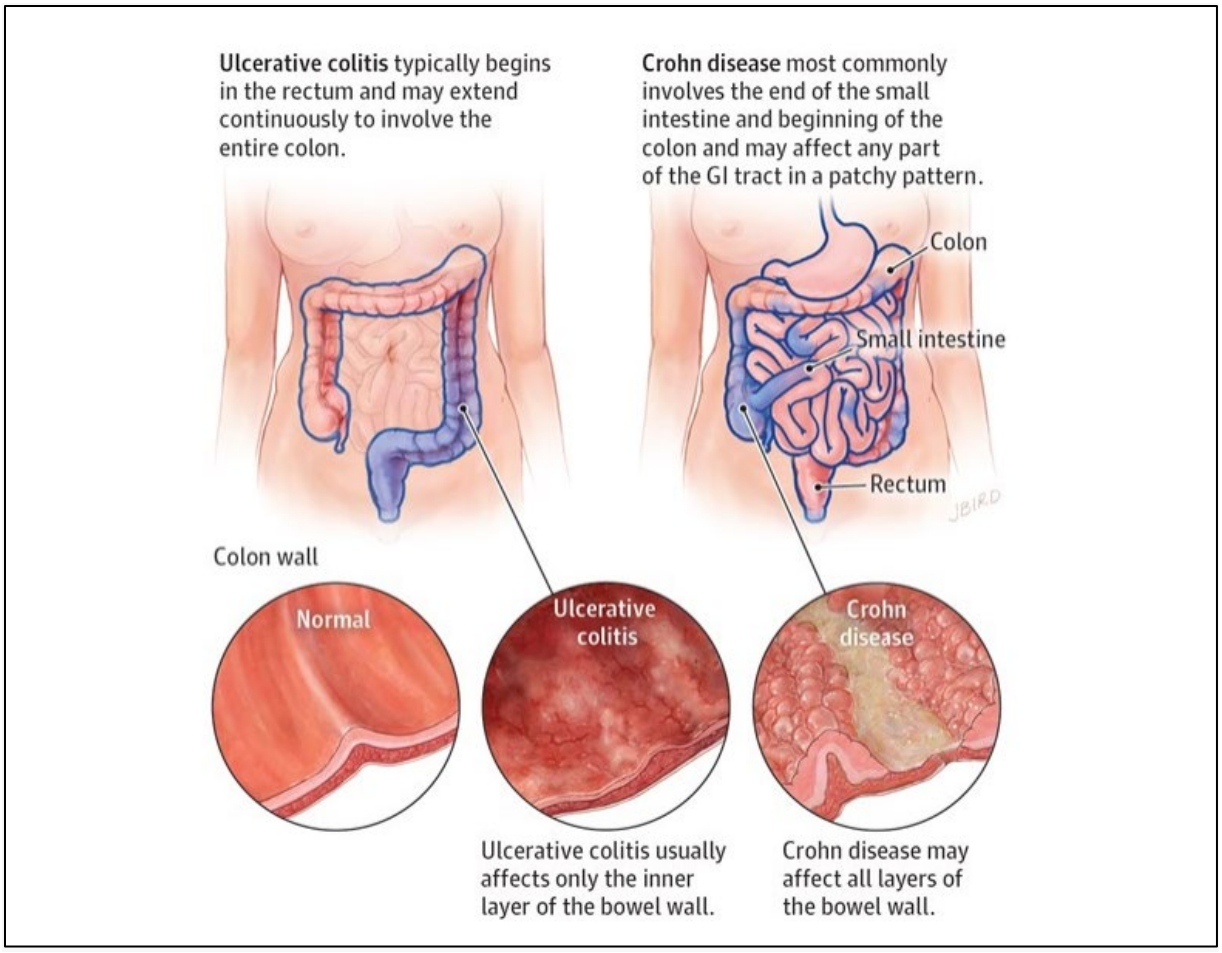

Figure 5. Differences between two idiopathic IBD subtypes: Crohn's disease (CD) and Ulcerative colitis (UC) (Jin, JAMA, 2014).

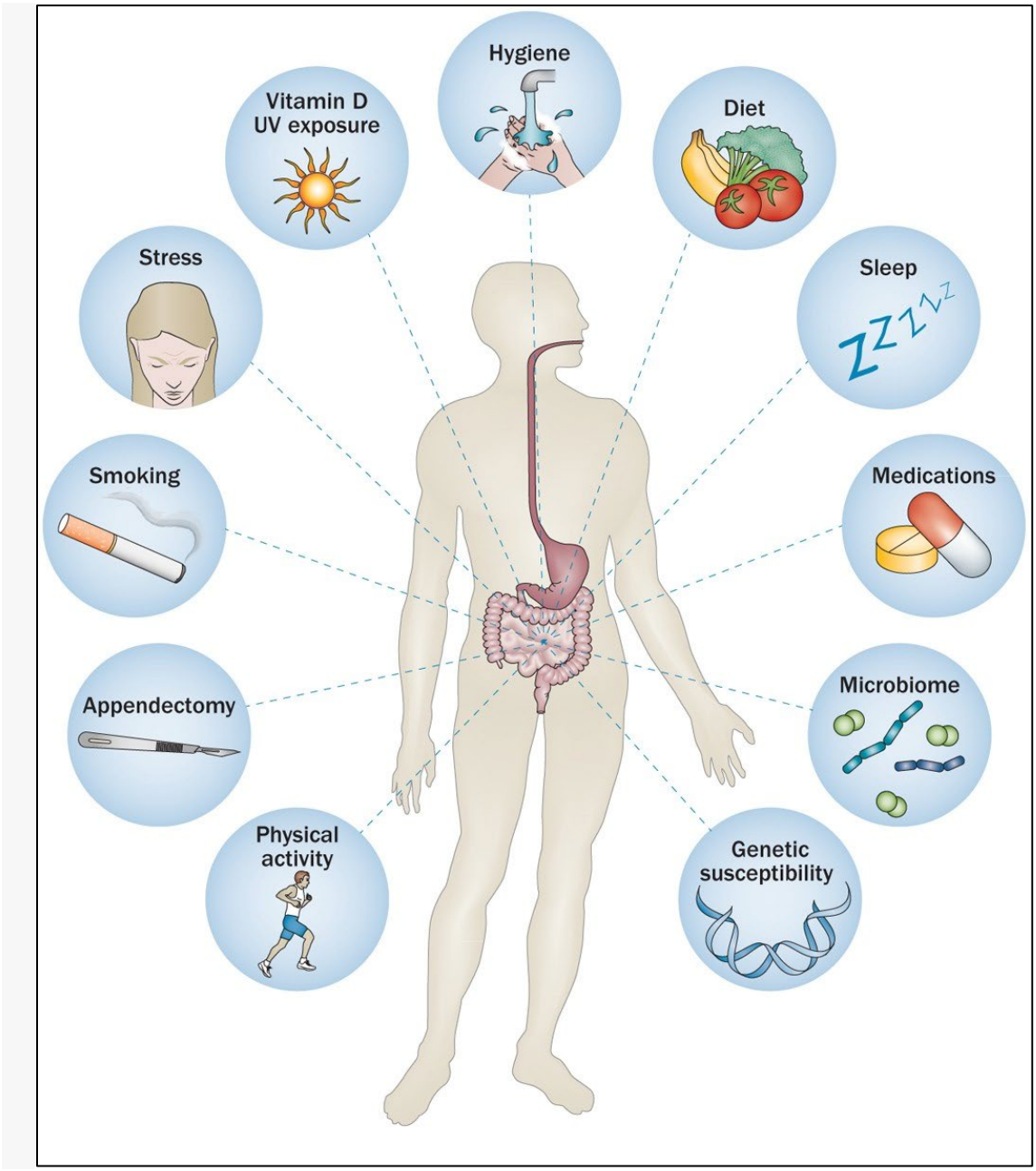

Figure 6. Risk factors for IBD (Ananthakrishnan, Nat Rev Gastroenterol Hepatol, 2015).

1.2.1 Intestinal fibrosis (IF): a frequent complication in IBD

One of the most frequently encountered and serious issues in CD is intestinal fibrosis (IF), affecting over a third of CD patients and resulting in intestinal blockages due to constrictions (D'Alessio et al., 2022; Y. Wang et al., 2022). IF leads to heightened levels of illness, necessitating extended hospital stays and surgical interventions, influencing the quality of life, and increasing CRC risk. While the effects of fibrosis in various organs (i.e., lung, kidney, liver) are extensively documented, exploring fibrosis in the intestinal context is only at the beginning. IF is a multifactorial condition that triggers an immune response, driven by both cellular and molecular components, that can also develop even after removing an inflammatory trigger and resolving inflammation. This pathological condition is characterized by the excessive accumulation of extracellular matrix (ECM), increasing submucosal recruitment of mesenchymal cells, and abnormal collagen deposition (types I, III, and V), often leading to bowel obstruction (Y. Wang et al., 2022). ECM is a complex and highly dynamic molecule network, like collagen and glycoproteins, responsible for cell and tissue structure stability (Karamanos et al., 2021). Notably, ECM is a crucial regulator of a plethora of both biological functions (i.e., cell signaling, tissue development and repair, regulation of biological processes and physical barrier) and pathological conditions (i.e., tissue fibrosis and cancer) as well (Karamanos et al., 2021; Koliaraki, Prados, Armaka, & Kollias, 2020; Lu, Neff, Quake, & Weissman, 2011; Valdoz et al., 2022). Matrix metalloproteinases (MMP) and their inhibitors, tissue inhibitors of metalloproteinases (TIMPs), mainly regulate ECM remodelling. MMPs are a large family of proteolytic enzymes involved in several functions, including the breakdown of ECM components, tissue remodelling, and cell migration, closely regulated by TIMPs (Cabral-Pacheco et al., 2020). Loss of tissue homeostasis, by alteration in MMPs/TIMPs balance, is responsible for pathophysiological processes such as IF, transforming epithelial cells from their usual polarized state into mesenchymal cells. Several studies reported changes in MMP2-MMP3-MMP8, MMP-9, and TIMP-1 expression in both in vivo studies and fibrotic biopsies from fibrotic CD patients (Breynaert et al., 2016; Dmochowska et al., 2020; Lawrance et al., 2003; Y. Wang et al., 2022). IF results from interplaying multiple cellular and molecular components, including cytokines, growth factors, and mesenchymal and non-mesenchymal cells. Mesenchymal cells, including fibroblasts, myofibroblasts, and smooth muscle cells, are committed to synthesising collagen and are crucial for IF development and progression (Santacroce, Lenti, & Di Sabatino, 2022). Furthermore, their excessive proliferation, under pro-inflammatory stimuli, is responsible for thickening the *muscularis mucosae* and *muscularis*

propria, typical histological features of IF. Fibroblasts are a highly heterogeneous cells population and the most common type in connective tissue involved in intestinal homeostasis by upholding structural integrity and contributing to tissue repair (Chalkidi, Paraskeva, & Koliaraki, 2022; Dick, Miao, & Limaiem, 2024; Talbott, Mascharak, Griffin, Wan, & Longaker, 2022). Under pro-inflammatory stimuli (i.e., PDGF, TGF-β, IGF-I, and EGF), fibroblasts have the potential to transform into myofibroblasts, key players in IF, sharing features of smooth muscle cells and fibroblasts, can contract, move, and secrete components of ECM and growth factors. Myofibroblast activation leads to migration to sites of injury aided by adhesion molecules such as fibronectin and N-cadherin (Burke, Cunningham, Sweeney, Docherty, & O'Connell, 2011; D'Alessio et al., 2022; Leeb et al., 2002). Beyond this mechanism, several hypotheses are responsible for mesenchymal cell proliferation, including bone marrow-derived fibrocyte recruitment ((D'Alessio et al., 2022; Uehara et al., 2010). Finally, inflammation can trigger the conversion of epithelial and endothelial cells into ECM-producing mesenchymal cells through processes like epithelial-mesenchymal transition (EMT) and endothelial-mesenchymal transition (EndMT) (Rieder et al., 2011; Santacroce et al., 2022; Yang et al., 2019). EMT is a complex cellular process based on the trans-cellular differentiation from epithelial to mesenchymal phenotype. EMT inducing changes in function, morphology, and molecular alterations, including downregulation of epithelial markers expression (i.e., E-cadherin, Zonulae Occludentes (ZOs), and cytokeratins) and up-regulation of mesenchymal cells markers (i.e., α smooth muscle actin (αSMA), vimentin, fibronectin, collagens) (Kalluri & Weinberg, 2009; Lovisa, Genovese, & Danese, 2019; Santacroce et al., 2022). Although mesenchymal cells play a pivotal role in IF, many non-mesenchymal cell types are also involved, including telocytes and innate lymphoid cells (ILCs) ((D'Alessio et al., 2022). Furthermore, immune components, by promoting pro-inflammatory cytokine network activation, play a critical role in the onset and progression of IF (Yang et al., 2019) (Figures 7 and 8). Although the regulatory mechanism of T cells in the intestine is still not completely understood, literature evidence-based suggests the crucial involvement of T cell subsets (i.e., Th1 with the pro-inflammatory role and Th2 and Th17 with pro-inflammatory and pro-fibrogenic functions) and their cytokines in IF development (D'Alessio et al., 2022; Friedrich, Pohin, & Powrie, 2019; Santacroce et al., 2022; Y. Wang et al., 2022; X. Wu et al., 2023). In particular, Th2 cells produce cytokines like IL-4, IL-5, and IL-13, associated with type 2 immune responses. In contrast, Th17 cells are characterised by the RAR-related orphan receptor γt (ROR-γt) expression producing IL-17, IL-21, IL-22, and IL-23 (Gieseck, Wilson, & Wynn, 2018; Y. Wang et al., 2022). Specifically, the predominant Th17-associated cytokines are IL-

17A, promoting fibrotic effects by influencing myofibroblasts and regulating EMT, and IL-23, stabilising Th17 (Latella & Viscido, 2020; Y. Wang et al., 2022). Additional research has demonstrated that IL-23 affects innate immune system cells and plays a role in producing inflammatory cytokines and causing tissue inflammation. Consequently, the significance of the IL-23/IL-17 axis in developing persistent intestinal inflammation in IBD has been emphasized in animal and human studies (Gaffen, Jain, Garg, & Cua, 2014). This pathway is particularly relevant to the understanding of CD's disease pathogenesis. The existing pharmaceutical solutions for IBD fall short in their ability to halt or treat fibrotic progression completely. Therefore, gaining insights into the cellular and molecular mechanisms responsible for gut fibrosis is crucial. In this context, targeting the IL-23/IL-17 axis may hold promise as a therapeutic strategy to prevent or treat IF in IBD patients. In the present work, we used chronic TNBS colitis, a well-known useful mouse model of intestinal fibrosis, reproducing tissue fibrosis and stenosis, typical of human CD (Wirtz et al., 2017).

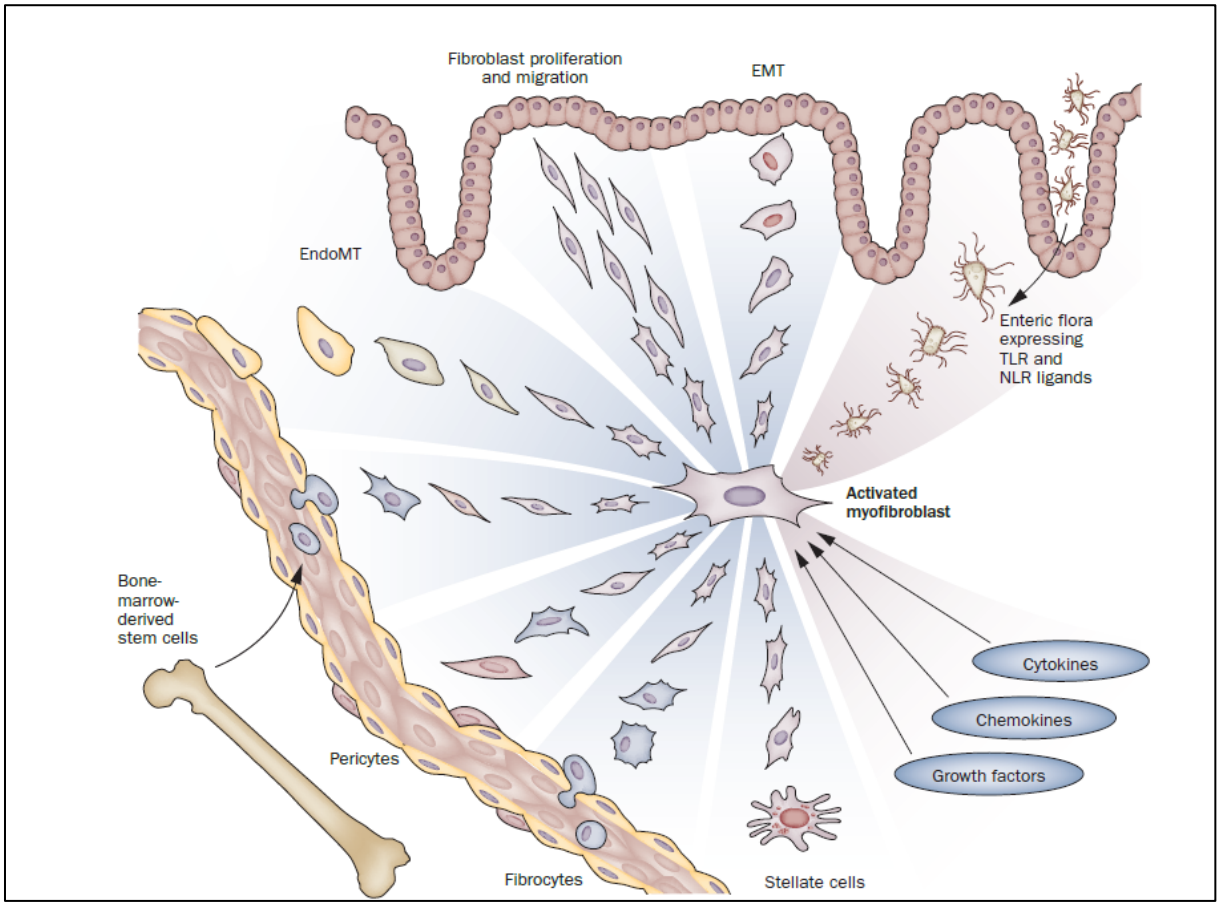

Figure 7. Cell types involved in initiating and mediating fibrogenesis in the inflamed gut (Rieder and Fiocchi. Nat Rev Gastroenterol Hepatol., 2009).

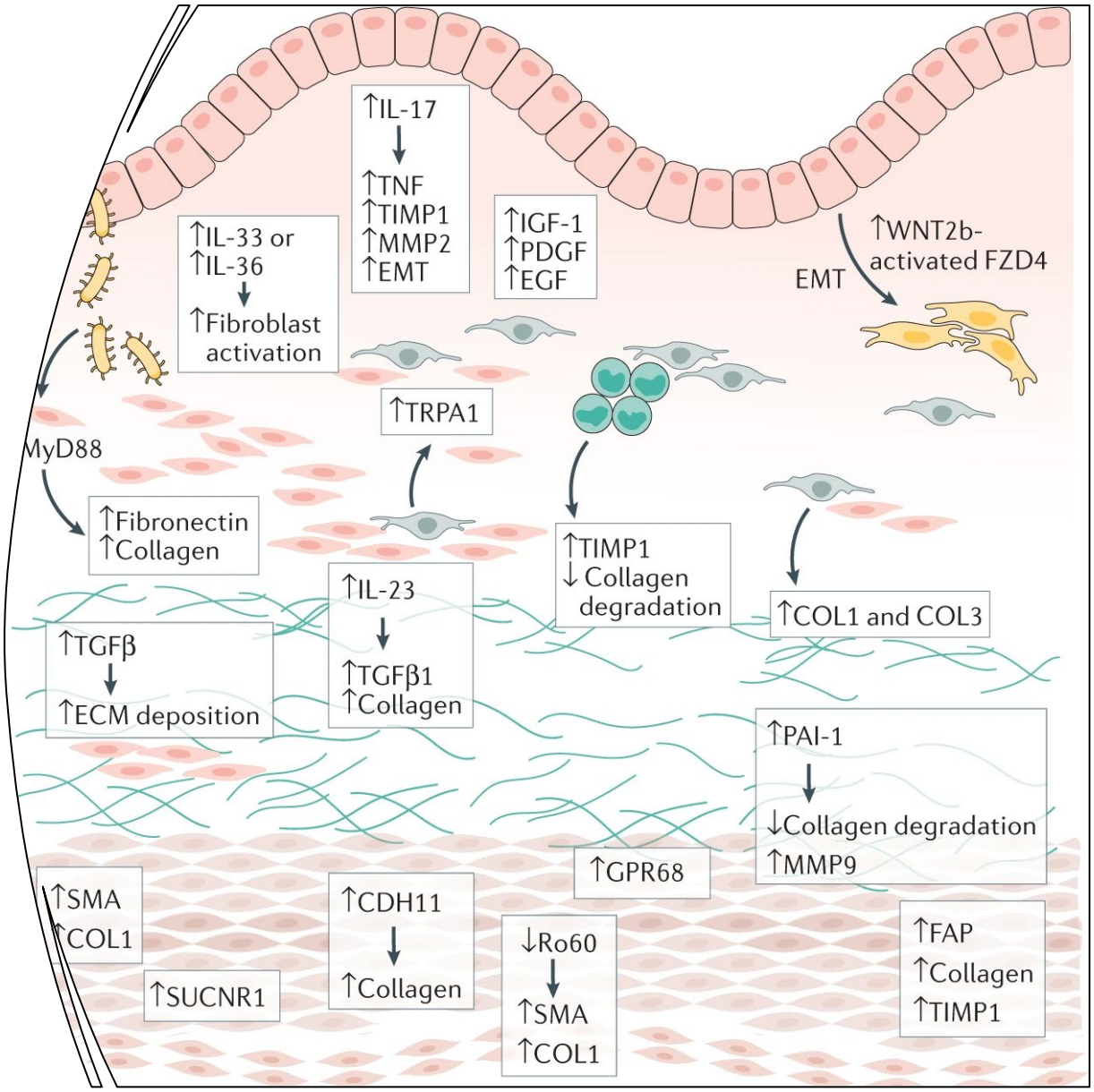

Figure 8. Molecular components involved in the pathogenesis of intestinal fibrosis (D'Alessio S. et al. Nat Rev Gastroenterol Hepatol. 2022).

1.3 Acylethanolamides (AEs)

Acylethanolamides (AEs) are bioactive lipid molecules that occur naturally and are composed of an acyl chain linked to ethanolamine through an amide bond (Figure 9). These compounds differ in their acyl chain length and level of unsaturation. Despite sharing a common structural foundation, AEs can engage with different receptors and elicit a diverse array of biological responses, including pain, inflammation, anxiety, stress, neurotransmission, and food intake (Bottemanne, Muccioli, & Alhouayek, 2018; Mock, Gagestein, & van der Stelt, 2023; Tsuboi, Uyama, Okamoto, & Ueda, 2018). AEs are synthesized on demand in response to external stimuli through a two-stage biosynthetic pathway involving several enzymes (Bottemanne et al., 2018; Di Marzo & Piscitelli, 2015). The initial step is orchestrated by a calcium-dependent N-acyltransferase (Ca-NAT), producing N-acylphosphatidylethanolamines (NAPEs). In the second stage, NAPE is hydrolysed by NAPE phospholipase D, the principal biosynthetic enzyme for AEs (Bottemanne et al., 2018; Okamoto, Morishita, Tsuboi, Tonai, & Ueda, 2004; Tsuboi et al., 2018). The main degradative AEs' enzyme is fatty acid amide hydrolase (FAAH), and N-acylethanolamide acid amidase (NAAA). The most encountered and extensively researched AEs include arachidonoylethanolamide (AEA), oleoylethanolamide (OEA), and palmitoylethanolamide (PEA). AEA binds cannabinoid receptors CB1 and CB2 (Devane et al., 1992; Maccarrone et al., 2015) and exerts many biological effects, including hypotension induction, neuroprotection, analgesic properties, and appetite stimulation. Moreover, AEA influences cell proliferation and apoptosis in inflammatory and cancer cells and exerts anti-depressive effects (Batkai et al., 2004; Cravatt et al., 2001; Gobbi et al., 2005; Iannotti, Di Marzo, & Petrosino, 2016; Kathuria et al., 2003; Maccarrone et al., 2015; Pacher, Batkai, & Kunos, 2006; Williams & Kirkham, 1999). OEA is produced from digested dietary fats in the small intestine and is well known for its anorexic effects, mediated by the PPARα receptor (O'Sullivan et al., 2022; Romano et al., 2014). Additionally, OEA can activate the GPR119 receptor, leading to increased GLP-1 levels, which are associated with satiety and is a weak agonist of TRPV1 (Romano et al., 2014).

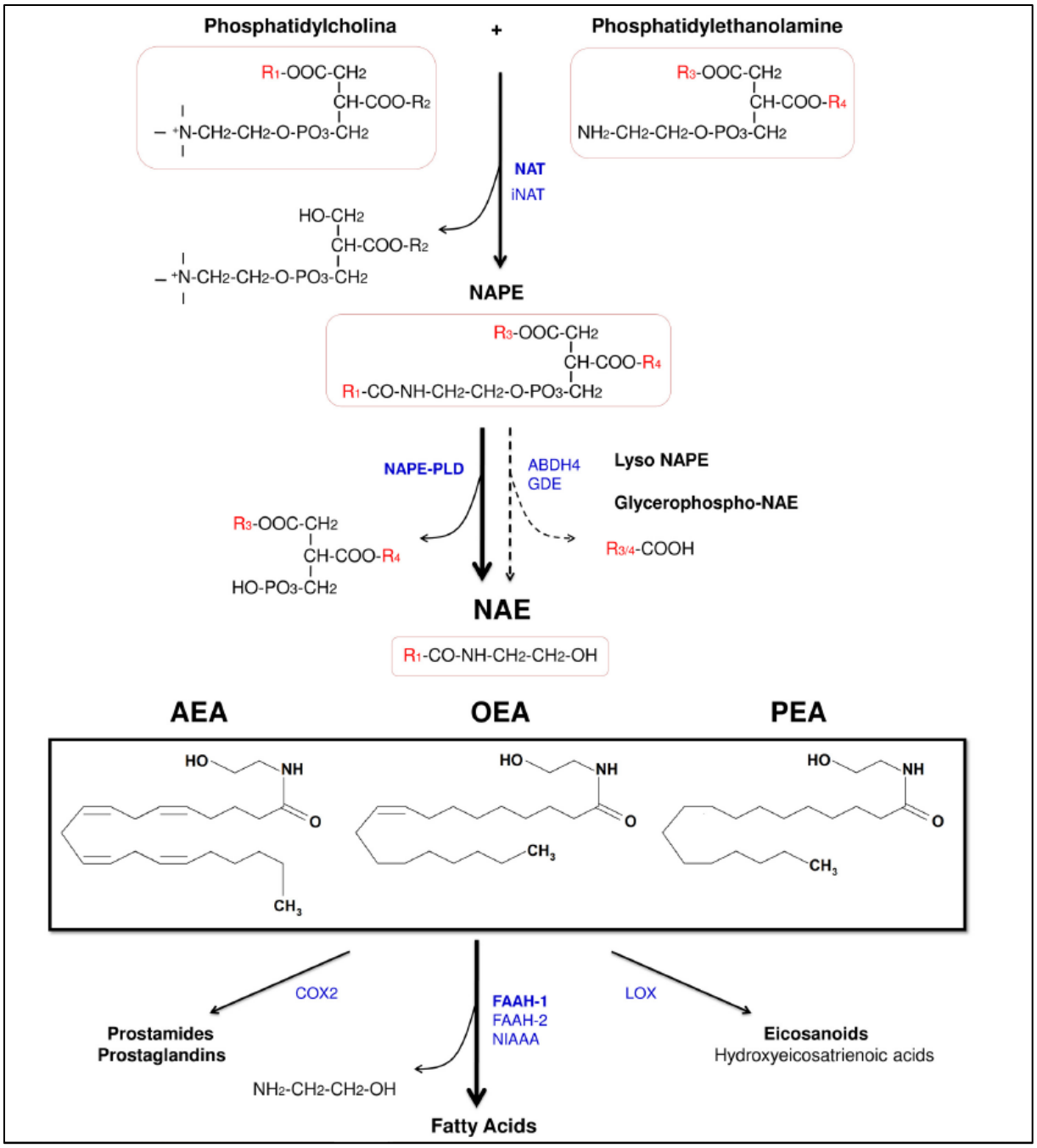

Figure 9. **Chemical structures of the acylethanolamides anandamide (AEA), oleoylethanolamide (OEA), and palmitoylethanolamide (PEA), and pathways for their synthesis and degradation** (Orio et al., Front Mol Neurosci. 2019).

1.3.1 Palmitoylethanolamide (PEA)

PEA is an endogenous fatty acid amide belonging to the family of AEs (Petrosino & Di Marzo, 2017). Many scientific studies investigating the effect of PEA have demonstrated a wide range of biological properties, including neuroprotective, anti-inflammatory, antioxidant, and analgesic functions by acting via several targets, such as PPARα and GPR55, TRPV1 and cannabinoid receptors that are, in turn, involved in several carcinogenesis mechanisms and inflammatory conditions (Fraguas-Sanchez, Martin-Sabroso, & Torres-Suarez, 2018; Petrosino & Di Marzo, 2017). Moreover, PEA does not directly interact with CB1 and CB2 receptors but can indirectly trigger their biological activity through the "*entourage*" effect by inhibiting FAAH, the enzyme responsible for breaking down endocannabinoids (De Petrocellis et al., 2002; Ho, Barrett, & Randall, 2008; Petrosino et al., 2019). PEA is biologically inactivated by N-acylethanolamide acid amidase (NAAA) (Bottemanne et al., 2018; Iannotti et al., 2016). (Figure 10). Of importance, PEA is also a food component considered an oral intestinal anti-inflammatory nutraceutical, marketed as a food component for special medical purposes in some European Countries. PEA's food sources are bovine milk, Common bean (*Phaseolus vulgaris*), garden pea (*Pisum sativum*), soy lecithin and peanut (*Arachis hypogaea*) (Gouveia-Figueira & Nording, 2014; Lam, Marczylo, & Konje, 2010; Petrosino & Di Marzo, 2017; Venables, Waggoner, & Chapman, 2005) (Figure 11). Interestingly, PEA has demonstrated the ability to inhibit the phosphorylation of kinases associated with pro-inflammatory pathways, such as mitogen-activated protein kinase (MAPK), c-Jun N-terminal kinase (JNK), extracellular signal-regulated kinases (ERK), and the nuclear translocation of NF-kB (Rieder et al., 2011). Additionally, PEA affects several cell lines and mouse models, including melanoma, neuroblastoma, and breast cancer (De Petrocellis et al., 2002; Hamtiaux et al., 2012; Stock et al., 2012). Moreover, PEA regulates critical enzyme expression involved in intestinal inflammation, such as COX-2 and inducible nitric oxide synthase (iNOS) (E. Esposito & Cuzzocrea, 2013). Furthermore, PEA alleviates inflammation in murine (Borrelli et al., 2015; G. Esposito et al., 2014) and human colon tissues (Couch, Tasker, Theophilidou, Lund, & O'Sullivan, 2017). Notably, PEA may counteract essential factors contributing to organ fibrosis, including α-SMA, the TGF-β1/SMAD signalling pathway, IL-4, and IL-13 (Ohara et al., 2018; Roviezzo et al., 2017). Furthermore, several of the primary targets affected by PEA's mechanisms of action, such as TRPV1, CB1, and CB2 receptors, are also involved in fibrotic and carcinogenic processes (Correia-Sa et al., 2021; Fraguas-Sanchez et al., 2018; Petrosino & Di Marzo, 2017). These observations raise the question of whether PEA might play a part in the development of intestinal cancer, given the well-documented link between intestinal

inflammation and the initiation of carcinogenesis and gut fibrosis (Terzic, Grivennikov, Karin, & Karin, 2010). However, the understanding of PEA's effects on colon carcinogenesis remains limited, with only one study reporting PEA's antiangiogenic effects on human colon carcinoma cell lines achieved through VEGF downregulation (Sarnelli et al., 2016). Finally, the effect of PEA in intestinal fibrosis is unknown with little notion reported in other organ fibrosis (Ohara et al., 2018; Roviezzo et al., 2017).

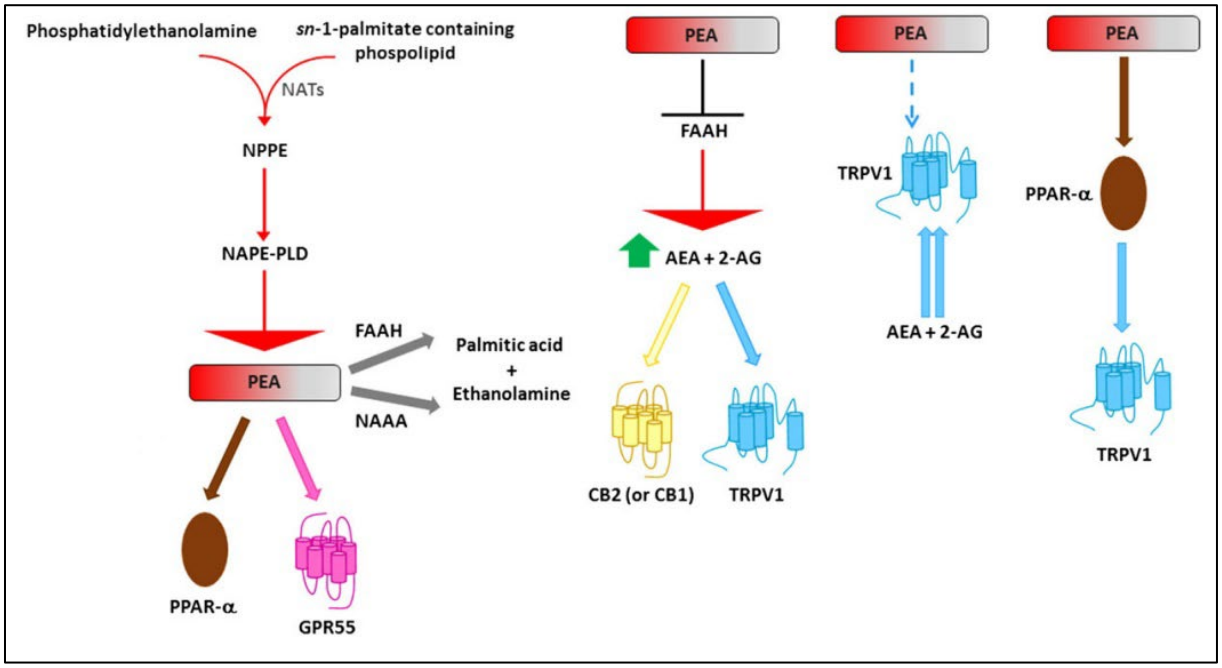

Figure 10. **Metabolic pathways and molecular targets of PEA** (Petrosino and Di Marzo. Br J Pharmacol. 2017).

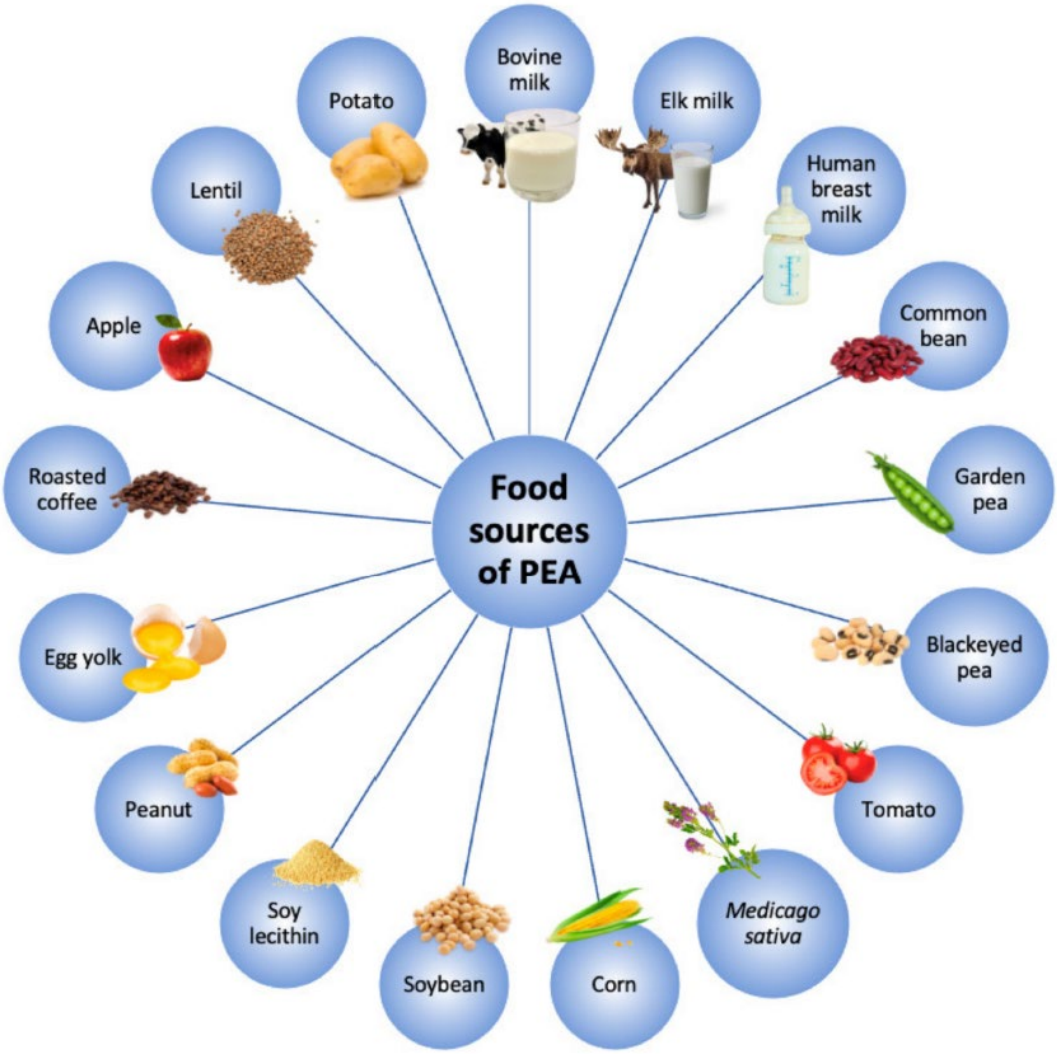

Figure 11. Food sources of Palmitoylethanolamide (PEA) (Noce et al. Pharmaceuticals (Basel), 2021).

1.4 N-acylethanolamide acid amidase (NAAA)

N-acylethanolamine acid amide hydrolase (NAAA) is a lysosomal N-cysteine hydrolase enzyme responsible for AEs degradation, preferentially PEA (Piomelli et al., 2020; Zhao, Tsuboi, Okamoto, Nagahata, & Ueda, 2007). NAAA is also expressed in humans and mice, sharing 76% of similarity sequences (Tsuboi et al., 2005). According to the literature, NAAA is highly expressed in macrophages and B lymphocytes, small and large intestines, and also in the prostate and lung epithelium (Alhouayek et al., 2015; Borrelli et al., 2015; A. I. Su et al., 2004; J. Wang et al., 2008). Many studies report its role in inflammatory disorders, chronic pain, and obesity (Piomelli et al., 2020). NAAA dysregulation is documented in few cancer types (i.e., triple-negative breast cancer, prostate cancer, ovarian and lung cancer) (Du et al., 2016; Gagliardi, Molinaro, Fresta, Duranti, & Cosco, 2022; Huang et al., 2021; Y. Liu et al., 2014; Sakura et al., 2016; J. Wang et al., 2008) with no reported published on its role in colon cancer. Noteworthy, several NAAA inhibitors have been developed (i.e. including AM9053) that showed promising anti-inflammatory, immune-modulating, and analgesic effects in vitro and in vivo due to the increase of AE levels (Bottemanne et al., 2021; Bottemanne et al., 2018; Sgroi et al., 2021). However, the role of NAAA in gut fibrosis is still uncovered to date. Continuous investigation within this domain suggests that the functions of NAAA in cancer may vary depending on the cancer subtype and its cellular context (Huang et al., 2021). Considering these discoveries, inhibiting NAAA has exhibited encouraging outcomes in cancer exploration by fostering an increase in AEs tissue levels (Bottemanne et al., 2018). In the cancer context, the role of NAAA was explored in Triple-negative breast cancer, both in vitro and in vivo. AM11095 (an NAAA inhibitor) showed in vitro beneficial effects by negatively influencing pro-inflammatory cytokines such as IL-6 and IL-8 release, suppressing NF-κB pathway activation, and decreasing expression of pro-angiogenic factors by up-regulating PEA levels. Moreover, AM11095 reduced tumor growth in mice. Interestingly, evidence suggests that NAAA is highly involved in the development and progression of prostate cancer. Foremost, NAAA is markedly expressed in prostate cancer cells (PC-3, DU-145, and LNCaP) compared to prostate epithelial cells (PrEC), with a concomitant up-regulation of endocannabinoids such as anandamide and 2-AG in prostate cancer. Furthermore, recent research on NAAA in the ovarian system suggests its potential involvement in ovarian cancer by modulating signalling pathways relevant to cancer progression. Due to its expression in immune cells, NAAA has been extensively studied also in inflammatory-based conditions, including atopic dermatitis, bowel inflammation, and neuroinflammation (Alhouayek et al., 2015; Bottemanne et al., 2021; Eberlein, Eicke, Reinhardt, & Ring, 2008; Malamas et al., 2020). According to the literature,

NAAA pharmacological inhibition led to an increase in PEA levels at the site of inflammation in preclinical models of ulcerative colitis, resulting in i) an alleviation of most colitis symptoms and ii) significant reduction of pro-inflammatory cytokines releasing in the gastrointestinal tract as well as in peripheral tissues (Alhouayek et al., 2015). Additionally, several scientific studies fully support NAAA inhibition in treating chronic inflammatory disorders (Bandiera, Ponzano, & Piomelli, 2014; Bonezzi et al., 2016; Pontis, Ribeiro, Sasso, & Piomelli, 2016; Ribeiro et al., 2015). Despite the promising pharmacological benefits of NAAA inhibitors in various inflammatory conditions, it's important to note that few NAAA inhibitors with sub-optimal druggability profiles have been discovered so far (Bandiera et al., 2014). Nevertheless, the knowledge of NAAA in gut fibrosis physiopathology and the effect of its inhibition on gut fibrosis is still unexplored.

1.4.1 Natural NAAA-Inhibitors

Exploring plant-based natural molecules offers a promising tool for developing new therapeutic strategies for inflammation, pain, and cancer due to their ability to interact with several targets. The literature describes a few natural compounds that can inhibit NAAA activity, but none of these molecules has been reported to exert anti-inflammatory properties within the gut. Among natural NAAA inhibitors, Atractylodin is a polyethylene alkyne compound from the root of *Atractylodes lancea* (Thunb) DC (Yang et al., 2020). This naturally potent and reversible NAAA inhibitor (IC50 = 2.81 μM) is reported to be effective in ameliorating LPS-induced microglia activation by elevating cellular PEA levels (Yang et al., 2020). Moreover, Atractylodin reduces pro-inflammatory cytokines release (i.e., TNF-α, IL-1ß, and IL-6). Diacerein (IC50 0.7uM) is an anthraquinone derivative found in Cassia plants and Rumex crispus. It exerts anti-inflammatory activity due to increased PEA levels *in vitro* and *in vivo* (Petrosino et al., 2015). None of these molecules have been reported to exert anti-inflammatory properties within the gut.

1.5 Role of diet and nutraceuticals in intestinal disorders

Diet and nutrition have been of growing interest in the context of intestinal diseases (Jayasinghe et al., 2024; Wark et al., 2020; Corsello et al., 2020; Chey et al., 2013). Extensive research has been focused on the correlation between dietary habits and the rising incidence of IBD and CRC in populations (Jayasinghe et al., 2024; Wark et al., 2020; Corsello et al., 2020; Chey et al., 2013). It is well-recognised that diet, nutraceuticals, and natural compounds are crucial in triggering and protecting against chronic inflammation leading to IBD and CRC

(Cassotta et al., 2023). Western diets, characterised by high consumption of fats, refined sugars, and animal proteins and low intake of vegetables and fruits, increase the risk of developing IBD and CRC by worsening inflammation and oxidative stress. It has also been reported that IBD patients'consumption of a Western diet is responsible for a worsening of symptoms. Conversely, anti-inflammatory diets rich in plant-based foods may help treat IBD and maintain remission. Specific dietary patterns, like the Mediterranean diet, which includes fruits, vegetables, whole grains, and healthy fats, have been shown to reduce inflammation and protect against CRC and IBD. Nutraceuticals were defined in 1989 by Stephen DeFelice as a combination of "nutrition" and "pharmaceuticals" and are referred to as a natural compound found in food and plants, able to promote health (Santini, Tenore, & Novellino, 2017). In the last decade, the nutraceutical approach has gained an increasing role in managing several chronic conditions due to its ability to enhance beneficial effects with reduced risk of adverse side actions. Interestingly, several nutraceuticals were considered complementary tools for managing common intestinal disorders, including IBD and CRC. In the context of IBD, evidence suggests nutraceuticals have the potential to reduce symptoms, improve the quality of life of IBD patients, and reduce risks of tumor development by improving host immunity (Ban et al., 2022; Gao, Xu, & Chen, 2020; Mijan & Lim, 2018). Among them, probiotics and phytochemicals, including polyphenols, exert the most promising effect due to their ability to mitigate pro-inflammatory signalling both *in vitro* and *in vivo* (including DSS and TNBS model of CD) (Ban et al., 2022; Danesi & Ferguson, 2017; Gao et al., 2020). Moreover, evidence suggests that polyphenols can influence intestinal flora, enhancing barrier function and intestinal health (Kaulmann & Bohn, 2016). Interestingly, nutraceuticals' clinical efficiency is also demonstrated in patients with a CD diagnosis by counteracting gut chronic inflammation, maintaining clinical remission, and improving quality of life (De Conno et al., 2022). Several natural products are described in the literature as natural bioactive that is gaining an increasing role in treating chronic diseases such as colorectal cancer (Kuppusamy et al., 2014; Rossi, Mirbagheri, Keshavarzian, & Bishehsari, 2018; Shehzad, Lee, & Lee, 2013).

Nutraceutical products have shown promise in reducing the risk of colon cancer and slowing its progression by modulating cell signalling and apoptotic mechanisms, including BCL-2, K-ras, MMP, and immune responses (Gamallat et al., 2016; Hossain et al., 2022; Kuppusamy et al., 2014). Moreover, nutraceuticals are displaying potential as supplementary components in cancer treatment overall, with a specific focus on their role in CRC immunotherapy (Bhatt, Redinbo, & Bultman, 2017; Rossi et al., 2018). Natural products are employed in the context of colon cancer in three main ways: i) prevention, ii) supplementation, iii) and treatment. As

previously described, many natural products are well-known for their ability to impact cellular and molecular mechanisms associated with CRC development. They offer several mechanisms for potential cancer prevention. Among them, products rich in antioxidants, including fruits, vegetables, and herbs, due to polyphenols and carotenoids, have been reported to reduce the risk of developing CRC by neutralising free radicals that can damage DNA and lead to cancerous cell changes (Marino et al., 2023; Islam et al 2022). Moreover, substances like curcumin possess anti-inflammatory properties and help prevent chronic colon inflammation, a risk factor for CRC development and progression (Ojo et al., 2022). Bioactive compounds, like resveratrol, are reported to impact cell signalling pathways involved in CRC, including the Wnt signalling pathway (Ji et al., 2013). In addition, natural products may also exert their cancer-preventive effects through epigenetic mechanisms, such as DNA methylation and histone modification, potentially regulating gene expression and suppressing the development of cancerous changes in cells (Geng et al., 2023). Natural products also have the potential to act as supplements, enhancing the sensitivity of drugs (Guo et al., 2023). Alterations in gut microbiota are strongly associated with the initiation and progression of colorectal carcinogenesis. Some natural products, particularly dietary fibres, prebiotics, and probiotics are recognised to enhance gut microbiota composition and are used to prevent CRC and support gut health (Kvakova et al., 2022). Several studies support the hypothesis that natural products may offer a promising strategy in CRC treatment by influencing MicroRNAs (miRNAs) expression (Guo et al., 2023). Briefly, miRNAs are non-coding RNA molecules known to act as gene expression regulation in many conditions, including CRC (Chao et al., 2022). It has been recently reported that products like curcumin, lignan, rosemary extracts, grape seed extract, and walnuts have been found to alter the miRNA expression profile by promoting apoptosis, inhibiting CRC cell proliferation, and reducing invasion and migration of CRC cells, demonstrating their potential as therapeutic agents.

The overall beneficial effects make nutraceuticals attractive for individuals looking to optimise health and well-being.

Aims

Intestinal diseases are common and encompass many manifestations, including inflammation, fibrosis, and cancer. Despite the notable advances in managing gut disorders, CRC is still challenging, and no significant progress has been made in the development of anti-fibrotic therapies. Based on this background, the present PhD project aims to provide potential innovative therapeutic targets for CRC and intestinal fibrosis by studying the functional role of PEA and/or its primary degradative enzyme inhibitor, NAAA. To pursue our aims, we first evaluated the role of PEA on CRC cell proliferation, migration, and cell cycle and the in vivo model of sporadic colon cancer. More in-depth studies were also performed to investigate the functional role of NAAA (i.e. PEA main degradative enzyme whose inhibition can increase endogenous PEA levels) in CRC in vitro and in vivo by performing the AOM model and xenograft model, and analysis of its expression in primary tumoral colon biopsies. Finally, we explored the role of endogenous PEA (via NAAA inhibition by using AM9053, a selective and reversible inhibitor) i) in vitro on bone-marrow-derived macrophages (BMDM), ii) in vivo by performing a TNBS-chronic model of intestinal inflammation reproducing IF, iii) and in human clinically diagnosed IF intestinal samples.

Materials and Methods

1.1 Drugs and reagents

Ultra-micronized PEA (um-PEA, powder particle size <10 μm, with the following distribution: <6 μm, 99.9%; <2 μm, 59.6%; <1 μm, 14.7%; <0.6 μm, 2%, as described in patent EP2475352 A1, with text from patent WO2011027373A1) was kindly provided by Epitech Group (Saccolongo, Italy). AM9053 (10-isothiocyanatodecyl benzene) was synthesised following previously documented methods (Malamas et al., 2020). Azoxymethane (AOM) and 2,4,6-trinitrobenzenesulfonic acid (TNBS) were obtained from Sigma-Aldrich (Italy). All reagents for cell cultures were purchased from Sigma-Aldrich (Milan, Italy), Bio-Rad Laboratories (Milan, Italy). The vehicles used for in vivo (ethanol/Tween20/saline in a ratio of 1:1:8, 2 mL/kg) and in vitro (0.1% ethanol) experiments had no impact on the studied responses.

1.2 Patient samples

Biopsies of primary colon tumors were collected from n=19 CRC-patients and characterized by using the tumor–node–metastasis (TNM) classification, ranging from T2 to T4 (pT2 [n = 6], pT3 [n = 7], and pT4 [n = 6]). The areas of the intestinal mucosa, defined as 'healthy', refer to the adjacent non-tumoral zone of the same patients. The Ethical Committee of University of Naples Federico II granted ethical approval for human studies, and all participants provided written informed consent.

Ileocolonic biopsies were collected from surgical specimens of n=10 patients, admitted for ileocolonic resection due to a CD diagnosis associated with intestinal fibrosis. The areas of the intestinal mucosa, defined as 'non-stenotic', are referred to the adjacent non-stenotic zone of the same patients. The University approved human studies of Naples Federico II clinical research ethics committee and A.O.R.N. Antonio Cardarelli (approval number 252). All patients enrolled in this study provided written informed consent**.**

1.3 Gene expression across Normal and Tumor tissue (GENT) data analysis

Relative gene expression values were obtained from interrogating the Gene Expression across Normal and Tumor tissue (GENT2) database (Park et al., 2019), in which the NAAA relative transcript levels of CRC and healthy control samples were available. The query output values were divided into healthy (Accession ID: E-TAMB-118, E-TAMB-176, GSE4107, GSE4183, GSE7307, GSE8671, GSE9254, GSE9452, GSE9686, GSE10191, GSE10616, GSE11831, GSE13367, GSE13471, GSE14580, GSE15960, GSE18426, GSE19963, GSE20916,

GSE21510, GSE32323, GSE37267, GSE37364, GSE38713, GSE39397, GSE40220, GSE40967, GSE41328, GSE43346 and GSE62932; n = 397) and tumoral samples (Accession ID: GSE2109, GSE4107, GSE4183, GSE4554, GSE8671, GSE13067, GSE13294, GSE13471, GSE14333, GSE14580, GSE15960, GSE17536, GSE17537, GSE18088, GSE18462, GSE19860, GSE20916, GSE21510, GSE23194, GSE26027, GSE26682, GSE26906, GSE27157, GSE29623, GSE30540, GSE31595, GSE32323, GSE33114, GSE34489, GSE35144, GSE35452, GSE35603, GSE35896, GSE37364, GSE37892, GSE38832, GSE39084, GSE40367, GSE40967, GSE41328, GSE43576, GSE52847, GSE54483, GSE60697, GSE62080, GSE62932, GSE64258, GSE64857, GSE71222 and GSE73883; n =3775) to analyze the difference of NAAA expression level.

1.4 Mice

All the experimental procedures and protocols were carried out in conformity with national laws and policies approved by the Italian Ministry of Health and performed according to ARRIVE guidelines. Mice used for *in vivo* procedures were kept in polycarbonate cages under a 12 h light/12 h dark cycle. All the cages were supplemented with environmental enrichment. All blindly randomized mice were used after one 1-week of acclimation (temperature 23 ± 2 °C; humidity 60%, free access to water and food). Six to eight-week-old female BALB/c nude mice, six-week-old male CD1 background mice, female C57BL/6J mice, and male C57BL/6J mice, weighing 20–25 g, were purchased by Charles River (Sant'Angelo Lodigiano, Italy). All the animals were fed ad libitum with standard food, except for the 2 h immediately preceding the administration of 2,4,6-trinitrobenzene sulfonic acid (TNBS). Before euthanasia via carbon dioxide, all animals were anesthetized using enflurane inhalation. Every possible measure was taken to reduce the number of animals used and any discomfort they may have experienced.

1.5 Cell lines

1.5.1Colorectal cancer cell lines

For *in vitro* experiments, we used Caco-2 and HCT116 (ATCC from LGC Standards, Milan, Italy). Both were cultured in Dulbecco's modified Eagle's medium (DMEM) containing 10% fetal bovine serum (FBS), 100 U/ml penicillin and 100 μg/ml streptomycin, 1% non-essential amino acids, 2 mM L-glutamine and 1 M HEPES. Cell viability was evaluated by trypan blue exclusion. All the cell lines used were free from mycoplasma contamination.

1.5.2 Healthy colonic epithelial cells (HCEC)

HCEC were a kindly gifted from Fondazione Callerio Onlus (Trieste, Italy) and, according to the supplier's recommendations, were cultured in Dulbecco's modified Eagle's medium (DMEM) supplemented with 10% FBS, 100 Units/ml penicillin, 100 µg/ml streptomycin, 200 mM L-Glutamine, 100 mM Na-pyruvate and 1 M HEPES. Cell viability was evaluated by trypan blue exclusion. All the cell lines used were free from mycoplasma contamination.

1.5.3 Human intestinal myofibroblasts (CCD-18Co)

CCD-18Co (human intestinal myofibroblast cell line, from ATCC) were cultured in Eagle's Minimum Essential Medium (EMEM) (ATCC) containing 10% fetal bovine serum, 2.5% Hepes, and 100 U/ml penicillin– streptomycin, according to the supplier's recommendations, in presence of TGF-β (10 ng/ml) at 37°C in a humidified 5% CO2 atmosphere. Cell viability was evaluated by trypan blue exclusion. CCD-18Co were free from mycoplasma contamination.

1.5.4. Murine bone marrow-derived macrophages (BMDM)

Bone-marrow derived macrophages were obtained by flushing mouse femurs and tibias with macrophage culture medium (RPMI 1640) containing, according to the supplier's recommendations 100 U/ml of penicillin/streptomycin, 1 mM Hepes (pH 7.4), and 10% fetal bovine serum (FBS)] and filtered by using 70-µm cell strainer. Cells were cultered in RPMI-1640 medium supplemented with macrophage colony-stimulating factor (M-CSF) (50 ng/ml) at 37°C in a humidified 5% CO2 atmosphere. After 6 days, BMDM were reseeded and pretreated with the non-cytotoxic AM9053 concentration (1µM for 1 hour) and after that were stimulated with lipopolysaccharide (LPS) (10 ng/ml) for 3 hours. This pharmacological schedule was chosen to have the most effective IL-23 release (Mathur et al. 2019).

1.6 In vivo studies

1.6.1 AOM model of colorectal cancer

The effect of um-PEA and NAAA was evaluated in a murine model of chemically AOM-induced colon cancer. AOM (40 mg/kg in total, intraperitoneally (ip) was administered in CD1 mice (Charles River, Sant'Angelo Lodigiano, Italy) at the single dose of 10 mg/kg once per week for four weeks. Um-PEA at a dose of 10 mg/kg was given (ip) three times per week for the experiment, starting one week before the first administration of AOM to appreciate its chemopreventive effect. Um-PEA dose was selected based on previous published work which showed the in vivo selective pharmacological effect of PEA in the intestine. AM9053 (20 mg/kg, i.p.) (Alhouayek et al., 2015) was given intraperitoneally three times per week, starting 1 week before the first administration of AOM. All mice were humanely euthanized 12 weeks after the first injection of AOM. Based on our laboratory experience, this time (at the used dose of AOM) was associated with the occurrence of a significant number of aberrant crypt foci (ACF, which are considered preneoplastic lesions), polyps and tumors (Izzo et al., 2008). As previously reported, the detection and quantization of ACF, polyps and tumors on the colon were performed (Pagano et al., 2017).

1.6.2 Xenograft model

A tumor xenograft model of CRC was established using BALB/c nude mice (Charles River, Sant'Angelo Lodigiano, Italy). The effect of the NAAA inhibitor AM9053 was evaluated on tumor formation induced by the subcutaneous injection of HCT116 cells ($2.5x10^6$, 200-µl PBS) into the back of the mice. AM9053, at the dose of 20 mg/kg (Alhouayek et al., 2015), was given peritumoral three times per week, and .tumor size measured and calculated for all the duration of the experiment. At 15 days after treatment started, mice were humanly killed, and tumors were excised, photographed, weighed, and processed.

1.6.3 TNBS model of intestinal fibrosis

Intestinal fibrosis was induced according to the method described by Wirtz et al. in 2017. This involved the use of a hydroalcoholic solution of TNBS, which compromised the integrity of the intestinal wall and allowed TNBS to enter. A pre-sensitization phase was initiated to initiate this process, involving the topical application of 1% TNBS. Subsequently, TNBS was administered intrarectally (under inhalation anesthesia) once a week for six weeks, with a progressively increasing dosage scheme (0.75%, 1.5%, 2.5% v/v), using a specialized

polyethylene catheter with a 1 mm diameter. AM9053, a potent and selective NAAA inhibitor described by Romano et al. in 2022, was injected intraperitoneally (20 mg/kg) thrice weekly. The mice's body weights were monitored weekly, and the disease activity index (DAI) score, which evaluated stool consistency and the presence of blood, was assessed every two days. After the study, on the 49th day, all the mice were humanely euthanized by exposure to CO2, and their colons were removed, washed, weighed, measured for length, and stored at -80 °C for further analysis.

1.7 Endoscopic analysis

Endoscopic analysis was performed at time zero and at the final time (49^{th} day) of TNBS model of intestinal fibrosis to assess the degree of intestinal inflammation and fibrosis using a high-resolution mini endoscopy. All mice were anesthetized by subcutaneous injection of alfaxolone (5 mg/kg) and xylazine (5 mg/kg) and examined by using a mini-endoscope (Mainz COLOVIEW® System, Karl Storz, Germany). Scoring of fibrosis activity was expressed by the modified murine endoscopic index of colitis severity (MEICS) based on the following four parameters: (i) thickening of the colon, (ii) stool consistency, (iii) changes of the vascular pattern, and (iv) fibrin visible (Becker et al., 2005). Endoscopic grading was performed for each parameter (scores 0–3), leading to a cumulative score between 0 and 15.

1.8 Cell viability assays

1.8.1 MTT assay

Bone Marrow-Derived Macrophage (BMDM) cells viability was assessed using the 3-(4,5-dimethylthiazol-2-yl)-2,5-diphenyltetrazolium bromide (MTT) assay (Buranaamnuay, 2021). BMDM cells ($3x10^4$ cells seeded in a 96-well plate), were pr-treated with AM9053 (0.03-10 μM) for 1h, then stimulated with LPS (50 ng/mL) for 3h and finally were incubated with MTT solution for 1 hour at 37°C. Subsequently, dimethyl sulfoxide (DMSO) was added to dissolve the formazan crystals, and the absorbance was measured at 570-590 nm using an iMarkTM microplate reader from Bio-Rad, located in Segrate, Italy.

1.8.2 Neutral Red

HCT116, CaCo2, and HCEC (1.5×10^4 cells density were seeded in a 96-well plate) cell viability was assessed by measuring the neutral red uptake (NR assay) as previously described (Romano et al., 2014). Cells were treated or not with AM9053 (0.1-3 uM, 24h) and were

incubated with NR dye solution (50 μg·ml−1 in 10% FBS) for 3 h at 37°C and then lysed with 1% acetic acid. The absorbance was read at 532 nm (iMarkTM microplate reader, Bio-Rad, Segrate, Italy). All results are expressed as percentage of cell viability. CCD-18Co ($4x10^3$ cells seeded in a 96 well plate) treated or not with AM9053 (0,03–10 μM) were incubated with NR dye solution (50 μg/ml in 10% FBS) for 3 h at 37°C and then lysed with 1% acetic acid. The absorbance was read at 532 nm (iMarkTM microplate reader, Bio-Rad, Segrate, Italy). All results were expressed as a percentage of cell viability.

1.9 BrdU Proliferation assays

Exogenous PEA experiments

HCT 116, Caco-2, HCEC were seeded in 96-well plates (1.0×10^4 cells per well), allowed to adhere (within 24 h) and starved by serum deprivation for 18 h. Tumoral and no-tumoral cells were all treated with um-PEA (1–30 μM). After 24, 48 and/or 72 h of treatment, pulsing cells were incubated with BrdU (10 μM) in the cell medium for 2 h. After that, the cells' proliferation was determined using the BrdU proliferation ELISA kit (Roche, Milan, Italy) according to the manufacturer's instructions. um-PEA antiproliferative effect (used at the submaximal concentration 10 μM) was also assessed (in HCT116 cells) in the presence of GW6471 (3 μM, PPARα antagonist); ML191 (1 μM, GPR55 antagonist); 5′-iodoresiniferatoxin (0.1 μM, TRPV1 antagonist); AM251 and AM630 (both 1 μM, CB1 and CB2 antagonist, respectively) (Alexander et al., 2019) [all from Tocris, Rodano, Italy and incubated 30 min before um-PEA (10 μM)]. All results are expressed as a percentage of cell proliferation.

NAAA inhbition experiments

HCT 116, Caco-2, HCEC, siNAAA-HCT116, and CCD-18Co (cultured under TGF-beta stimulation) were seeded in 96-well plates (1.0×10^4 cells per well), allowed to adhere (within 24 h) and starved by serum deprivation for 18 h. After 24 hours of no-cytotoxic AM9053 treatment (0.1-3 μM [HCT116], 3 μM [Caco-2, HCEC, an siNAAA-HCT116], and 0.03–1 μM [CCD-18 Co]), pulsing cells were incubated with BrdU (10 μM) in the cell medium for 2 h. After that, the BrdU proliferation ELISA kit (Roche, Milan, Italy) was performed according to the manufacturer's instructions. Using this assay, the antiproliferative effect of AM9053 was evaluated (in HCT116 cells) in the presence of GW6471 (3 μM, PPAR-α antagonist), 50 -iodoresiniferatoxin (0.1 μM, transient receptor potential vanilloid 1 [TRPV1] antagonist), and AM251 and AM630 (both 1 μM, CB1 and CB2 receptor antagonists, respectively) (Alexander

et al., 2021)(all from Tocris, distributed by Bio-Techne, Milan, Italy) and incubated 30 min before AM9053 (3 μM). The results are expressed as a percentage of cell proliferation.

1.10 Cell Cycle Analysis

Cell cycle analysis was performed according to BD Pharmingen™ BrdU Flow Kit (BD Biosciences, San Jose, CA USA) and conducted on HCT116 cells (1.5×10^5 cells seeded in a 6-well plate), overnight serum deprived and treated or not with um-PEA (30 μM) for 24 h, and HCT116 cells and/or siNAAA-HCT116 (1.5×10^5 cells seeded in a six-well plate), overnight serum deprived and treated or not with AM9053 (3 μM) for 24 h. Cells were revealed using BriCyte flow cytometer (Mindray, Trezzano sul Naviglio Italy), gated based on forward and side scatter to separate debris. Then the cellular events were further gated based on their BrdU and 7-AAD content. Data were analyzed by FlowJo v10 software (Tree Star, Ashland, OR, USA) and expressed as fold change of the cells in each cell cycle phase.

1.11 Scratch assay

Exogenous PEA experiments

Sub-confluent HCT116 and Caco-2 cell lines were trypsinized and plated on a 2-well culture-insert (ibidi GmbH, Gräfelfing, Germany) inserted on a 24-well plate (5 × 104 cells/70 μL) and left to adhere overnight. After this time, the insert was removed, and cells were washed with phosphate buffer saline (PBS 1×) and treated with mitomycin C 30 μg/mL (Sigma-Aldrich, Milan, Italy) in serum-free media to inhibit cell proliferation completely. After 2 h, tumoral cells were treated with um-PEA (30 μM) for 24 h. Wound area recovery was observed under a phase-contrast microscope (Leica, Wetzlar, Germany) and photographed at the time zero point (right after the mitomycin C removal) and after 24 h of treatment. Successively, by using the ImageJ software, the size of the opened area was measured from the digital images. The results are expressed as % of scratch closure (time zero/time 24 h × 100). Two images were acquired for each well, and at least 3 replicates were analyzed for each treatment. Four independent experiments were independently carried out.

NAAA inhbition experiments

The scratch assay was performed on subconfluent HCT116 and/or Caco-2 trypsinized and plated on μ-Dish 35-mm culture inserts (ibidi GmbH, Gräfelfing, Germany) ($5x\ 10^4$ per 70 μl per area). After 24 h, sterile tweezers gently removed inserts and a scratch was made in the

monolayers. Cells were then incubated with mitomycin C 30 μg/ml (Sigma-Aldrich, Milan, Italy) in serum-free media to inhibit cell proliferation. After 2 h, CRC cells were treated with AM9053 (3 μM, 24 h). Using this assay, the effect of AM9053 on HCT116 cell migration was also evaluated in the presence of GW6471 (3 μM, PPAR-α antagonist), 50 -iodoresiniferatoxin (0.1 μM, TRPV1 antagonist), and AM251 and AM630 (both 1 μM, CB1 and CB2 antagonists, respectively) (all from Tocris, distributed by BioTechne, Milan, Italy) and incubated 30 min before AM9053 (3 μM). Wound area recovery was observed under a phase-contrast microscope (Leica, Wetzlar, Germany) and photographed at Time 0 point (right after the mitomycin C removal) and after 24 h from the pharmacological treatment. The size of the opened area was measured by Fiji (NIH) software. Two images were acquired for each well, and at least three replicates were analysed for each treatment. The results are expressed as % of scratch closure (Time 0 area - 24h area⁄Time 0 area * 100).

1.12 Transfection

HCT116 cells ($1.5x10^5$ cells seeded in a six-well plate) were transfected with siRNA for NAAA (Trilencer-27 siRNA duplex, OriGene, Rockville, MD, USA) (10 nM) and/or a standard negative control (5 nM), resuspended in MegaTran 2.0 Transfection Reagent (OriGene, Rockville, MD, USA) and Opti-MEM® (Thermo Fisher Scientific, Waltham, MA, USA) in a total volume of 100 μl and added drop by drop to cells for 4 h. The transfection was then stopped by adding DMEM supplemented with 20% FBS overnight and replaced with complete culture medium incubated at 37ºC, 5% CO2 for 48 h. Silencing efficiency was controlled by performing RT-PCR, and the obtained siNAAA-HCT116 was used as a due.

1.13 Gene expression analysis by quantitative Real-Time q-PCR

RNAs were extracted from a) murine colons derived from the in vivo model of CRC (xenograft model and AOM model) and from in vivo model of intestinal fibrosis chemically induced by TNBS; b) bone marrow-derived macrophages and c) human intestinal fibrosis biopsies. Human and murine tissues were later collected and stored in RNA to stabilize and store RNAs (Thermo Fisher Scientific, USA). RNAs were extracted from a) homogenized mice colon tissue by using FastPrep™ (MP Biomedical, USA) in Purezol Reagent (Biorad, Milan, Italy); b) colorectal cancer cells, human healthy cell line, and BMDM in Purezol Reagent; and c) human colon biopsies (from CRC patients and fibrotic patients) by using RNeasy®Mini Kit (Qiagen, Germany), all according to the manufacturer's protocol. RNA's quantification and quality analysis was performed using a NanoDrop™ One C spectrophotometer (Thermo Fisher

Scientific, USA). Retro-transcription was performed using the High-Capacity cDNA Reverse Transcription Kit (Applied Biosystem, USA). Reverse transcription polymerase chain reaction (RT–qPCR) was performed using Fast SYBR^{TM} Green Master Mix (Applied Biosystem, USA). Target gene expression calculation was normalized to the reference housekeeping gene glyceraldehyde-3-phosphate dehydrogenase (GAPDH) and expressed using the 2-ΔCt formula.

1.14 Western blot analysis

Exogenous PEA experiments

Western blot analysis was performed to investigate the expression of cyclin B1, CDK1, MMP2 and TIMP1 in the HCT116 tumoral cell line alone or the presence of um-PEA (30 μM, 24 h). Cells were lysates in RIPA buffer (10 mM Tris-Cl (pH 8.0), 1 mM EDTA, 140 mM NaCl, 1% Triton X-100, 0.1% (v/v) sodium deoxycholate, 0.1% SDS) supplemented with protease (Roche, Monza, Italy) and phosphatase inhibitors (Sigma-Aldrich, Milan, Italy). Forty micrograms of protein extract was fractionated by 12% SDS-PAGE according to the manufacturer's protocols (Bio-Rad, Milan, Italy). After incubation with 5% (w/v) non-fat milk in TBS-T (10 mM Tris, pH 8.0, 150 mM NaCl, 0.5% (v/v) Tween-20) for 60 min, the membranes were incubated overnight with anti-Cyclin B1 (1:2000, Cell Signaling, Danvers, MA, USA), anti-CDK1 (1:1000, Invitrogen, Carlsbad, CA, USA), anti-MMP2 (1:1000, Invitrogen, Carlsbad, CA, USA) and anti-TIMP1 (1:200, Invitrogen, Carlsbad, CA, USA). After that, anti-mouse IgG secondary antibodies (1:3000, Cell Signaling, Danvers, MA, USA), linked to horseradish peroxidase, were added. The signal was visualized by enhanced chemiluminescence using Chemidoc XRS (Biorad, Milan, Italy) and analyzed using Image Lab version 6.10.7. α-tubulin (1:1000, Cell Signaling, Danvers, MA, USA) was used as housekeeping normalizing protein.

NAAA inhbition experiments

Xenograft samples derived from tumor-bearing mice, treated or not with AM9053, were pounded in liquid nitrogen and lysed in RIPA buffer (10-mM Tris–Cl [pH 8.0],1-mM EDTA, 140-mM NaCl, 1% Triton X-100, 0.1% [v/v] sodium deoxycholate and 0.1% SDS) supplemented with protease (Roche, Monza, Italy) and phosphatase inhibitors (Sigma-Aldrich, Milan, Italy); 50 μg of protein extracts was fractionated by 8% SDS-PAGE according to the manufacturer's protocols (Bio-Rad, Segrate, Italy). After incubation with 5% (w/v) non-fat milk in TBS-T (10-mM Tris, pH 8.0, 150-mM NaCl and 0.5% [v/v] Tween 20) for 60 min, the

membranes were incubated overnight with fresh PathScan® Multiplex Western Cocktail (Rabbit, 1:1000, Cell Signalling, Catalogue Number 5301, Danvers, MA, USA), and after that, fresh secondary antibody anti-rabbit IgG (1:2500, Promega, Catalogue Number S3731, Milan, Italy), linked to HRP, was added. The signal was visualized by enhanced chemiluminescence using Chemidoc XRS (Bio-Rad, Segrate, Italy) and analysed using Quantity One Software Version 4.6.8. Ras-related protein (Rab-11) was used as housekeeping normalizing protein.
Moreover, whole-cell lysates were obtained from BMDM cell line or tissue lysed with RIPA buffer (50 mM Tris–HCl, pH 7.4, 150 mM NaCl, 1% NP-40, 1 mM EDTA, 0.25% sodium deoxycholate, 1 mM NaF, 10 μM Na_3VO_4, 1 mM phenylmethylsulfonylfluoride, 10 μg/ml aprotinin, 10 μg/ml pepstatin, 10 μg/ml leupeptin) as previously described (Ammendola, Parisi, Esposito, & Cattaneo, 2021). Bio-Rad protein assay was used to determine proteins concentration (BioRAD, Hercules, CA, USA). Forty micrograms of whole lysates were resolved on 10% SDS-PAGE and proteins were transferred by blotting onto PVDF membranes. Membranes were incubated with anti-phospho-STAT3 Y705 antibody from Cell Signalling Technology (Cat. 9131) (Denvers, MA, USA) or anti-NAAA antibody from MyBiosource (Cat. MBS2001655) (San Diego, CA, USA) and probed with appropriate horseradish peroxidase-conjugated secondary antibodies from Bioss Antibodies (Woburn, MA, USA). Proteins were visualized by enhanced chemiluminescence reagent (Amersham Biosciences, Buckinghamshire, UK) and were quantified using densitometry (Chemidoc, Bio-Rad). The same filters were re-probed with an anti-tubulin antibody from Santa Cruz Biotechnology (Cat. sc-5274) (Irvine, CA, USA) to normalize the amount of loaded proteins**.**

1.15 Tumor secretome collection

Tumor-bearing nude mice treated or not with the NAAA inhibitor AM9053 (20 mg/kg) were killed with enflurane/CO2 15 days after treatment started, tumors were excised and cultured in DMEM, without FBS, for 24 h. The conditioned mediums were collected and added to HCT116 or Caco-2 cells for 24 h at 37ºC. After that, CRC cells were washed in PBS and used for further analyses.

1.16 Oncogenic array

Tumor secretomes collected (as above stated) from tumor-bearing nude mice, treated or not with AM9053, were analyzed by using the oncogenic array Proteome Profiler Human XL Oncology Array Kit (R&D Systems, Minneapolis, MN, USA) following the manufacturer's instructions.

1.17 DNA Fragmentation Assay

HCT116 cells were seeded in 10 cm culture dishes (5×10^5 cells per well), allowed to adhere (within 24 h) and starved for 18 h. Then, cells were treated with vehicle or um-PEA (30 μM). After 24 h of treatment, cells were washed twice in PBS, and incubated in DNA-lysis Buffer (50 mM Tris pH 7.5, 100 mM NaCl, 5 mM ethylenediaminetetraacetic acid, 1% sodium dodecyl sulphate, 0.5 mg/mL proteinase K) for 1 h at 55 ◦C before extraction with phenol/chloroform/isoamyl alcohol. The suspension was then centrifuged (4000 rpm) for 5 min. DNA was precipitated with 1 volume of 5 M NaCl and 2.5 volumes of 95% (v/v) ethanol. The isolated DNA was resolved on a 1.5% agarose gel containing GreenSafe DNA Gel Stain (Canvax, Cordoba, Spain) in 40 mM Tris-acetate-EDTA buffer with electrophoresis at 80 V for 30 min. DNA fragments were visualized and photographed under ultraviolet light using Chemidoc XRS (Biorad, Milan, Italy).

1.18 Enzyme-linked immunosorbent (ELISA) assay

ELISA assay was performed from supernatants of BMDM 1 h pre-treated or not with AM9053 (1μM) before LPS (10 ng/ml) exposure for 3 hours. According to the manufacturer's instructions, the murine IL-23 was detected using the ELISA kit protocol (R&D, Minneapolis, USA). Data were expressed as the pg/mL of cytokine quantity.

1.19 Histological Analyses

1.19.1 Haematoxylin-Eosin Staining

Haematoxylin-Eosin (H&E) staining was performed using formaldehyde fixed tissues, dehydrated in a series of ethanol solutions, and embedded in paraffin to visualize colon anatomy. To pursue our aim, 5 μm thick sections were dewaxed in xylene for 10 minutes followed by dehydration in graded alcohol. According to the literature, colon sections were treated with hematoxylin for 8 minutes and eosin for 2 minutes, rinsed, dehydrated in alcohol, cleared with xylene, and mounted. Histological evaluation was performed under a light microscope (Leica, Germany), and images were captured using a 10X objective.

1.19.2 Masson’s Trichome Staining

Masson’s Trichome staining was performed using formaldehyde-fixed tissues, dehydrated in ethanol solutions, and embedded in paraffin to ascertain collagen deposition. 5 μm thick colon sections were first hydrated and incubated in Bouin’s Solution at 56°C for 15 minutes, then

staining with Weigert's Iron Haematoxylin solution for 5 minutes. Subsequently, slides were immersed in Phosphotungstenic/Phosphomolybdic acid solution for 5 minutes, Aniline Blue Solution for 5 minutes, and 1% Acid Acetic for 2 minutes.
After staining, slides were rinsed, dehydrated in alcohol, cleared with xylene, and mounted. Slides were examined under a light microscope (Leica, Germany), and images were captured using a 10X objective.

1.20 Immunofluorescence evaluation

Immunofluorence on frozen tissues

Frozen sections (10 μm) in Cryobloc Compound (Diapath, Martinengo, Italy) of tumor explanted from xenograft tumor-bearing mice, treated or not with the NAAA inhibitor AM9053 (20 mgkg1, peritumorally), were fixed in 4% paraformaldehyde and then blocked with PBS containing 2% BSA, 2% goat serum and 0.1% Triton (all from Sigma-Aldrich, Milan, Italy) for 60 min at room temperature and incubated overnight at 4ºC with the human anti-Ki67 (1:400, Abcam, Cambridge, UK). All sections were then incubated for 30 min at room temperature with Alexa Fluor 594-conjugated goat anti-rabbit IgG (1:1000; Jackson ImmunoResearch, Cambridge, UK), followed by incubation for 5 min at room temperature with DAPI (1:25,000; Invitrogen, Waltham, MA, USA). Sections were mounted with glycerol (Sigma-Aldrich, Milan Italy) and acquired/analysed using Axio Imager M2P combined with the high-end fluorescence imaging system ApoTome.2 (Zeiss, Jena, Germany). Images were acquired with an objective of 20x.

Immunofluorence on paraffin-embedded tissues

Slides of colon tissue (5 μm) were deparaffinized with xylene and rehydrated with decreasing gradient alcohol. Antigen retrieval was carried out through pressure-cooking slides for 3 min in the Diva Decloaker solution 10X (Biocare Medical, CA, USA). The slides were treated for 2 h in 5% albumin bovine serum (BSA) in PBS to avoid non-specific interactions of antibodies. Immunostaining was performed by incubation overnight with anti-α-SMA (1:100, Alexa Fluor®488, Cat. AB124964, Abcam) at 4°C. The slides were mounted on microscope slides by Mounting Medium (Cat. AB104135, Abcam) and then counterstained with DAPI (Cat. AB228549, Abcam) for nuclear staining. The images were acquired at room temperature and detected under 40X magnification using a laser-scanning confocal microscope with an

AiryScan2 module (Zeiss, LSM 900, Germany). Three fields for each colon were analyzed by Zeiss Zen Blue edition software.

1.21 Flow cytometry

Lymphocytes isolated from MLNs were washed in FACS buffer (PBS containing 1% BSA and 0.02% NaN_2) and stained directly with the following conjugated antibodies: CD3 (1:200, clone 17A2), CD4 (1:200; clone GK1.5; BioLegend), CD8 (1:200; clone 5H10-1; BioLegend), CD25 (1:200; clone 3C7; BioLegend) for 60 min at 4°C. After washing, cells were fixated, permeabilized, and stained intracellularly with IFN-γ (1:200; clone XMG1.2, Cat. no:505807; BioLegend), IL-4 (1:200; clone clone 11B11, Cat. no:504103; BioLegend), IL-17A (1:200; clone TC11-18H10.1; BioLegend) and FoxP3 antibody (1:200; clone MF-14; BioLegend). Th1, Th2, Th17 and regulatory T cells (Treg) populations were defined as $CD4^+INF\text{-}\gamma^+$, $CD4^+IL\text{-}4^+$, $CD4^+IL\text{-}17^+$ and $CD4^+CD25^+FoxP3^+$ cells respectively (Vellecco et al., 2023). At least 1×10^4 cells were analysed per sample, and positive and negative populations were determined based on the staining obtained with related IgG isotypes. Flow cytometry was performed on BriCyte E6 flow cytometer (Mindray Bio-Medical Electronics, Nanshan, China) using MRFlow and FlowJo software operation (Raucci et al., 2022).

1.22 Hydroxyproline assay

Hydroxyproline concentration is determined by the reaction of oxidized hydroxyproline with 4-(dimethylamino) benzaldehyde, which results in a colorimetric (560 nm) product proportional to hydroxyproline content, a significant component of collagen. The hydroxyproline kit assay (Merck, Milan, Italy) was conducted by following manufacturer instructions on human biopsies to ascertain fibrosis. Results were expressed as absorbance values at 560 nm.

1.23 Analysis of AEs Levels by LC-APCI-MS

Frozen tissues derived from xenograft murine tumors, murine colonic samples, and human specimens were homogenized in a solution of chloroform/methanol/TRIS-HCl 50 mM, pH 7.4 (2:1:1, by vol), containing 5 pmol of $[^2H]_8$-AEA, 50 pmol of $[^2H]_4$-PEA and $[^2H]_2$-OEA (Cayman Chemicals, Vinci, Italy) as internal standards. The extracts were purified by open-bed chromatography on silica gel. The eluted fractions (90:10 by vol) containing AEA, PEA, and OEA were analysed by liquid chromatography–atmospheric pressure chemical ionization–mass spectrometry (LC-APCI-MS) by using a Shimadzu (Shimadzu, Kyoto, Japan) HPLC apparatus (LC-10ADVP) coupled to a Shimadzu (LCMS-2020) quadrupole MS via a Shimadzu APCI

interface. LC-APCI-MS analyses of AEA, PEA and OEA were performed in the selected ion-monitoring (SIM) mode (Di Marzo et al., 2001; Marsicano et al., 2002), using m/z values of 356 and 348 (molecular ion + 1 for deuterated and undeuterated AEA), 304 and 300 (molecular ion + 1 for deuterated and undeuterated PEA), and 328 and 326 (molecular ion + 1 for deuterated and un-deuterated OEA). The AEA, PEA and OEA levels were determined based on their area ratio with the internal standard signal areas to provide the amounts in pmol per milligram of lipid extract.

1.24 Statistical analyses

The study was designed to generate groups of equal size, using randomization and blinded analysis. All data were expressed as mean ± SEM and GraphPad Prism 8 software (USA) was used for statistical analysis. The D'Agostino and Pearson (≥8n per group) or Shapiro–Wilk (≤8n per group) tests were used to determine if a data set was well modelled by a normal distribution or not. Data were tested using unpaired, paired Student's t-test and/or Mann-Whitney test to determine differences between the two group's comparisons. For multiple group comparisons, data were compared via one-way analysis of variance (ANOVA) with Dunnett's post hoc test and/or Tukey's post hoc test analysis. Nonnormal data were compared via Kruskal–Wallis with Dunn's test. Two-way ANOVA was used to compare different concentration–effect curves, followed by Bonferroni's test. Post hoc tests were run only when F achieved $P < 0.05$ and there was no variance inhomogeneity. A p-value<0.05 was considered significant.

Results

Chapter 1: Role of Palmitoylethanolamide in Colorectal Cancer (CRC)

1.1 PEA selectively inhibits colon cancer cell proliferation rate

To investigate the functional role of PEA in colon carcinogenesis, we evaluated the effect of um-PEA treatment on cell proliferation, using BrdU assay, up to 96 hours of treatment. We first exposed HCT116 cells at um-PEA (1-30 μM). Our results revealed that um-PEA (1–30 μM) treatment reduced, in a concentration-dependent manner, the proliferation rate up to 96 hours of exposure (Figure 12 A–C). Noteworthy, 30 μM um-PEA treatment significantly reduced cell proliferation after 24 h compared with the other timepoints (Figure 12 D). We also evaluated whether um-PEA treatment improved cell proliferation rate of non-metastatic Caco2 (Figure 12 E). Data showed that um-PEA treatment could also reduce the proliferation of these cells. Of prominence, um-PEA treatment did not influence HCEC proliferation in any concentration tested, suggesting a cancer cells-selective action (Figure 12 F).

1.2 PEA exerts the antiproliferative effect in CRC cell lines

We further explored antiproliferative mechanisms of action of um-PEA on HCT116 cells. With this purpose, we exposed HCT116 to um-PEA submaximal concentration (10 uM for 24h) in the presence of selective antagonists of its primary target (i.e., GW6471 (PPARα antagonist), 5'-iodoresiniferatoxin (TRPV1 antagonists), ML191 (GPR55 antagonist), AM251 (CB1 antagonist) and AM630 (CB2 antagonist) (Alexander et al., 2019). The antiproliferative effects of PEA were partially counteracted by PPAR-α and GPR55 selective antagonists, suggesting their involvement in the PEA mechanism of action (Figure 13).

1.3 PEA triggers cell cycle arrest by inducing DNA damage

Next, we addressed whether um-PEA would affect HCT116 cell-cycle progression using BrdU/7-AAD staining. Um-PEA treatment (30 μM for 24 h) resulted in an accumulation of cells in G2/M phase with a significant reduction in the number of cells in the S phase by flow cytometry analysis (Figure 14 A-B). Since cyclin B1/CDK1 complex expression is a well-known complex that regulates G2/M phase, we evaluated whether um-PEA could influence this complex. Our results revealed that um-PEA treatments increase protein and gene expression of the cyclin B1/CDK1 complex (Figure 14 C-D). It is well known that an arrest of the G2/M checkpoint accompanies the induction of DNA damage. Since PEA induced cell-cycle arrest in

the G2/M phase, we evaluated if um-PEA treatment could cause DNA damage of CRC cells by DNA fragmentation assay. As agarose gel electrophoresis showed, there is a functional correlation between cell cycle arrest in G2/M and the induction of DNA damage following um-PEA treatment (30 μM, 24 hours) (Figure 14 E).

1.4 PEA impact colon cancer cell migration

Migration is a well-established cancer cell's ability to disseminate from the primary tumor site, spreading tumor cells to other body parts. Considering the above discussion, we investigated whether um-PEA treatment could influence HCT116, and Caco-2 cell migration by performing a scratch analysis assay. Um-PEA treatment significantly reduced the proliferation rate of HCT116 cells after mitomycin C pre-treatment (Figure 15 A). We next focused on crucial matrix metalloproteinases (MMPs) expression and protein tissue inhibitor matrix metalloproteinase 1 (TIMP1), critical molecules related to cancer disease progression. As corroborated by data, um-PEA treatment impacted MMP-2 and TIMP-1 gene and protein levels in the HCT116 cell line (Figure 15 B-C). Um-PEA treatment also significantly reduced the proliferation rate of Caco-2 cells after mitomycin C pre-treatment (Figure 15 D). Finally, we investigated whether um-PEA could affect expression of other pertinent genes involved in the process of epithelial-mesenchymal transition (EMT, which is one of the primary processes that lead to the invasion and migration of epithelial cells involved in the progression of cancer (Song et al., 2016); these include the zinc finger proteins SNAI1 and SNAI2 (SLUG), twist family BHLH transcription factor 1 (TWIST), transforming growth factor beta (TGF-β), E-cadherin, and vimentin (Figure 16 A-F). As corroborated by data, um-PEA did not affect the EMT gene's expression. All our results indicate um-PEA's function in lowering both tumor growth and tumor cell migration.

1.5 PEA inhibits tumor development in AOM-sporadic model of CRC

To further investigate on um-PEA effect in vivo, we used the Azoxymethane (AOM)-mouse model of colon cancer (Neufert et al., 2007). When the carcinogenic agent AOM was administered alone, it most likely caused of aberrant crypt foci (ACF) (Figure 17 A), polyps (Figure 17 B) and tumors (Figure 17 C). According to our findings, um-PEA (10 mg/kg), administered intraperitoneally every two days for 13 weeks, dramatically decreased both the overall number of tumors (Figure C) and the number of AOM-induced ACF preneoplastic lesions (Figure 17 A). Um-PEA showed a tendency to decrease the number of polyps as well

(35.63% inhibition), however, this trend was not statistically significant (Figure 17 B). Based on our findings, we determine that the administration of um-PEA is efficient.

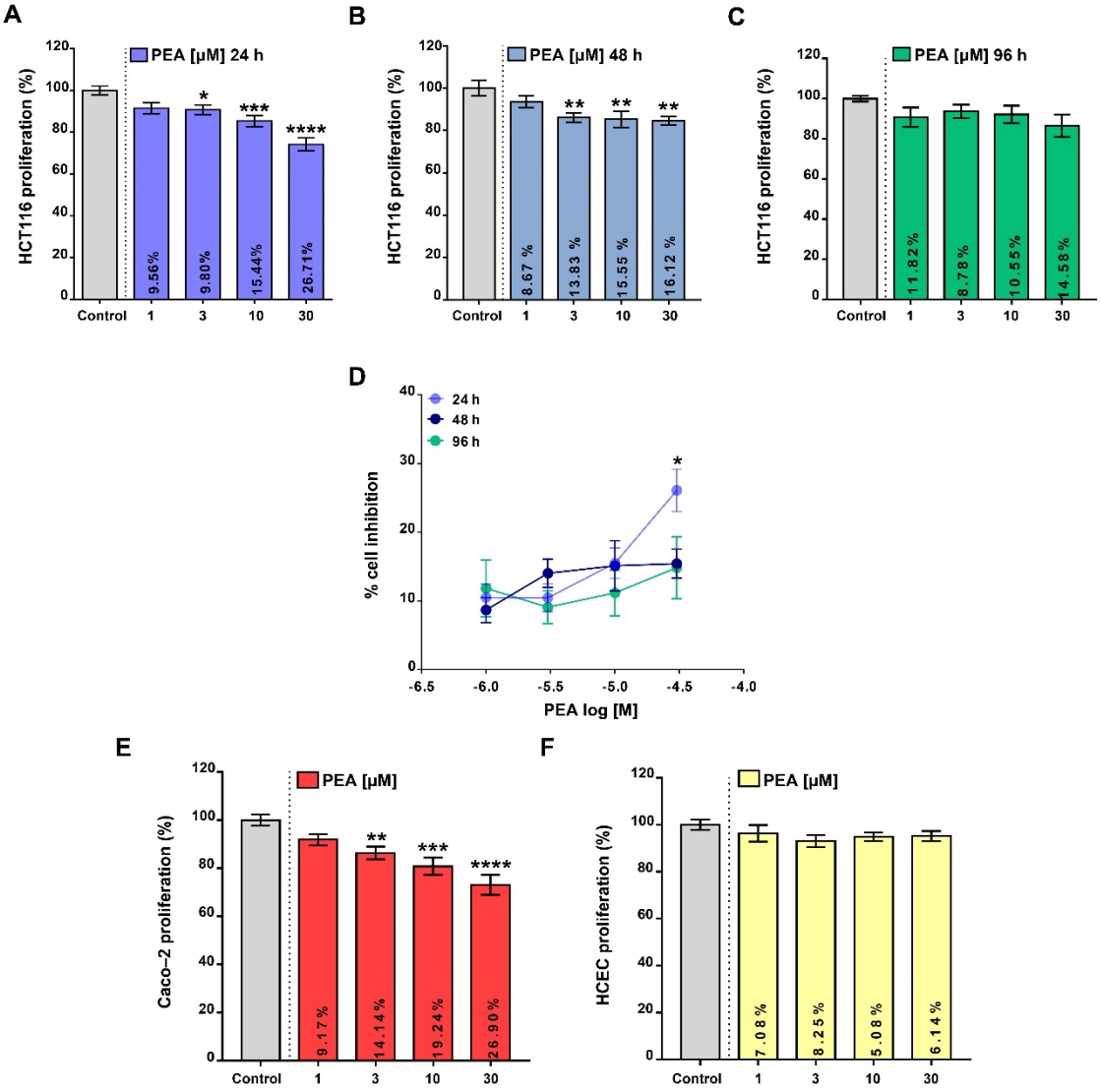

Figure 12. Palmitoylethanolamide impacts tumor cell proliferation. Cell proliferation rate of the colorectal cancer cell line HCT116 alone or in the presence of ultramicronized palmitoylethanolamide (PEA, 1–30 µM) for 24 **(A)**, 48 **(B)** and 96 h **(C)**. In **(D)** the effect of the time course of PEA pharmacological treatment (up to 96 h) is reported, expressed as a percentage of cell proliferation inhibition. * $p < 0.05$ vs. 48 and 96 h as assessed by two-way ANOVA. Effect of PEA treatment (1–30 µM for 24 h) on Caco-2 cells **(E)** and human healthy colonic epithelial cells (HCEC) **(F)**. All the data are expressed as a percentage of cell proliferation (n = 3 or 5 independent experiments). Inserted into the columns, the means of the % of cell proliferation inhibition versus the control are reported. All the values are expressed as means ± SEM; * $p < 0.05$, ** $p < 0.01$, *** $p < 0.001$ and **** $p < 0.0001$ vs. control, as assessed by one-way ANOVA followed by Dunnett's multiple comparisons.

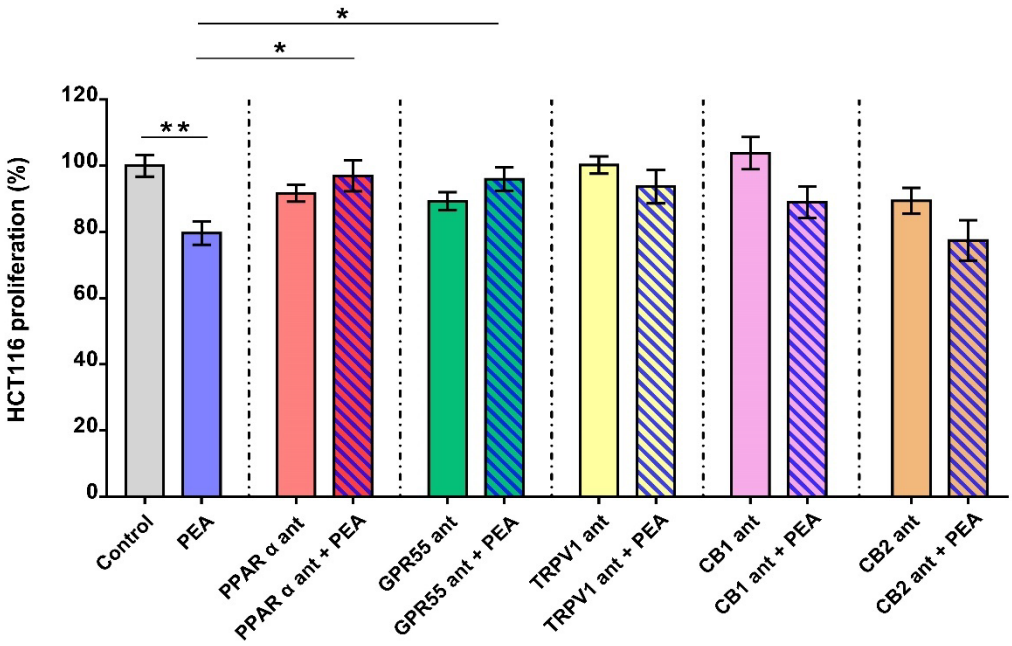

Figure 13. Palmitoylethanolamide's pharmacological mechanism of action. Antiproliferative effect of the submaximal concentration of ultramicronized palmitoylethanolamide (PEA, 10 μM, 24 h) evaluated in the presence of GW6471 (3 μM, PPARα antagonist, red column); ML181 (10 μM, GPR55 antagonist, green column); 5′-iodoresiniferatoxin (0.1 μM, TRPV1 antagonist, yellow column); AM251 (1 μM, CB1 antagonist, pink column) and AM630 (1 μM, CB2 antagonist, orange column). All results are expressed as percentage of cell proliferation (n = 4 independent experiments) and as means ± SEM; ** $p < 0.01$ vs. control; * $p < 0.05$ vs. PEA as assessed by one-way ANOVA followed by Tukey multiple comparisons test.

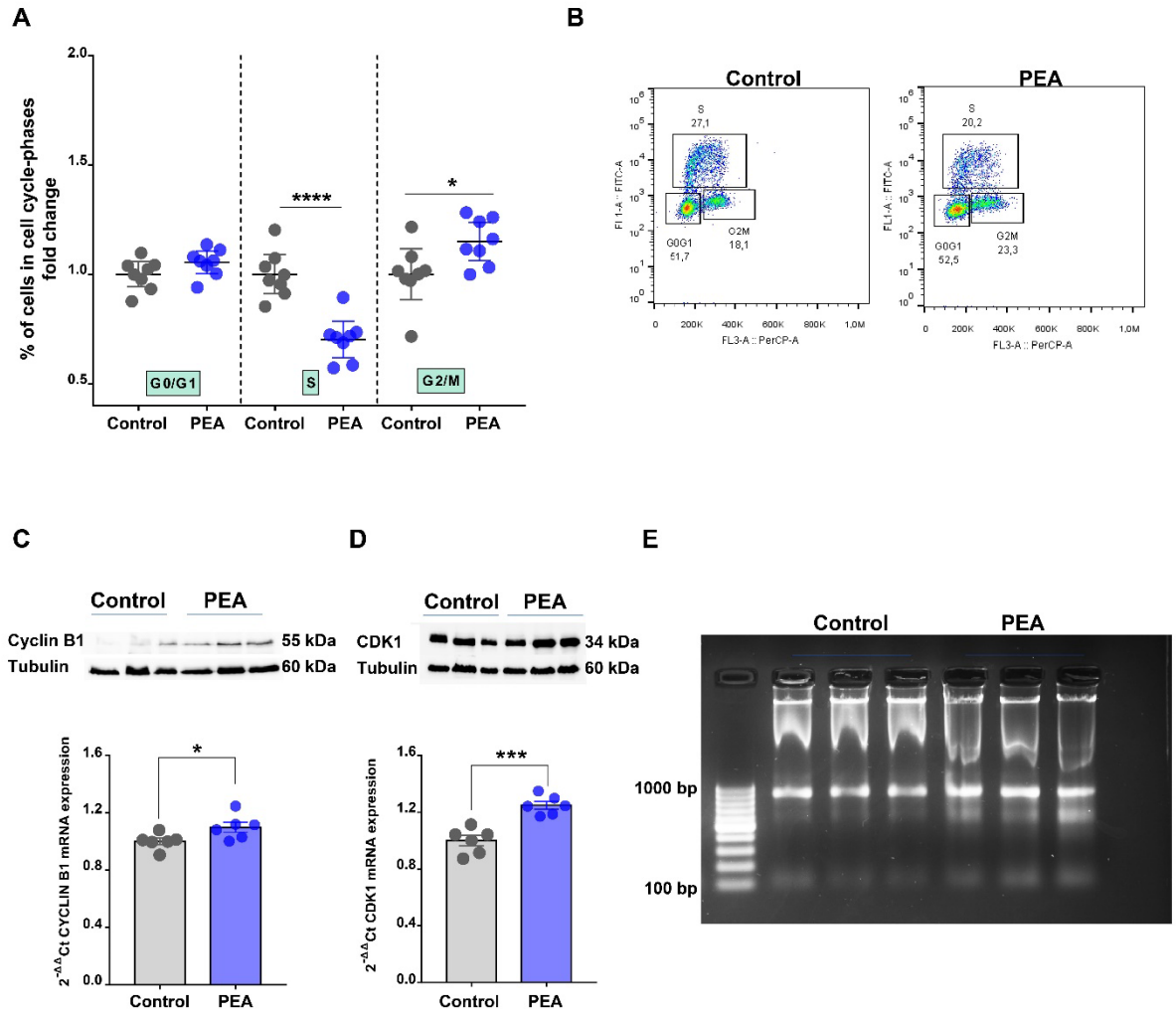

Figure 14. Palmitoylethanolamide induces cell cycle arrest. (A) Cell cycle analysis of HCT116 cells treated or not with ultramicronized palmitoylethanolamide (PEA, 30 µM, 24 h) by flow cytometry. Results are expressed as fold change of the cells in each cell cycle phase (n = 8). Values are expressed as means ± SEM; * $p < 0.05$ and **** $p < 0.0001$ vs. control (Student's t-test). **(B)** Representative density plots and cell percentage indicate the G0/G1, S and G2/M phase distribution of HCT116 cells treated with um-PEA (30 µM, 24 h). **(C)** Gene and protein expressions of cyclin B1 and **(D)** cyclin-dependent kinase 1 (CDK1) in HCT116 cells, alone or in the presence of PEA (30 µM, 24 h). Gene expression was measured by reverse transcription quantitative polymerase chain reaction (RT-qPCR) and calculated using the 2-ΔΔCt formula (n = 6). In contrast, protein expression was evaluated by Western blot analysis and normalized to the housekeeping protein α-tubulin (n = 3). Values are expressed as means ± SEM; * $p < 0.05$ and *** $p < 0.001$ vs. control as assessed by Student's t-test. **(E)** Detection of DNA ladder in HCT116 treated (um-PEA) or not (ctrl) with um-PEA (30 µM, 24 h) by standard agarose gel electrophoresis. The first lane represents the standard molecular size marker.

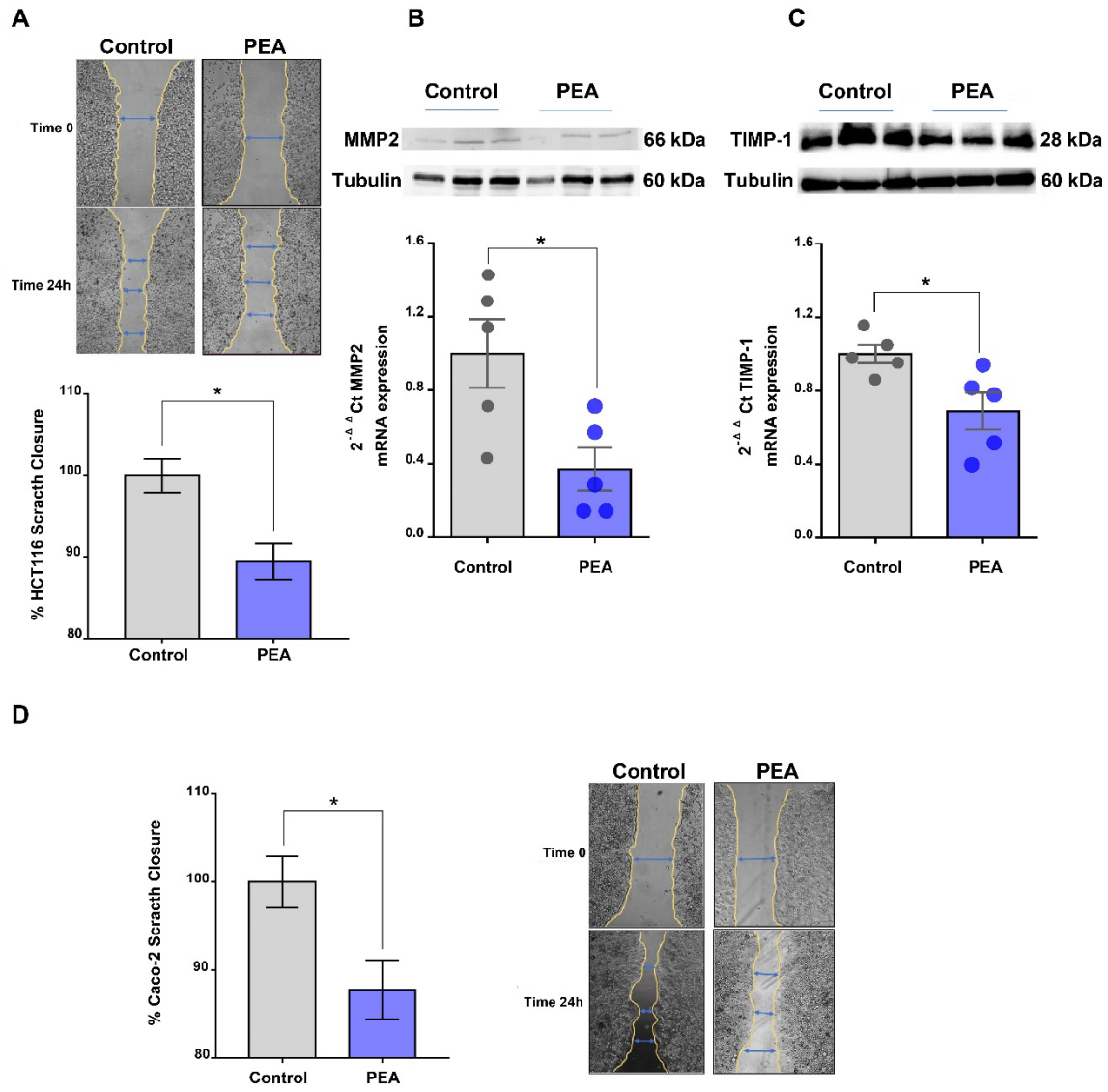

Figure 15. Palmitoylethanolamide affects tumor cell migration. (A) In vitro scratch assay performed in HCT116 cells alone or the presence of ultramicronized palmitoylethanolamide (PEA, 30 μM, 24 h). The scratches are expressed as a percentage of scratch closure (n = 4 experiments). Representative images of the scratch areas, at time zero and 24 h, of HCT116 cells alone or in the presence of PEA (30 μM, 24 h) are reported on top of the graph. Gene and protein expressions of matrix metalloproteinase type 2 (MMP2). Magnification: 4×. **(B)** and tissue inhibitor matrix metalloproteinase 1 (TIMP1) **(C)** in HCT116 cells, alone or in the presence of PEA (30 μM, 24 h). Gene expression was measured by RT-qPCR and calculated by using the 2-ΔΔCt formula (n = 5). In contrast, protein expression was evaluated by Western blot analysis and normalized to the housekeeping protein α-tubulin (n = 3). **(D)** In vitro scratch assay performed in Caco-2 cells alone or the presence of PEA (30 μM, 24 h). The scratches are expressed as percentage of scratch closure (n = 4 experiments). Next to the graph, representative images of the scratch areas at time zero and time 24 h for Caco-2 cells alone or in the presence of PEA (30 μM, 24 h) are reported. Values are expressed as means ± SEM; * $p < 0.05$ vs. control as assessed by Student's t-test. Magnification: 4×.

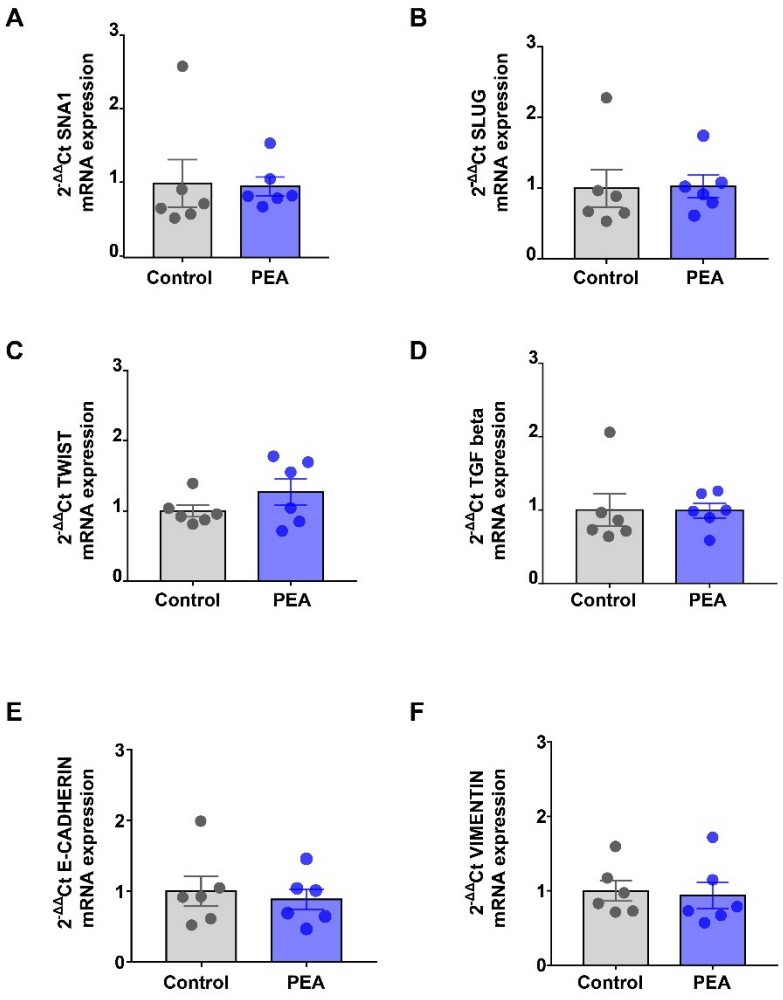

Figure 16. Palmitoylethanolamide effects on epithelial to mesenchymal transition (EMT). Gene expressions of SNAI1 (Snail Family Zinc Finger 1, **(A)**, SLUG (Zinc Finger Protein SNAI2, **(B)**, TWIST (twist family BHLH transcription factor 1, **(C)**, TGF-β (transforming growth factor beta, D), E-cadherin **(E)** and Vimentin **(F)** in HCT116 cells, alone or in presence of ultramicronized palmitoylethanolamide (PEA, 30 µM, 24 h). Gene expression was measured by qRT-PCR and calculated using the 2-ΔΔCt formula (n = 6). Values are expressed as means ± SEM and Student's t-test was performed.

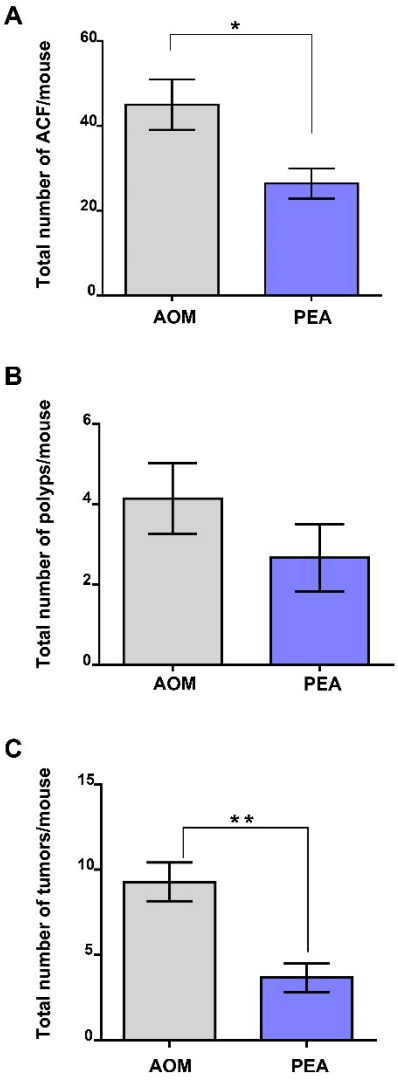

Figure 17. Effect of palmitoylethanolamide treatment in the murine azoxymethane (AOM) model of colon cancer. Total number of aberrant crypt foci (ACF) **(A)**, polyps **(B)** and tumors **(C)** derived from the administration of AOM (40 mg/kg, intraperitoneally) in mice treated or not with ultramicronized palmitoylethanolamide (PEA, 10 mg/kg, intraperitoneally, three times/week for 13 weeks), (n = 6–7 mice per experimental group). Results are expressed as means ± SEM; * $p < 0.05$ and ** $p < 0.01$ vs. AOM as assessed by Student's t-test.

Chapter 2: Role of NAAA inhibition in Colorectal cancer (CRC)

1.1 AM9053, by inhibiting NAAA, affects CRC development and growth in vivo.

We first used the xenograft model of CRC to investigate the functional role of NAAA in in vivo CRC growth. Colorectal cancer was induced by HCT116 cells subcutaneous (s.c.) injection into the back of immunodeficient BALB/c mice, which establishes a well-known method to evaluate tumor growth (threshold cycle—Ct ± SD: NAAA 25.3 ± 0.287; GAPDH 17.24 ± 0.191, n = 6). AM9053, a selective, potent, and slowly reversible NAAA inhibitor (IC50 = 30 nM), was administered intraperitoneally every two days (20 mg/kg). AM9053 has been proposed as a helpful tool chemical to research NAAA functions and has previously been used for systemic administrations (Alhouayek et al., 2015; Bottemanne et al., 2018). After 15 days of treatment, AM9053 was able to reduce, in a significant manner, the xenograft tumor volume, compared to the control group (Figure 18 A). As shown in figure 18 B, tumors of AM9053-treated group were smaller, with significantly lower weights (Figure 18 C). It has already been demonstrated that AM9053-induced NAAA inhibition raises AEs levels, with the specific AEs varying according to the disease and the tissue under study (Bottemanne et al., 2018). While PEA and anandamide levels remained unchanged, there was a notable increase in OEA levels in our CRC xenograft tumors (Figure 18 D-F). We subsequently looked at the expression of Ki-67, pAKT, ERK1/2, and pS6 in the xenograft frozen tumor sections and protein lysates, respectively, to understand the pathways linked to the decrease in tumor growth that was shown following NAAA pharmacological inhibition. High-end immunofluorescence images, as shown in Figure 18 G, confirmed significantly fewer red Ki-67-positive cells in frozen sections of AM9053-treated tumors (lower images) than in vehicle-treated tumors (upper images). This finding was further supported by the red positive cells' intensity mean value (Figure 18 H). In conclusion, we find that NAAA has a functional role in CRC development and that its pharmacological modulation by AM9053 can impact the tumor's growth by lowering the Ki-67 expression in vivo.

1.2 NAAA inhibition influences EGF family member expression in tumor secretome.

The tumor secretome comprises numerous factors released by tumor cells and other interacting cell types, collectively contributing to the promotion and maintenance of tumor growth (Xue, Lu, & Lai, 2008). Thus, we extracted the secretome from the tumor to further confirm NAAA's functional role in tumor growth. The schematic illustration given in Figure 19 A illustrates xenografts. Notably, initial data showed that the tumor secretome identified a trend of down-regulation of NAAA expression in HCT116 cells (Figure 19 B) and in the Caco-2 cell line, an adenocarcinoma cell line (Figure 19 C), which expresses NAAA (basal NAAA expression: Ct ± SD: NAAA 26.37 ± 0.295; GAPDH 17.95 ± 0.259, n = 6). To investigate the molecular mechanisms underlying the decrease in tumor growth brought about by the pharmacological NAAA inhibition, we studied the global changes in protein expression in the tumor secretome acquired from xenograft mice treated or not with AM9053. We discovered consistent changes in the protein expression levels of Erb-B1, Erb-B2, Erb-B3, and AREG in tumor secretomes obtained from mice treated with AM9053, using a well-controlled and commercially available oncogenic proteome array (Figure 19 D). All of these proteins are noteworthy since they belong to the EGF family and have a well-established function as master regulators of the proliferation of tumor cells (Yarden & Sliwkowski, 2001). When taken as a whole, NAAA inhibition alters the tumor secretome's composition, harming EGF family members' expression.

1.3 AM9053 exerts anti-proliferative effects selectively in CRC cell line.

The above data led us to further investigate how AM9053 affects CRC cells *in vitro*. First, AM9053 didn’t exhibit cytotoxic effects in either tumoral HCT116 (Figure 20 A) and healthy HCEC (Figure 20 B) at doses ranging from 0.1 to 3 μM. The antiproliferative activity of the NAAA inhibitor was next examined on HCT116 cells, the same colorectal adenocarcinoma cell line used to create xenograft tumors, using the bromodeoxyuridine incorporation assay. Notably, our findings showed that AM9053 (0.1–3 μM) had an IC50 value ± SD of 1.056 ± 0.285 μM and decreased the proliferation rate after 24 hours of exposure (Figure 20 C). Moreover, AM9053 (3 μM) confirmed its antiproliferative effect also on Caco-2 cells (% Caco-2 cell proliferation, mean ± SD: control 100 ± 4.14; AM9053 3 μM 80.95 ± 12.02; n = 7, $P < 0.01$). In contrast, the proliferation rate of the healthy HCEC line (Figure 20 D), which also produces NAAA (NAAA expression [Ct ± SD: NAAA 26.13 ± 0.155; GAPDH 17.46 ± 0.17, n = 6]), was unaffected by AM9053 treatment (3 μM, 24-hour exposure). These findings highlight the selective action of NAAA in tumor cell proliferation. To ascertain the

pharmacological mechanism of action behind the observed antiproliferative effect of NAAA inhibition, we treated HCT116 with AM9053 in the presence of specific antagonists of the primary targets accountable for AEs action (Di Marzo & Piscitelli, 2015); these antagonists included GW6471 [PPAR-α antagonist], 50-iodoresiniferatoxin [TRPV1 antagonist], AM251 [CB1 antagonist], and AM630 [CB2 antagonist] (Alexander, et al., 2021). It's interesting to note that, whereas CB1 and CB2 antagonists did not significantly reverse the antiproliferative impact of AM9053, PPAR-α, and TRPV1 did (Figure 20 E). Overall, our findings imply that the pharmacological inhibition of NAAA has antiproliferative effects at least partially mediated by TRPV1 and PPAR-α.

1.4 AM9053 inhibits tumor cell migration rate in vitro

Next, we addressed whether AM9053 would affect HCT116 cell-cycle progression using BrdU/7-AAD staining. AM9053-treated cells were found to have a significantly larger percentage of S-phase cells compared to the control group, as demonstrated in Figure 21 A and the representative density plots reported in Figure 21 B. Additionally, there was a significant decrease in the fraction of G0/G1 phase cells. Cyclin A2 is crucial in controlling the start and course of DNA synthesis and activating cyclin-dependent kinase 2 (CDK2) during the S phase (Heichman & Roberts, 1994). Data shown AM9053 decreased the expression of both cyclin A2 (Figure 21 C) and CDK2 (Figure 21 D), which are known to regulate the G2/M phase, without affecting cyclin B1 (Figure 21 E) or cyclin-dependent kinase 1 (CDK1) expression (Figure 21 D). These results are consistent with the blocking of the S phase. Furthermore, when pretreatment with mitomycin C prevented the proliferation of HCT116 (Figure 22 A) and Caco-2 (Figure 22 B) cells, AM9053 significantly reduced their migration. Figure S3C shows that the PPAR-α or TRPV1 antagonists did not affect AM9053's effect on migration, in contrast to the data on cell proliferation (Figure 22 D). These findings imply that NAAA inhibition may contribute to migration and proliferation through a distinct mechanism of action (i.e., participation of PPAR-α and TRPV1 in migration but not in proliferation). Taken together, our findings highlight the critical function that NAAA plays in CRC cell proliferation. NAAA inhibition's antiproliferative effect is mediated by PPAR-α and TRPV1 and is based on cell cycle arrest in the S phase, most likely because of down-regulating cyclin A2/CDK2.

1.5 Transient NAAA knock-down results in antiproliferative effects

We further explored if NAAA silencing could replicate the NAAA antiproliferative effect. To pursue this aim HCT116 cells were effectively knocked down for NAAA (siNAAAHCT116)

using siRNA (Figure 23 A). In contrast to treatment with siRNA scrambled sequence, NAAA silencing did not influence HCT116 cell viability for 72 hours. However, it is noteworthy that NAAA silencing considerably reduced cell proliferation compared to the scramble control (Figure 23 B). Furthermore, AM9053 did not significantly suppress the proliferation of siNAAA-HCT116 cells, demonstrating the specificity of AM9053 as an NAAA inhibitor (Figure 23 B). Figure 4c and the representative dot plots in Figure 4d show that siNAAA-HCT116 cells had a much greater percentage of cells in the S phase and a corresponding decrease in the number of cells in the G0/G1 phase, which is consistent with the effects shown by AM9053. Accordingly, this effect was connected to the reduction in cyclin A2 expression (Figure 23 E), despite no change in CDK2 expression (Figure 4f). Likewise, no discernible impact was noted on the manifestation of cyclin B1 (Figure 23 G) and CDK1 (Figure 23 H), which govern the G2/M phase. Together, these findings provide compelling evidence for and point to a significant function for NAAA in regulating the cell cycle and proliferation of colorectal cancer.

1.6 Human CRC biopsies showed a down-regulation of NAAA expression

The final goal of our study was to compare NAAA expression in primary human colon cancer tissues to that of their nearby non-tumor counterparts. Our findings demonstrate a considerable down-regulation of NAAA mRNA levels in surgically resected colorectal adenocarcinomas (Figure 24 A). Tumors were classed as pT2, pT3, and pT4 according to the tumor-node-metastasis staging approach (Edge & Compton, 2010). Interestingly, we found that NAAA expression dramatically decreased only in stages pT2 and pT3, with no alterations reported in pT4 tumors (Figure 25 B). These results were supported by the analysis of human CRC tissues that were accessible in the public gene expression GENT2 database (Park, Yoon, Kim, & Kim, 2019), where a down-regulation of NAAA expression in CRC biopsies (Figure 25 C). Bottemanne et al. (2018) reported that NAAA is responsible for PEA, OEA, and AEA hydrolysis. Therefore, we proceeded to measure the substrates of NAAA in eight human CRC specimens compared to eight healthy specimens. We discovered a direct correlation between NAAA's significant reduction in CRC tissues and higher levels of PEA, OEA, and anandamide

(Figure 25 D-F). Together, these findings provide credence to the hypotheses that NAAA is involved in human CRC, with its expression significantly downregulated and the tissue quantities of its three primary substrates rising as a result.

1.7 Human CRC biopsies showed AEs main targets dysregulation.

Lastly, as we discovered a significant up-regulation of PEA, OEA, and anandamide levels in human CRC tissues we further examined the expression of their primary targets, PPAR-α, TRPV1, and cannabinoid (CB1 and CB2) receptors (Di Marzo & Piscitelli, 2015). As shown by the data, the expression of CB receptors showed a substantial decrease (Figure 26 A-B). In contrast, TRPV1 and PPAR-α mRNA expression did not show any statistically significant differences (Figure 26 C-D). These findings suggest that CRC has downregulated some of the most well-known AEs targets.

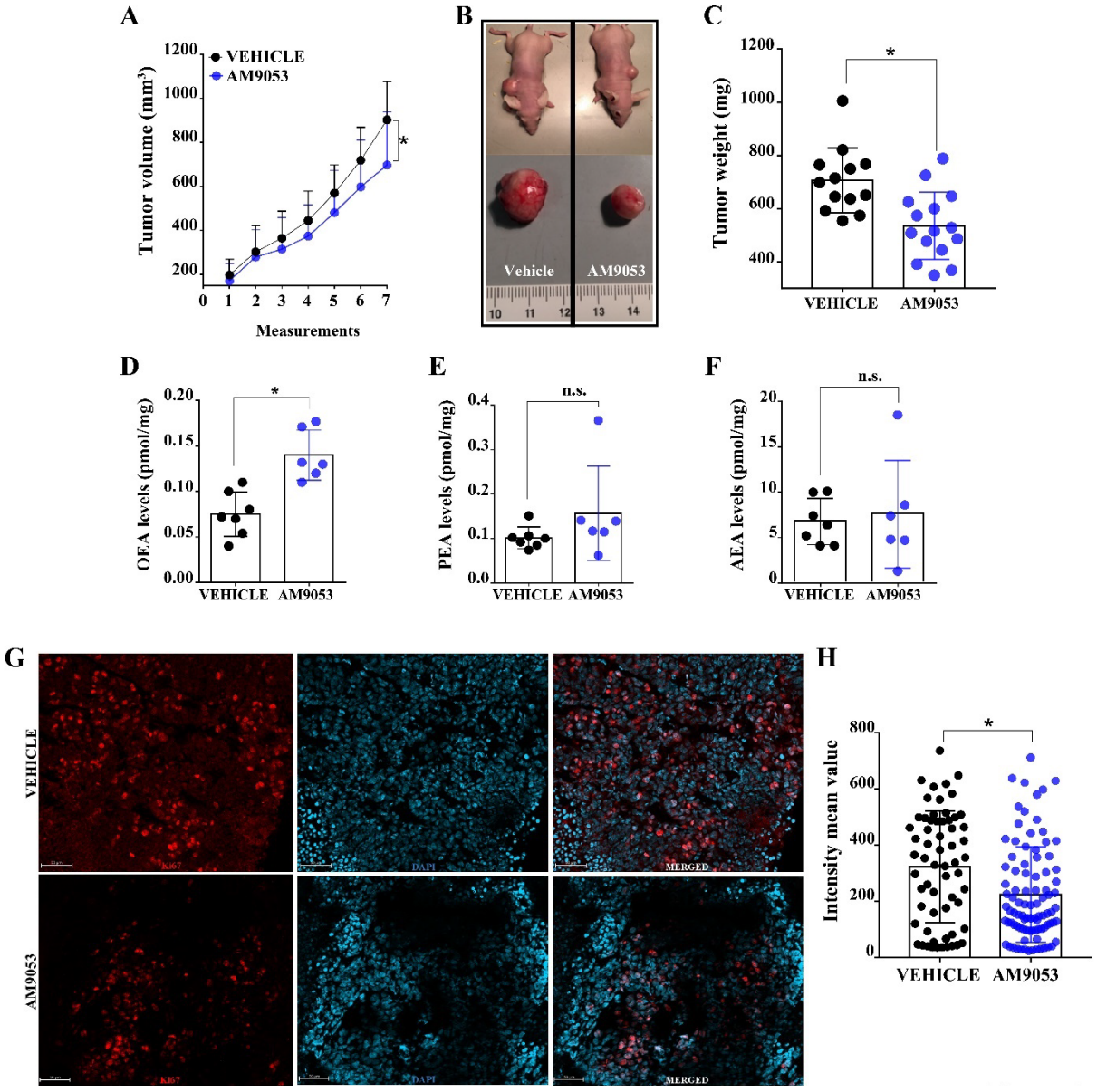

Figure 18. N-acylethanolamine acid amidase (NAAA) selective inhibition ameliorates CRC growth in vivo. **(A)** Effect of the NAAA inhibitor AM9053 (20 mg/kg, peritumorally) on in vivo tumor growth, measured as tumor volume (mm3), over 15 days (seven measurements). Each dot represents the mean ± SD of 13 mice for vehicle and 15 mice for AM9053 experimental groups; *P < 0.05 versus vehicle by two-way ANOVA. **(B)** Representative macroscopic pictures of tumor-bearing mice (upper images) as well as of the explanted tumors (lower images), with the respective treatments, at the day of the kill. **(C)** Weights (reported in mg) of the xenograft tumors explanted from tumor-bearing mice treated (n = 15) or not (n = 13) with AM9053 (20 mg/kg, peritumorally). **(D-F)** Endogenous-level measurements of NAEs: N-oleoylethanolamide, OEA (d), N-palmitoylethanolamide, PEA (E) and anandamide (AEA) **(F)** in mouse xenograft tumors treated (n = 6) or not (n = 7) with AM9053 (20 mg/kg, peritumorally). The levels of NAEs are reported as pmol·mg−1 of wet tissue weight. **(G)** Representative high-end fluorescence images of Ki-67 expression in frozen sections of tumors explanted from tumor-bearing mice treated (lower images) or not (upper images) with AM9053 (20 mg/kg, peritumorally). Ki-67 staining is visualized in red, and nuclei were counterstained with DAPI in blue. Magnification: 20× (white scale bar 50 μm). **(H)** Graph showing the intensity mean value (±SD) of red Ki-67-positive cells. Values are expressed as means ± SD; *P < 0.05 versus vehicle, as assessed by Student's t test; n.s., not significant.

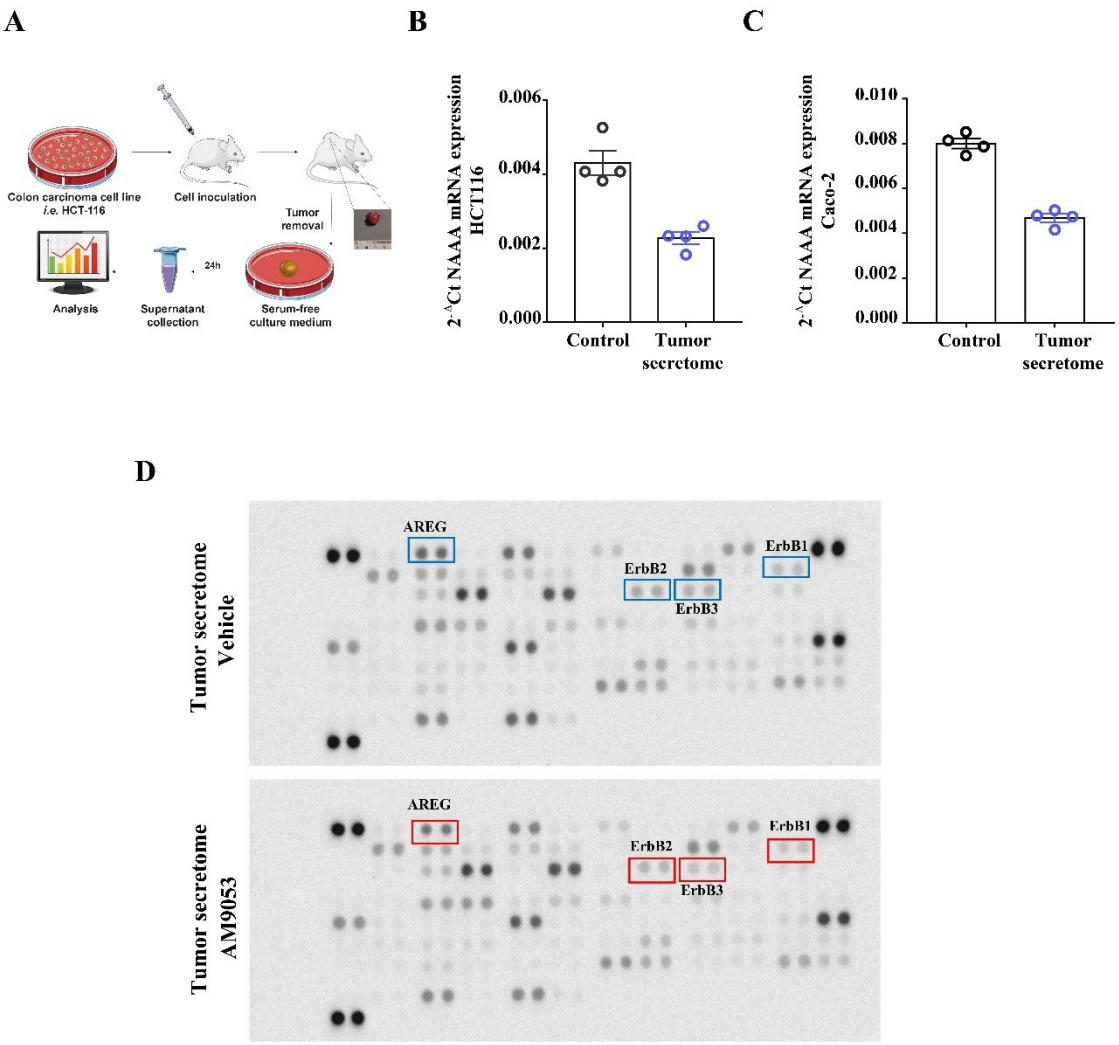

Figure 19. (A) Schematic illustration of the tumor secretome obtained from mouse xenograft tumors treated or not with AM9053 (20 mg/kg, peritumorally). NAAA gene expression in HCT116 (B) and Caco-2 cells (C), alone or in presence of tumor secretome (24-h time exposure) obtained from mice xenograft tumors (n = 4). NAAA expression was measured by qRT-PCR and calculated by using the 2-ΔCt formula. **(D)** Human oncology array performed on the tumor secretome obtained from mouse xenograft tumors treated (lower membrane) or not (upper membrane) with AM9053 (20 mg/kg) (n = 4 pooled tumor secretomes per experimental group). Erb-B1, Erb-B2, Erb-B3 and AREG dot proteins are indicated as rectangles on the images. Exploratory data not subjected to statistical analysis.

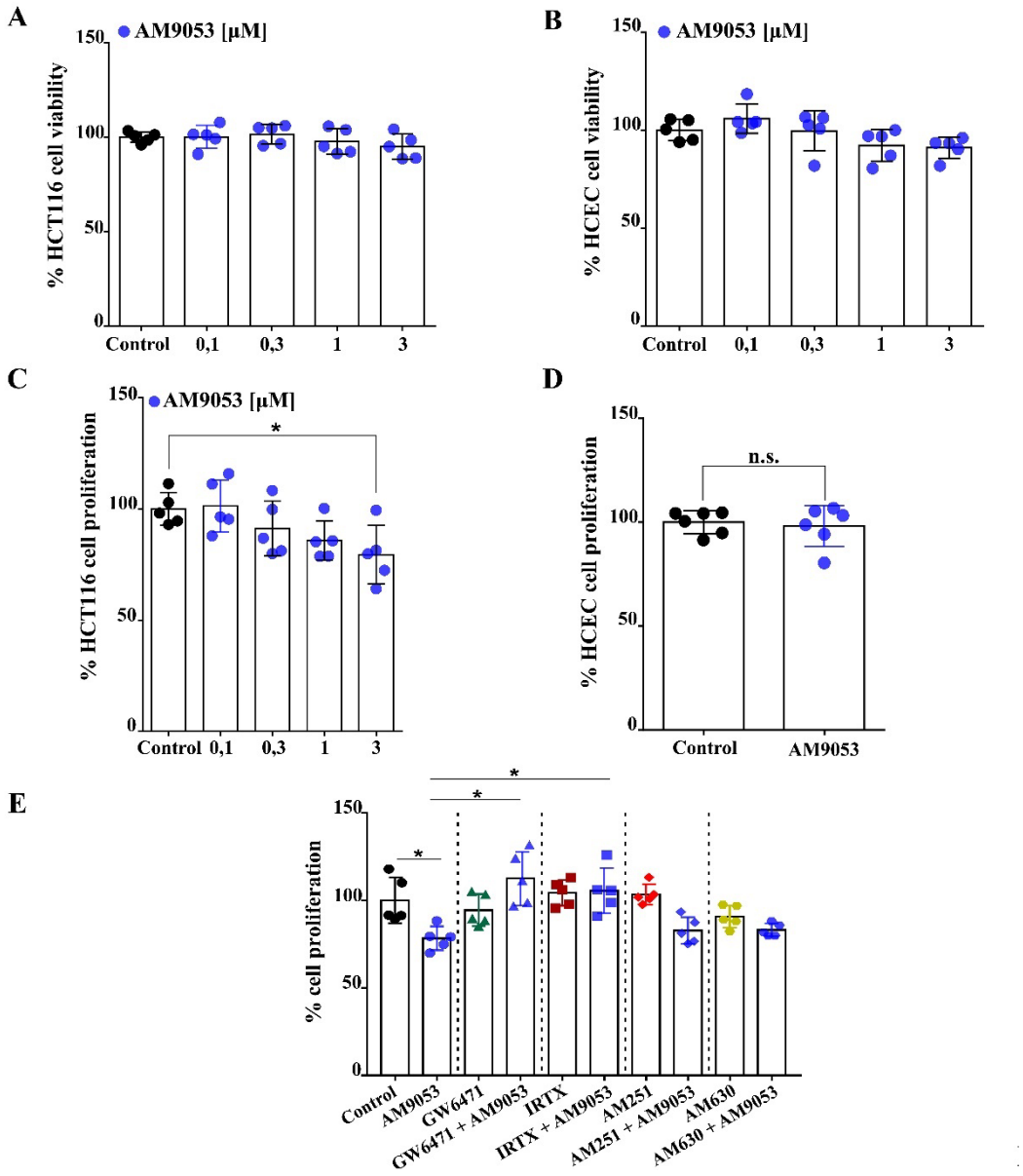

Figure 20. The N-acylethanolamine acid amidase (NAAA) selective inhibitor AM9053 impacts tumor cell proliferation. (A) Cell viability assay in HCT116 and **(B)** in healthy human colonic epithelial cells (HCEC) alone or in the presence of AM9053 (0.1–3 µM, 24 h) (n = 5). Results are expressed as mean ± SD. **(C)** Cell proliferation rate of HCT116 cells incorporating bromodeoxyuridine (BrdU), alone or in the presence of AM9053 (0.1–3 µM, 24 h). Results are expressed as percentage of cell proliferation (n = 5 independent experiments). Values are expressed as means ± SD; *P < 0.05 versus control, as assessed by one-way ANOVA followed by Dunnett's multiple comparisons test. **(D)** Cell proliferation rate of HCEC incorporating BrdU, alone or in the presence of AM9053 (3 µM, 24 h). Results are expressed as percentage of cell proliferation (n = 6). Values are expressed as means ± SD; n.s., not significant as assessed by unpaired Student's t-test. **(E)** The antiproliferative effect of AM9053 (3 µM) was also evaluated in the presence of GW6471 (3 µM, PPAR-α antagonist), 5′-iodoresiniferatoxin (I-RTX 0.1 µM, TRPV1 antagonist), AM251 (1 µM, CB1 antagonist) and AM630 (1 µM, CB2 antagonist). All results are expressed as percentage of cell proliferation (n = 5 independent experiments) and as means ± SD; *P < 0.05 versus control and/or AM9053 as assessed by one-way ANOVA followed by Tukey's multiple comparisons test.

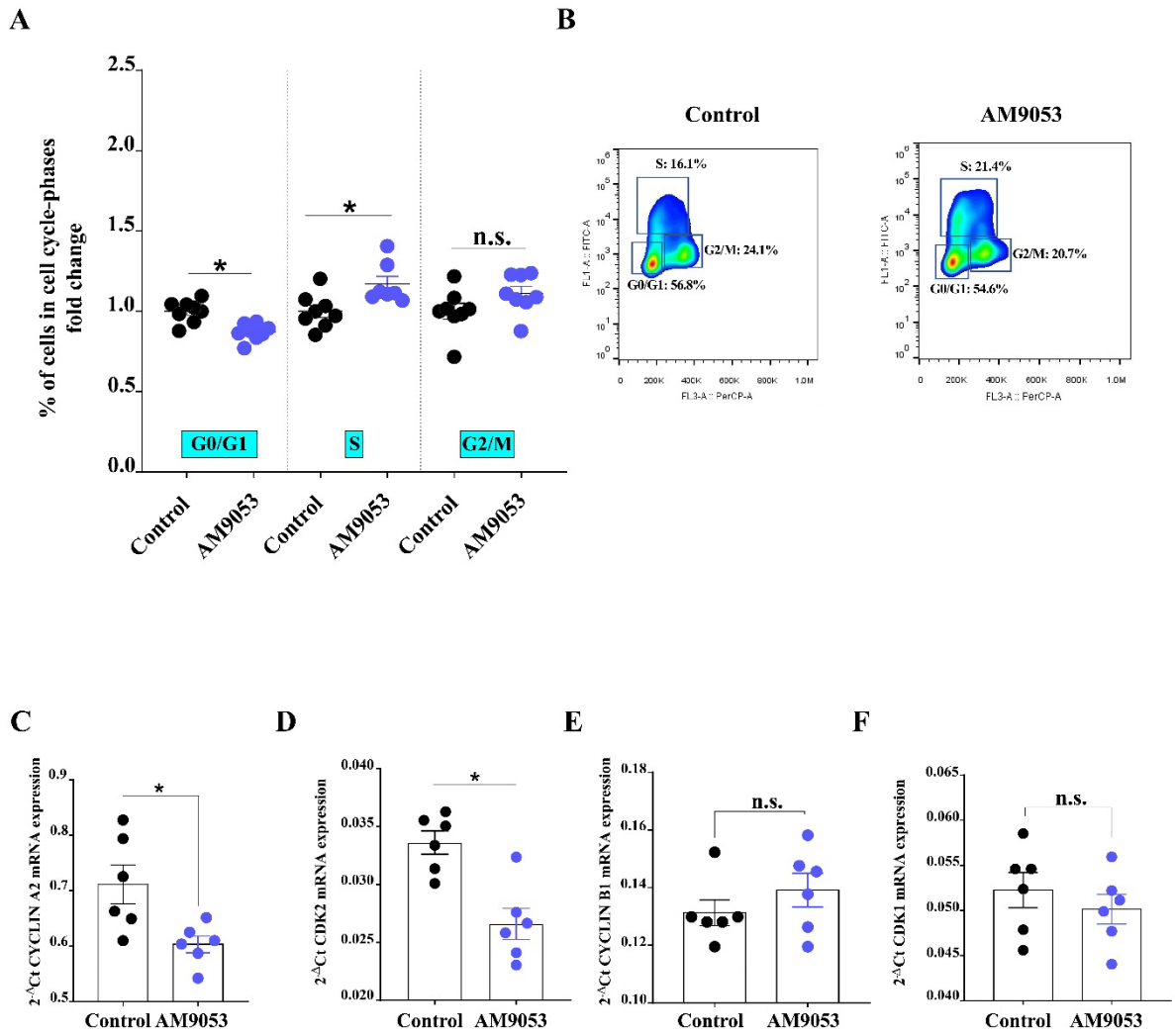

Figure 21. AM9053 blocks tumoral cell cycle. (A) Cell cycle analysis by flow cytometry of HCT116 cells treated or not with AM9053 (3 µM, 24 h). Results are expressed as fold change of the cells in each cell cycle phase (n = 8 independent experiments) to uniform the % values of the cells in each phase of the cell cycle. Values are expressed as means ± SD; *P < 0.05 versus control, as assessed by unpaired Student's t test and/or Mann–Whitney test. **(B)** Representative density plots and cell percentage, indicating the G0/G1-, G2/M- and S-phase distribution of HCT116 cells treated (right figure) or not (left figure) with AM9053 (3 µM, 24 h). Gene expression, in HCT116 cells, alone or in the presence of AM9053 (3 µM, 24 h), of cyclin A2 **(C)**, cyclin-dependent kinase 2 (CDK2) **(D)**, cyclin B1 **(E)** and cyclin-dependent kinase 1 (CDK1) **(F)**. Gene expression was measured by qRT-PCR and calculated by using the 2−ΔCt formula (n = 6 independent experiments). Values are expressed as means ± SD; *P < 0.05 versus control and analysed by Student's t-test; n.s., not significant.

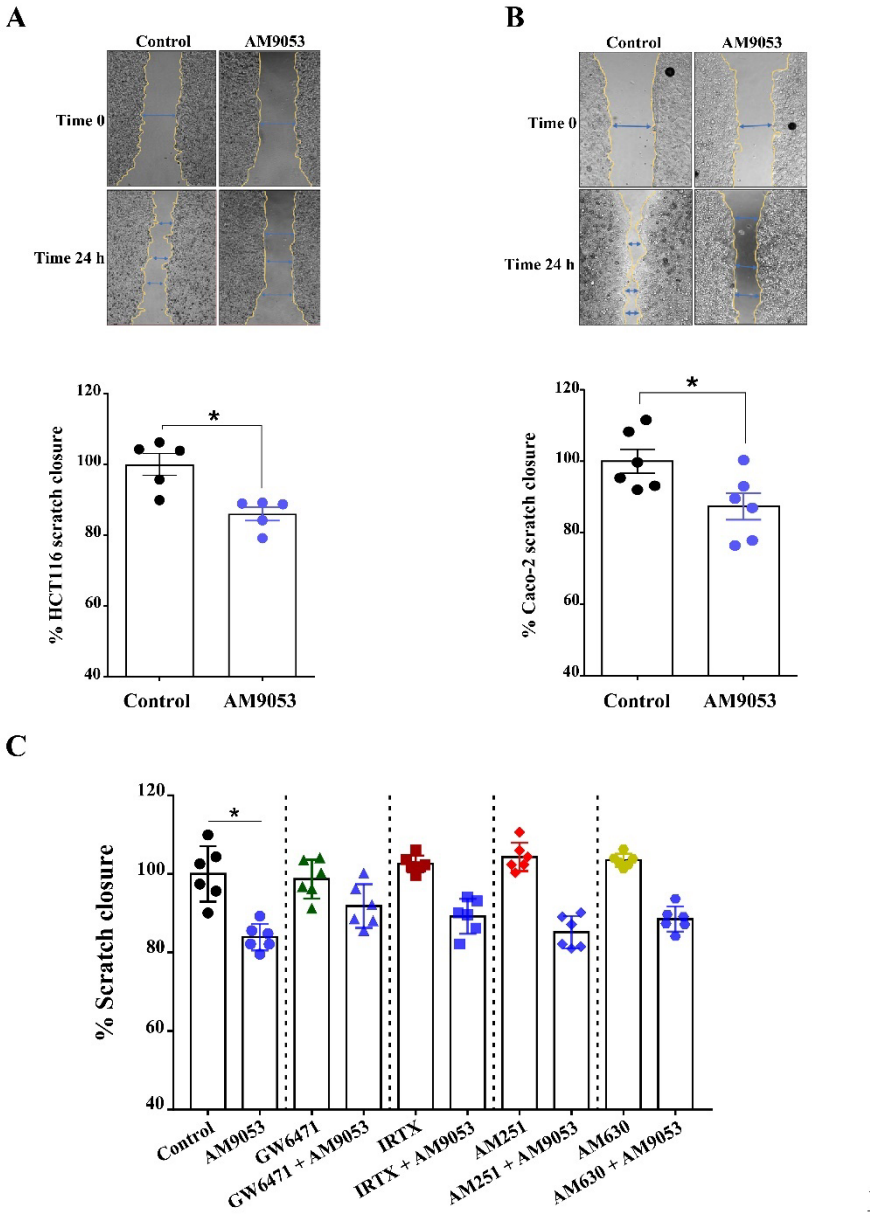

Figure 22. **AM9053 effects on tumoral cell migration in vitro.** In vitro scratch assay in HCT116 **(A)** and Caco-2 **(B)** cells alone or in presence of AM9053 (3 µM, 24 h). The scratches are expressed as percentage of scratch closure (n = 5 independent experiments) to uniform the number of pixels per area of the scratch closure. Representative fields are shown on top of each figure. All the results are expressed as means±SD; * P< 0.05 vs control, as assessed by Student's t-test. The effect of AM9053 (3 µM) in HCT116 cell migration **(C)** was also evaluated in presence of GW6471 (3 µM, PPAR-α antagonist); 5'-Iodoresiniferatoxin (I-RTX 0.1 µM, TRPV1 antagonist); AM251 (1 µM, CB1 antagonist) and AM630 (1 µM, CB2 antagonist). All results are expressed as percentage of scratch closure (n = 6) and as means±SD; *P < 0.05 vs control as assessed by one-way ANOVA followed by Tukey multiple comparisons test.

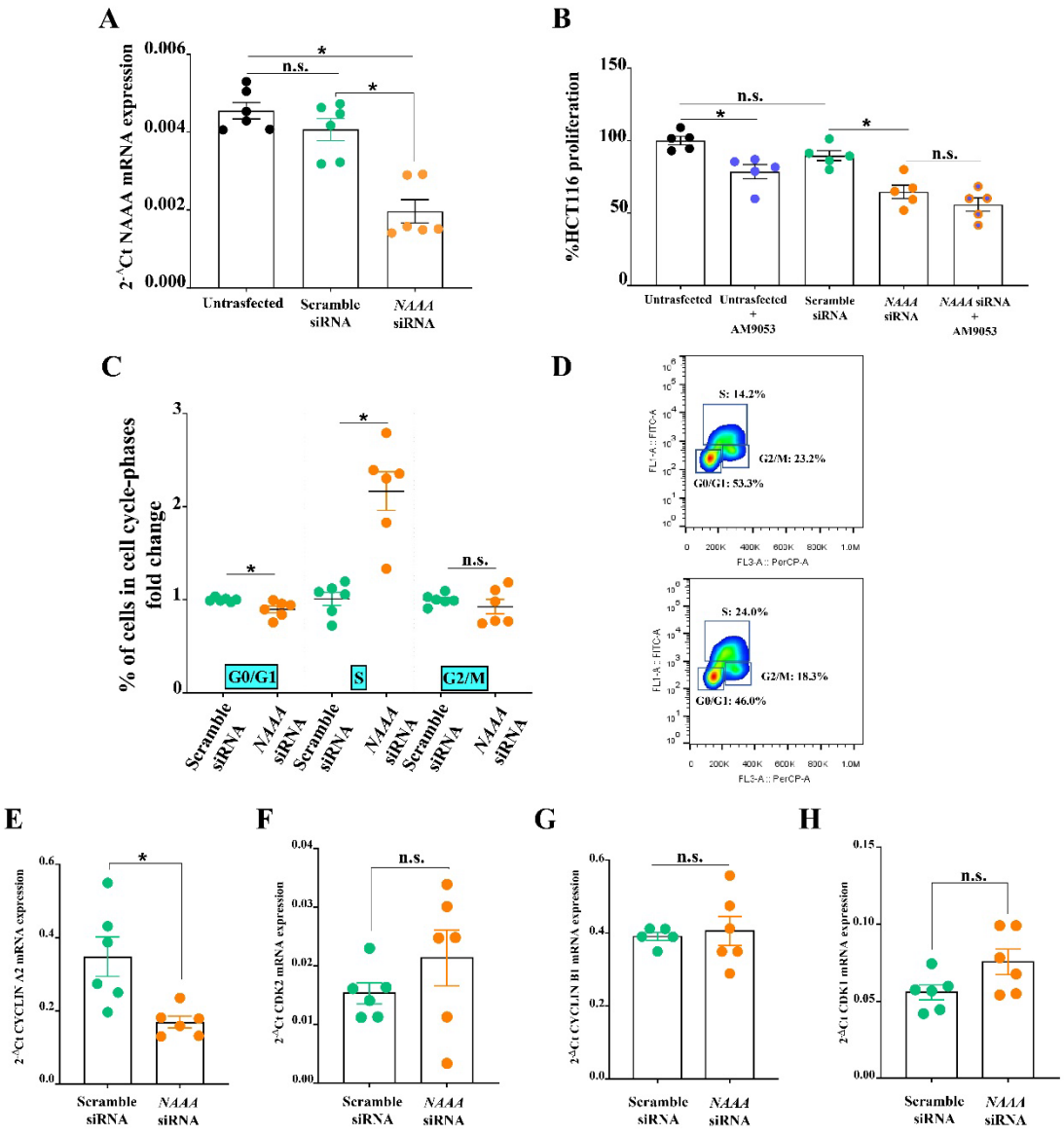

Figure 23. Transient knock-down of N-acylethanolamine acid amidase (NAAA) is associated with an antiproliferative effect. (A) NAAA gene expression in HCT116 cells alone (untransfected) or in the presence of scramble small interfering (si)RNA and/or NAAA siRNA (n = 6 independent experiments). NAAA gene expression was measured by qRT-PCR and calculated by using the 2−ΔCt formula. Values are expressed as means ± SD; *P < 0.05 versus scramble siRNA and/or NAAA siRNA as assessed by one-way ANOVA followed by Kruskal–Wallis comparisons test; n.s., not significant. **(B)** Cell proliferation rate of HCT116 cells incorporating BrdU in the following conditions: alone (untransfected), untransfected in the presence of AM9053 (3 μM, 24 h), scramble siRNA, NAAA siRNA and NAAA siRNA in the presence of AM9053 (3 μM, 24 h). Results are expressed as percentage of cell proliferation (n = 5 independent experiments) and as means ± SD; *P < 0.05 versus untransfected and/or NAAA siRNA, as assessed by one-way ANOVA followed by Tukey's multiple comparisons test; n.s., not significant. **(C)** Cell cycle analysis by flow cytometry of HCT116 cells in the presence of scramble siRNA and/or NAAA siRNA. Results are expressed as fold change of the cells in each cell cycle phase (n = 6) to uniform the % values of the cells in each phase of the cell cycle. Values are expressed as means ± SD; *P < 0.05 versus scramble siRNA, as assessed by unpaired Student's t-test. **(D)** Representative density plots and cell percentage, indicating the G0/G1-, G2/M- and S-phase distribution of HCT116 cells in the presence of scramble siRNA (upper figure) and/or NAAA siRNA (lower figure). Gene expression, in HCT116 cells in the presence of scramble siRNA and/or NAAA siRNA, of cyclin A2 **(E)**, CDK2 **(F)**, cyclin B1 **(G)** and CDK1 **(H)**. Gene

expression was measured by qRT-PCR and calculated by using the 2−ΔCt formula (n = 6). Values are expressed as means ± SD; *P < 0.05 versus scramble siRNA, as assessed by Student's t-test; n.s., not significant.

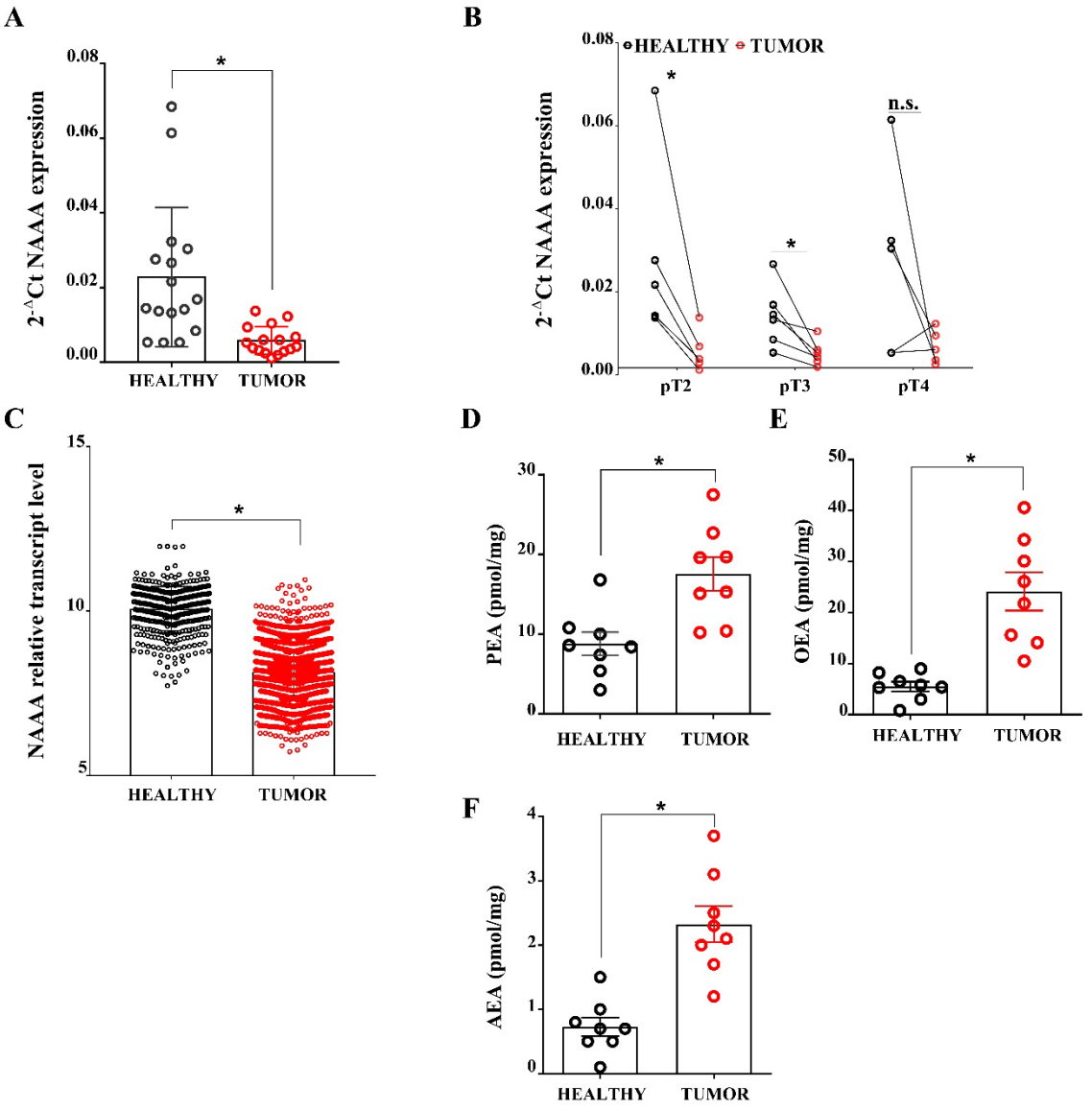

Figure 25. N-acylethanolamine acid amidase (NAAA) expression and Acylethanolamide (AE) levels in human colorectal cancer tissues. NAAA gene expression in **(A)** human colon cancer tissues versus adjacent non-tumor colon specimens (defined as 'healthy') (n = 16) and **(B)** different tumor stages (pT2 [n = 5], pT3 [n = 6] and pT4 [n = 5]). NAAA expression was measured by qRT-PCR and calculated by using the 2−ΔCt formula. **(C)** NAAA relative transcript levels to housekeeping genes (expressed as log2) in healthy (n = 393) and colorectal cancer patients (n = 3769) extrapolated from Gene Expression across Normal and Tumor tissue (GENT2) database interrogation. Endogenous-level measurements of Acylethanolamides (AEs): N-palmitoylethanolamine (PEA) **(D)**, N-oleoylethanolamine (OEA) **(E)** and anandamide (AEA) **(F)** in human colon cancer tissues (n = 8) and adjacent non-tumor colon specimens (n = 8). The levels of AEs are reported as pmol·mg−1 of wet tissue weight. All the data are expressed as means ± SD; *P < 0.05 versus 'healthy', as assessed by paired Student's t-test; n.s., not significant.

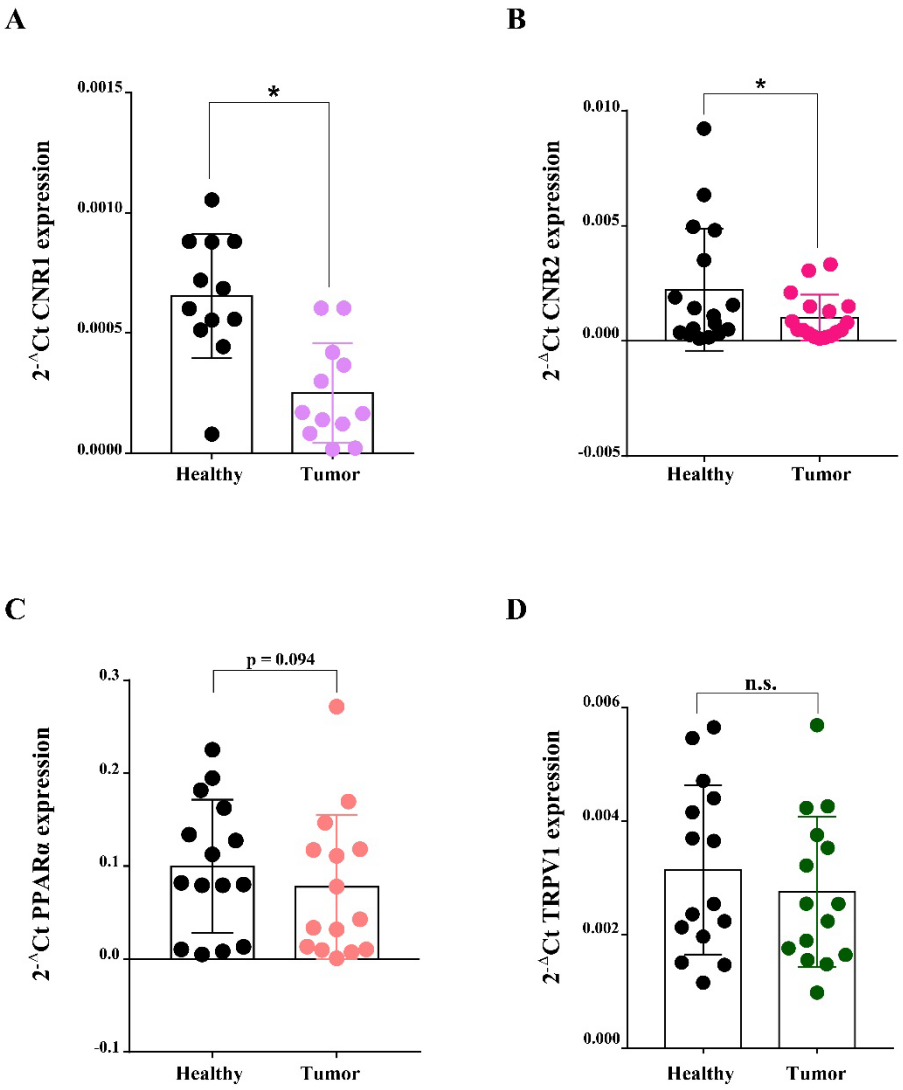

Figure 26. NAE target expression in colorectal cancer human tissues. PPARα **(A),** CB1 **(CNR1, B)** CB2 **(CNR2, C)** and TRPV1 **(D)** gene expression in human colon cancer tissues vs adjacent non-tumor colon specimens (defined as "healthy") (n = 19). Genes expressions were measured by qRT-PCR and calculated by using the 2-ΔCt formula. Data are expressed as means±SD; * $P < 0.05$ vs "healthy", as assessed by paired Student's t-test; ns = not significant.

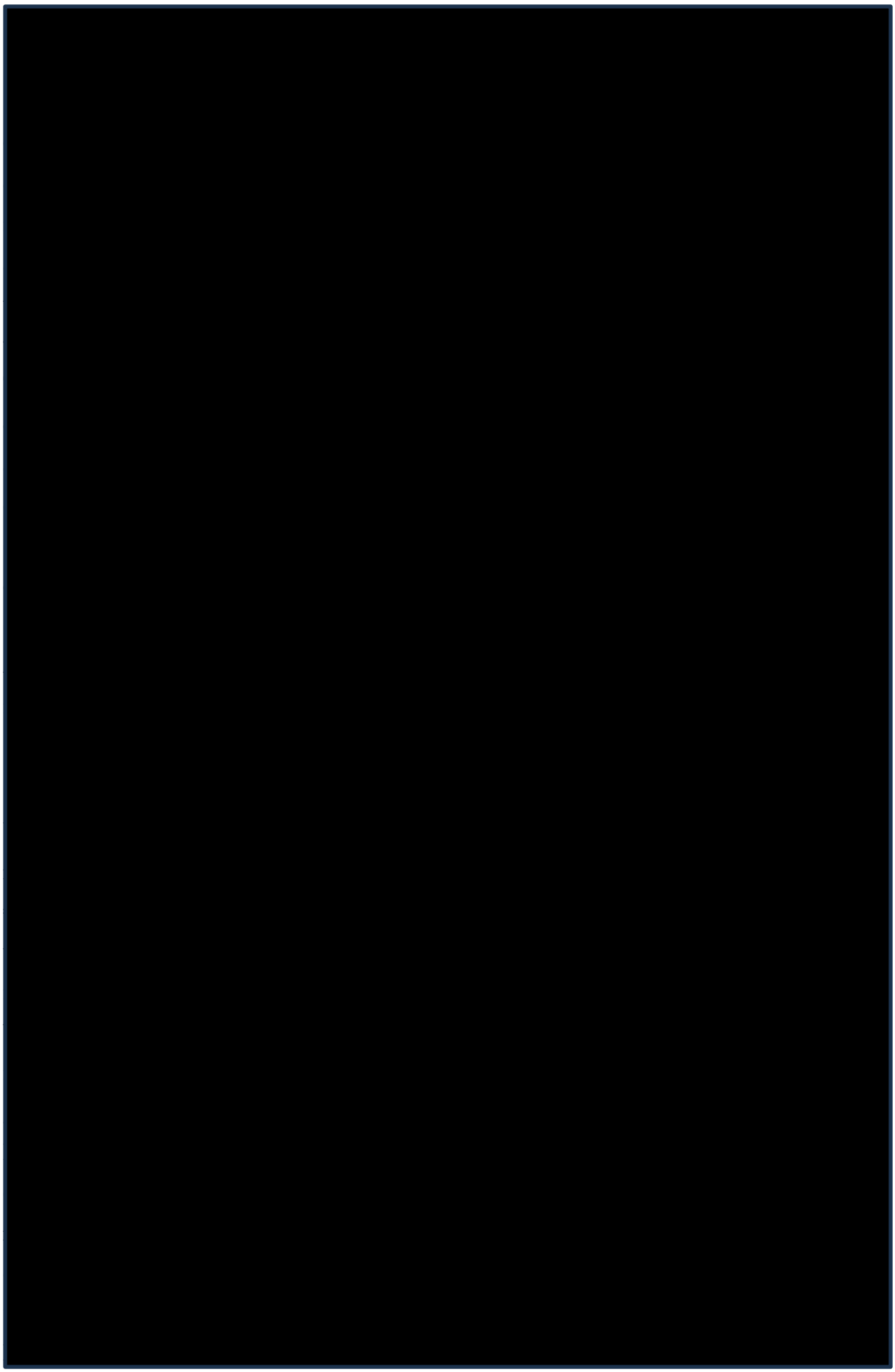

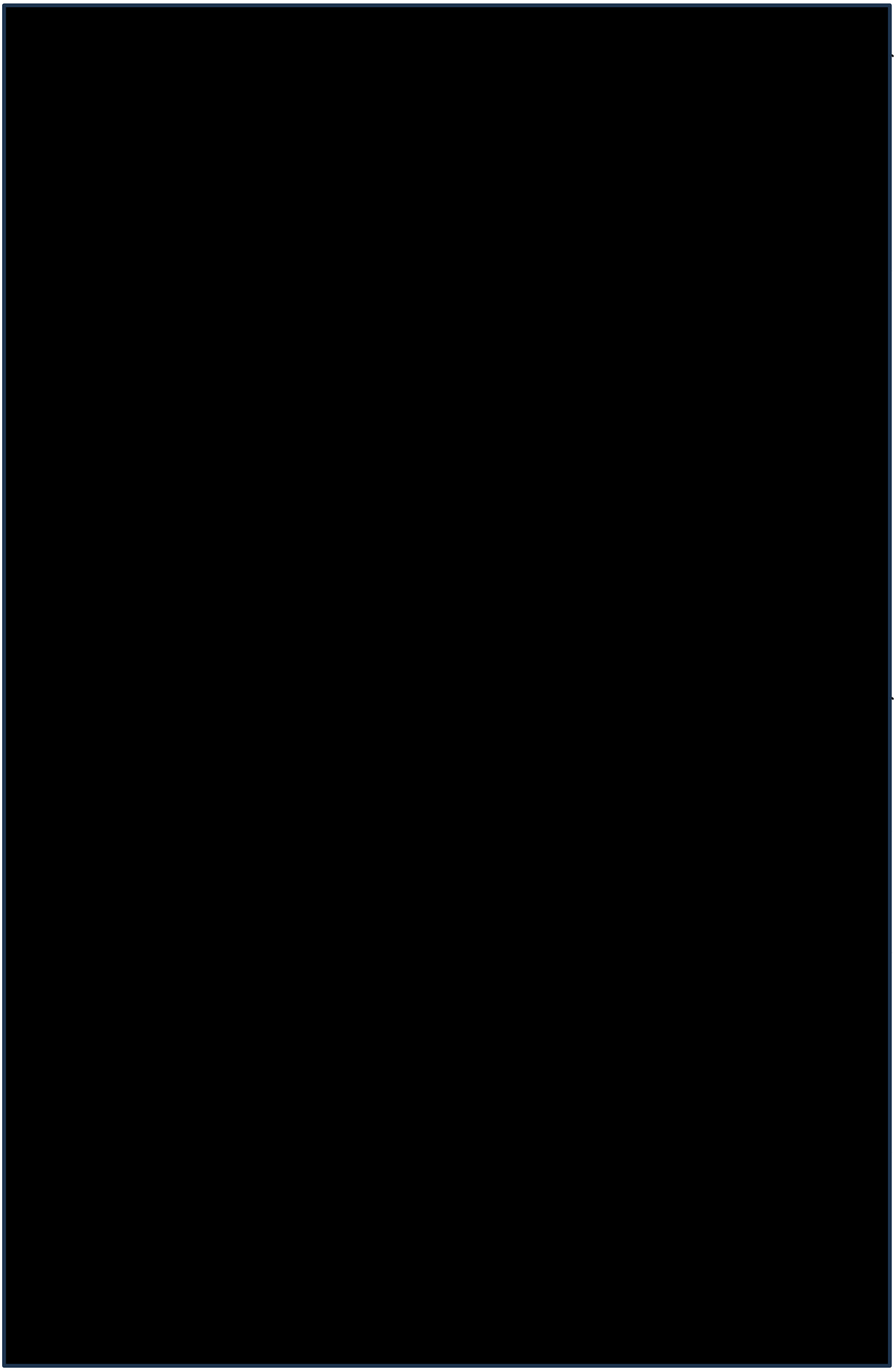

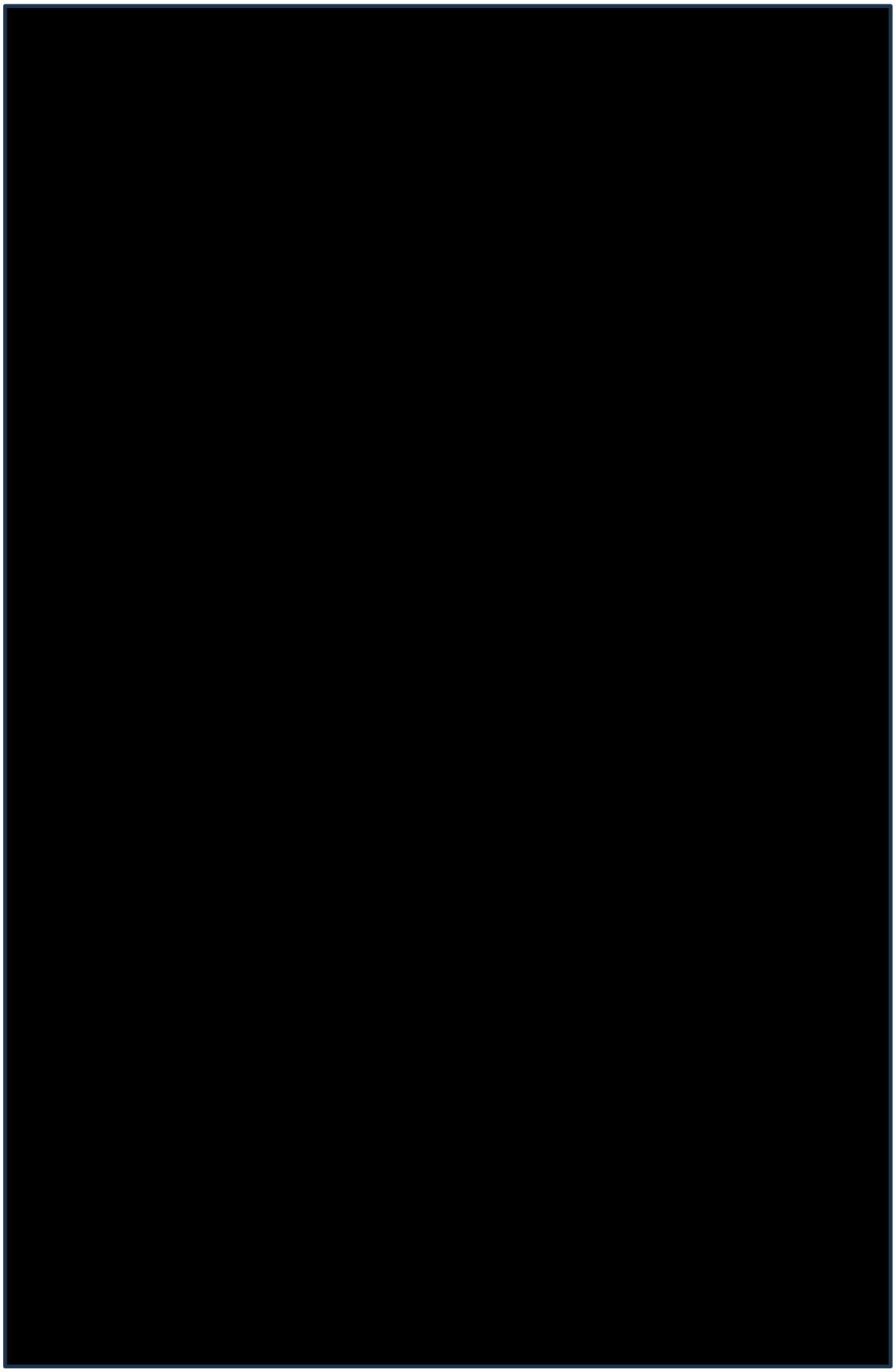

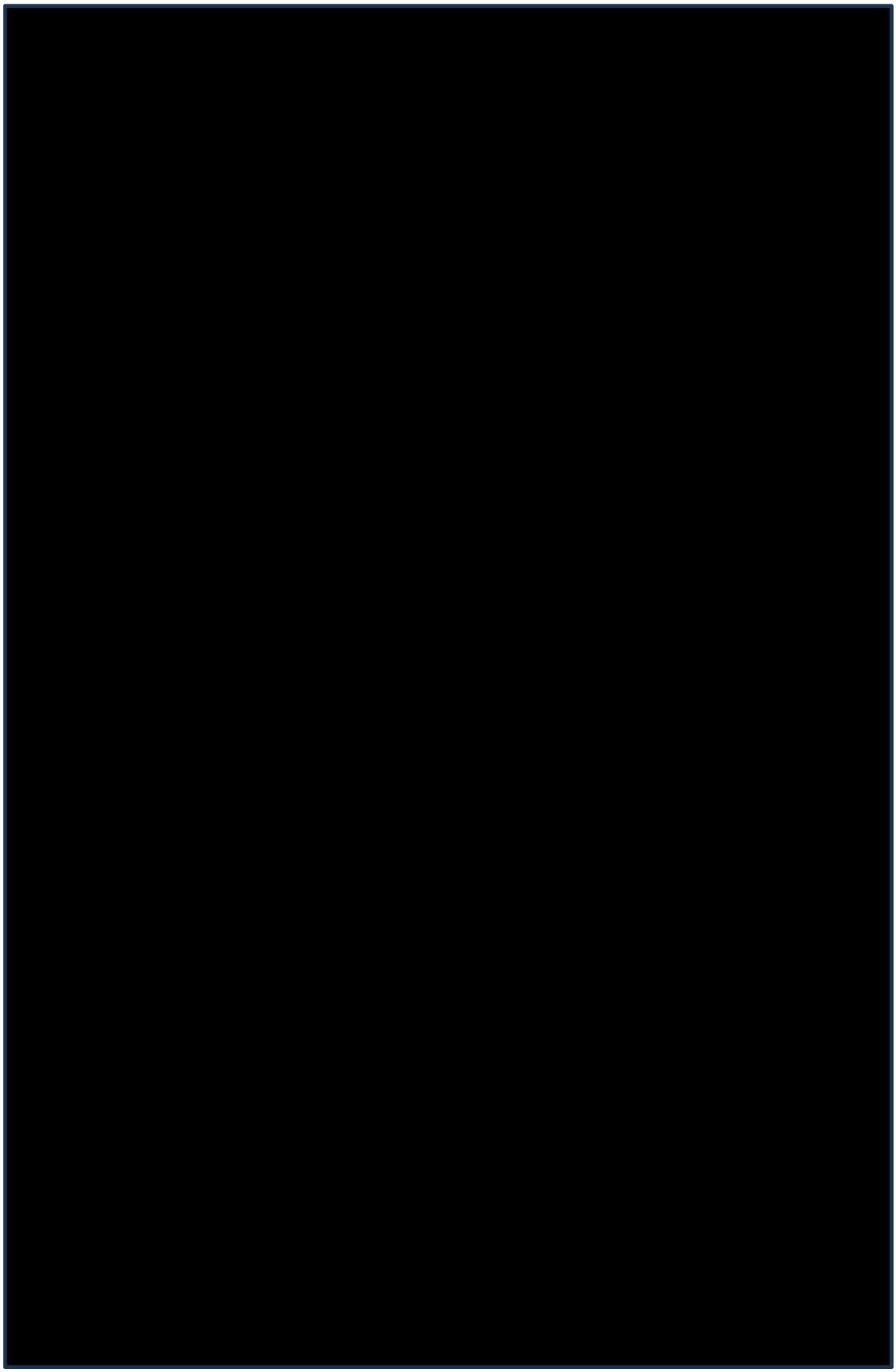

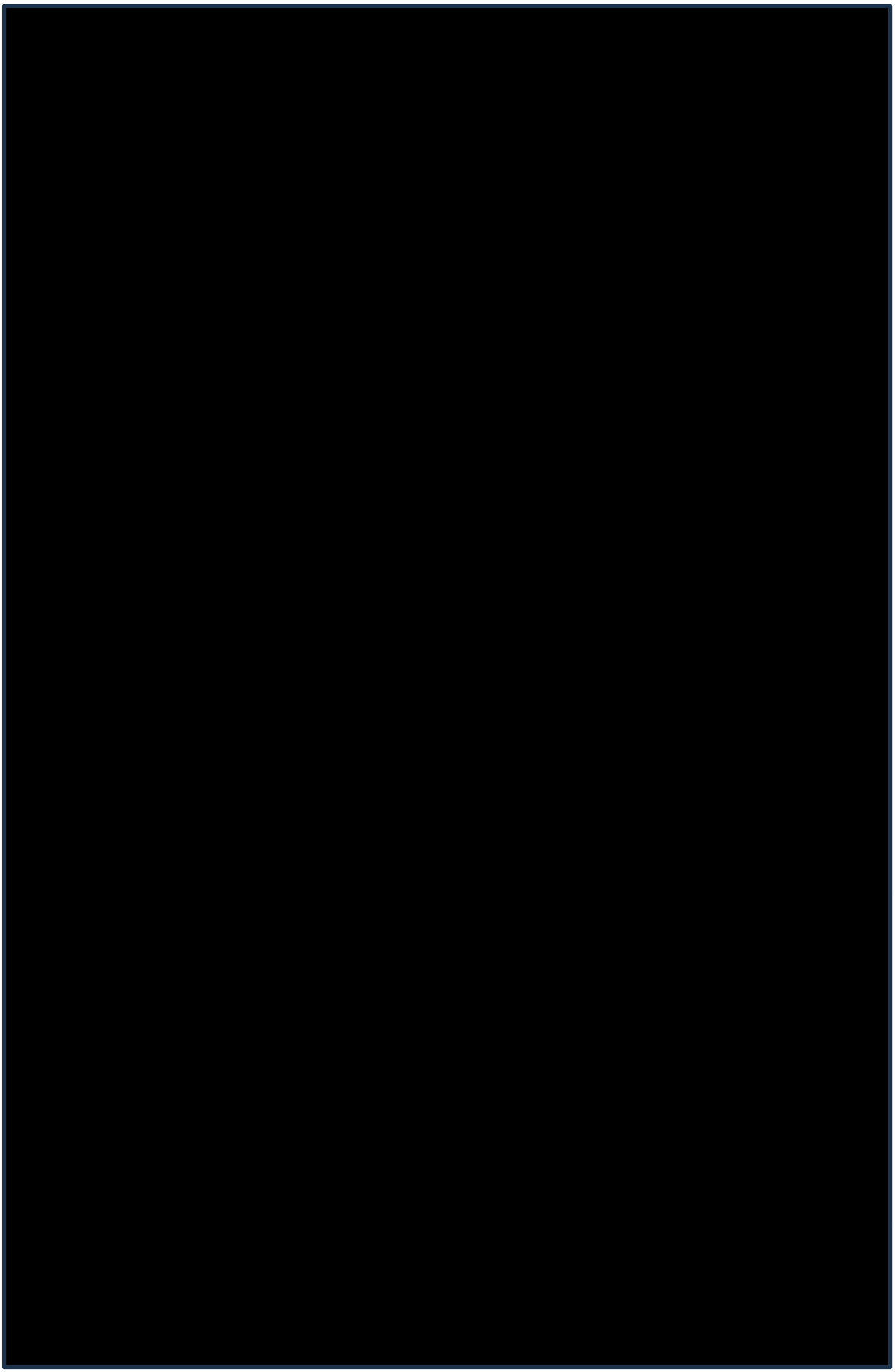

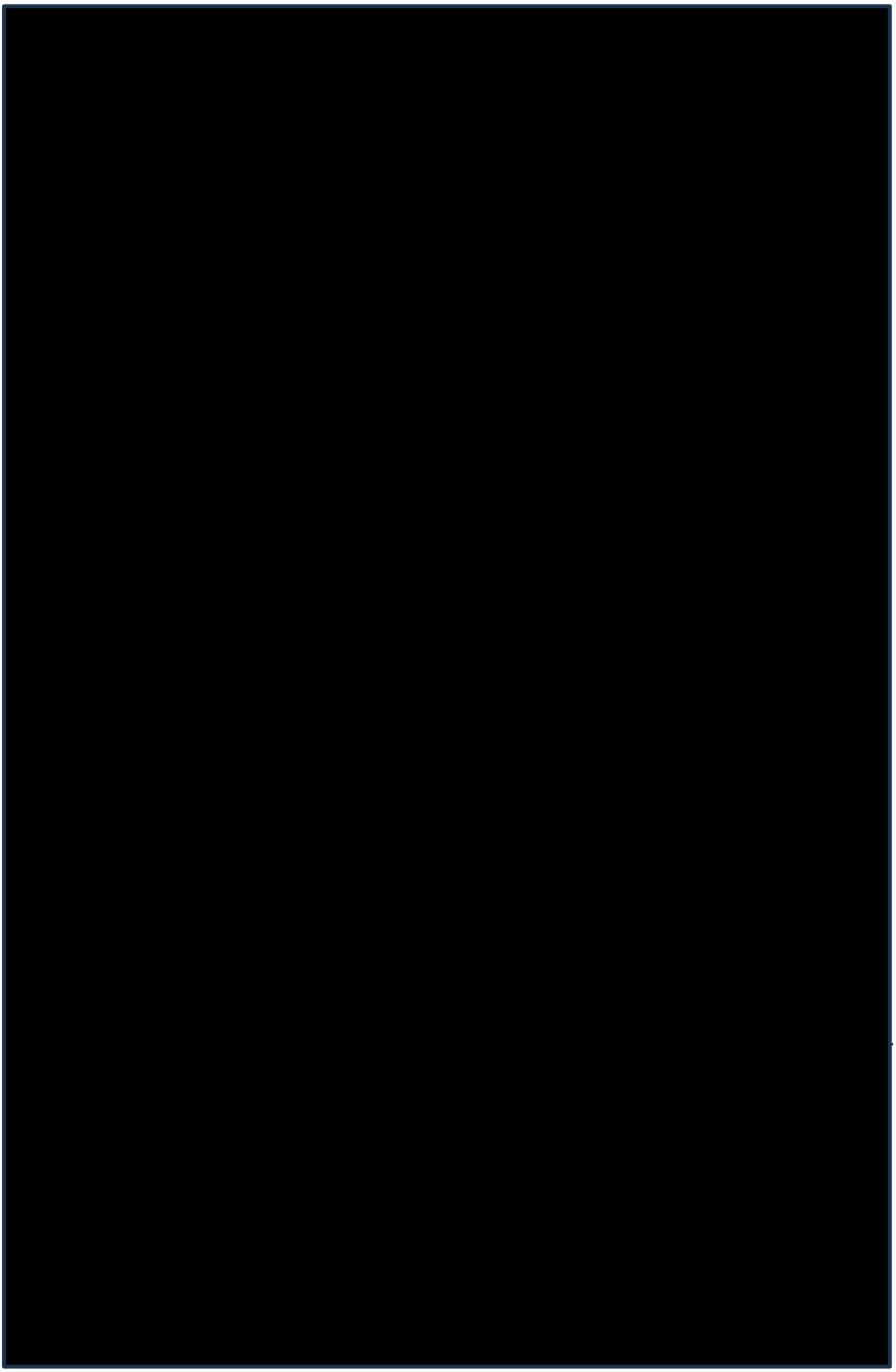

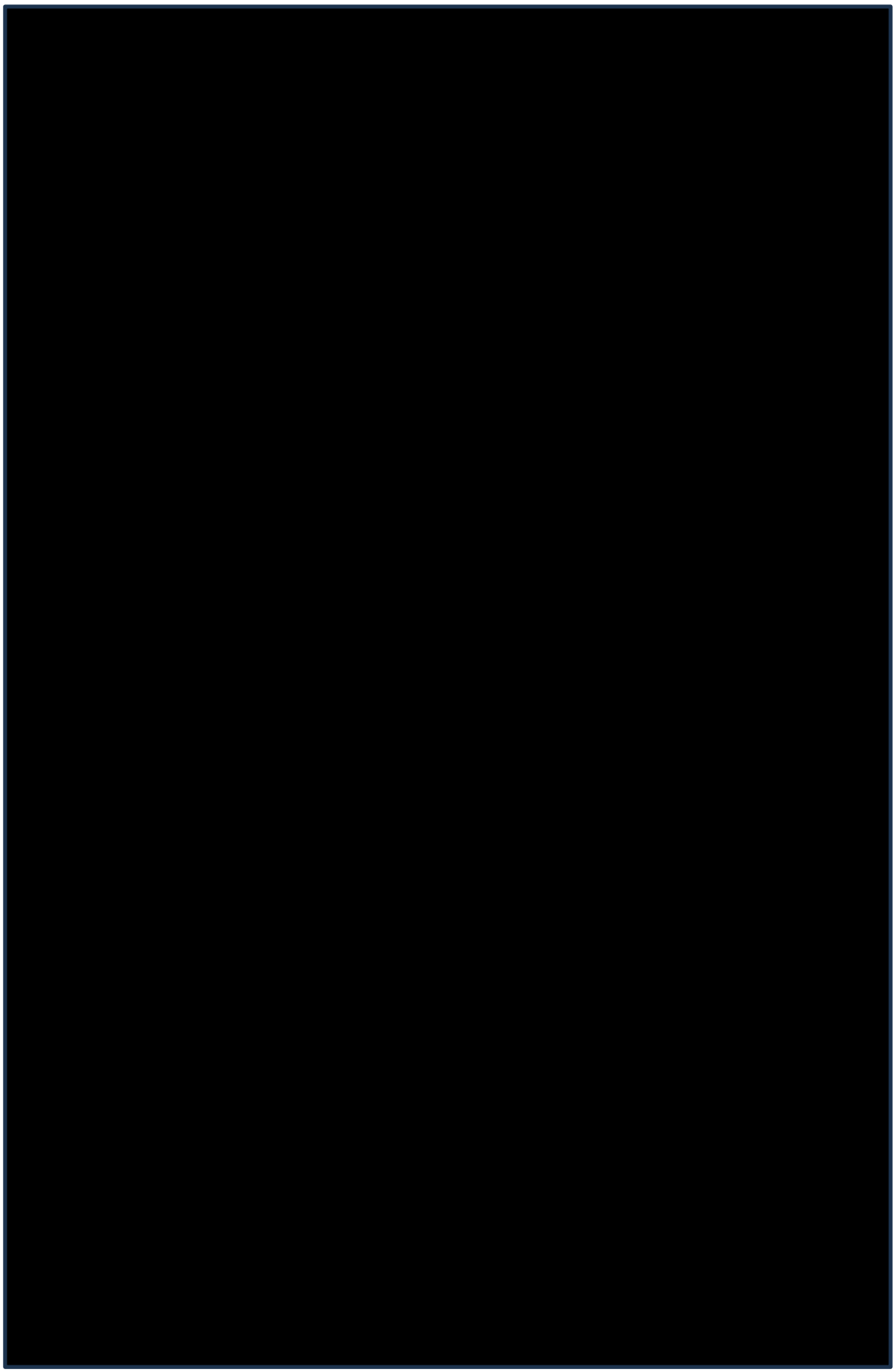

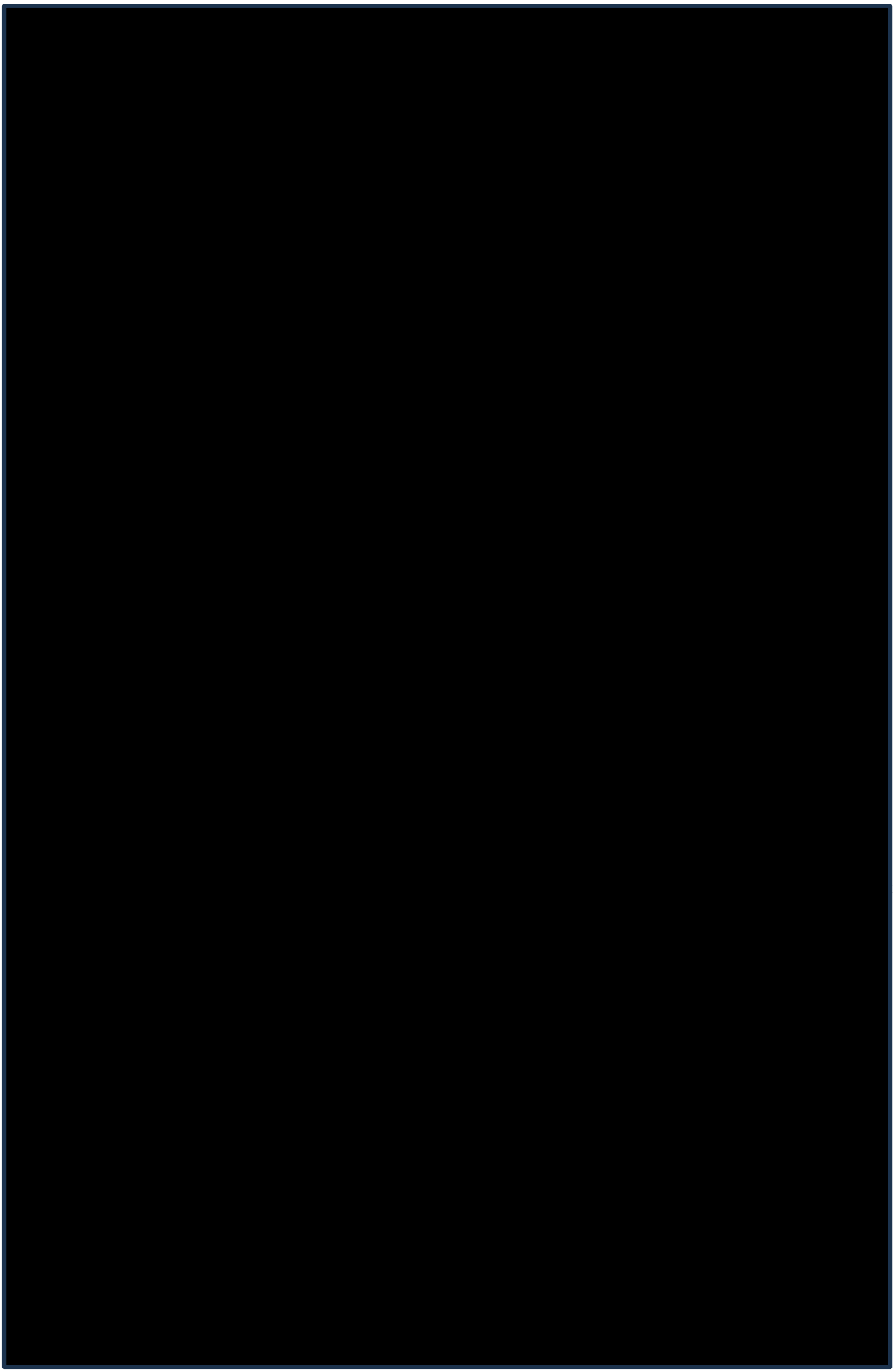

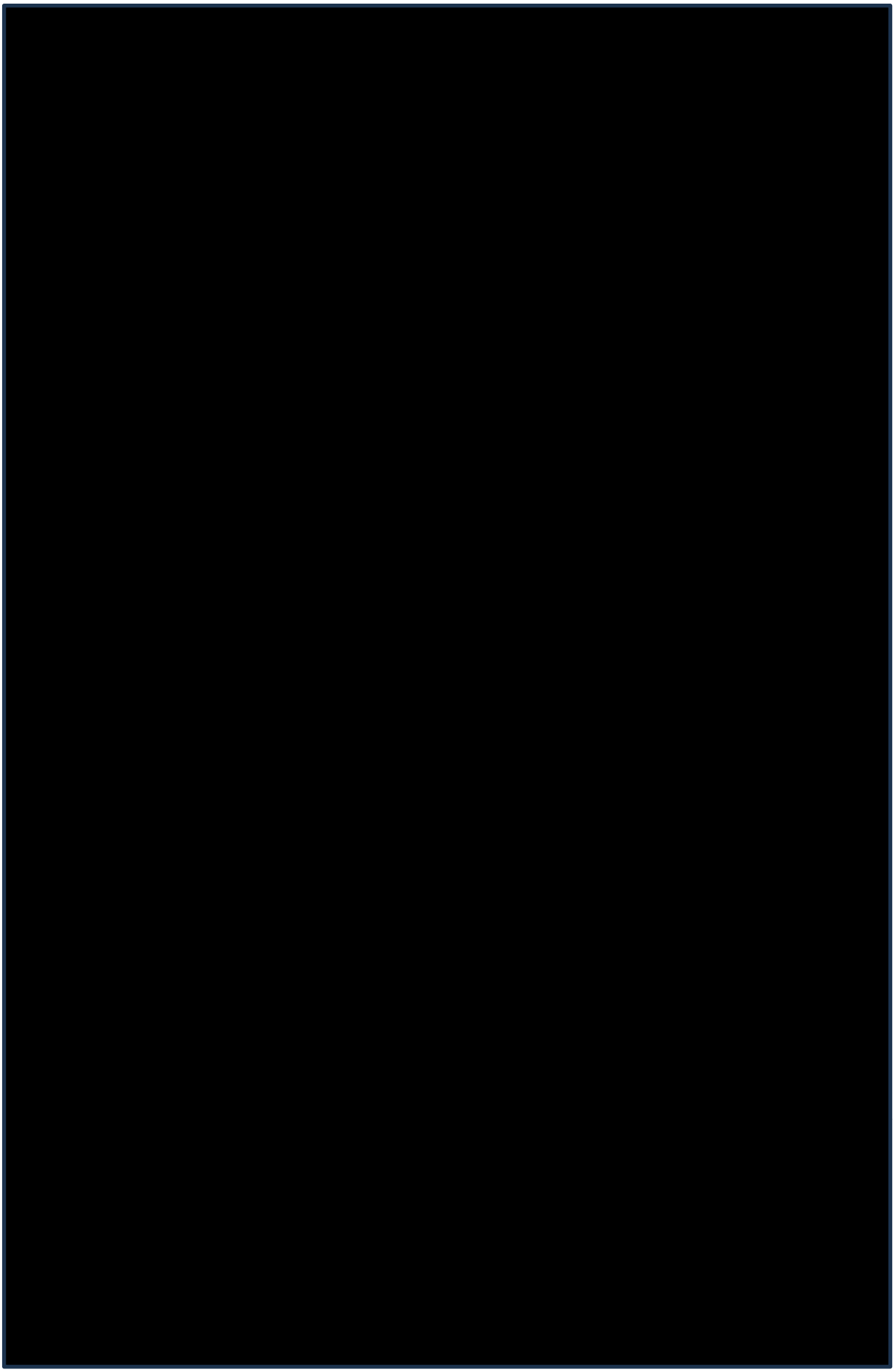

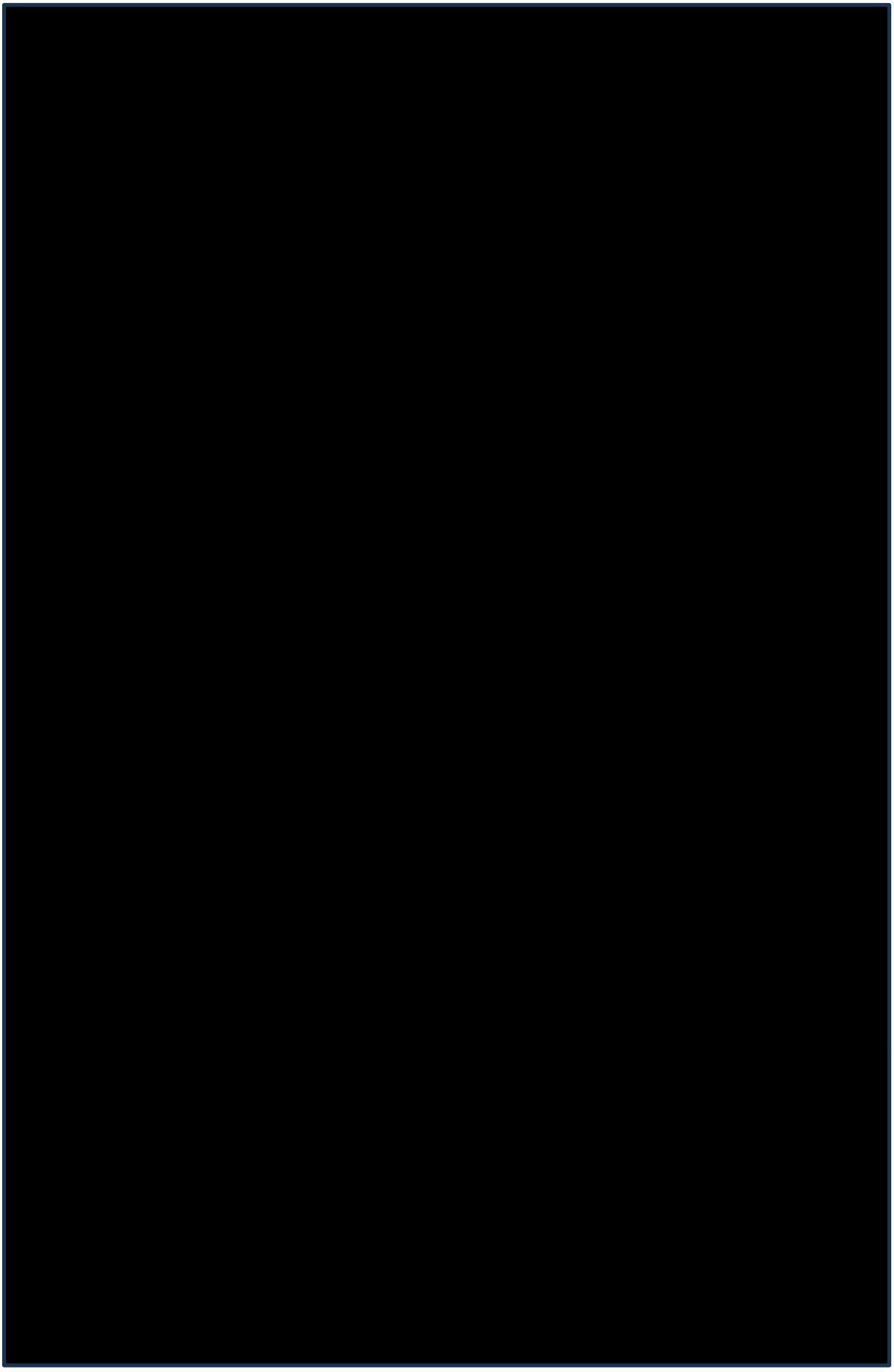

Discussion

Part I: Palmitoylethanolamide influences colon cancer cell proliferation and migration, impacts tumor cell cycle, and exerts beneficial effects in vivo

Although previous studies elucidated PEA's role in breast cancer, prostate cancer, melanoma, neuroblastoma, and lung cancer, its implication in CRC has been incompletely understood, with only one study reporting PEA antiangiogenetic effects on human colon carcinoma cell lines mediated by VEGF downregulation (Sarnelli et al., 2016). Here, we provide new insight into PEA's beneficial impact in vitro as well as in vivo model of CRC, by testing um-PEA. This Ph.D. work showed that the um-PEA affects CRC cell growth, exerts an anti-migratory activity, influences the tumor cell cycle, and effectively reduces cancer development in AOM-model of CRC. First, by analyzing um-PEA's effect on cell proliferation, we tested different time points (up to 96h of exposure) to observe the maximum antiproliferative during incubation. Since the most promising timepoint was 24 hours and 30 μM concentration exerted the most significant antiproliferative effect, we chose this specific timepoint for subsequent testing. The reduced um-PEA's impact after 24 hours of incubation may be attributed to twofold hypotheses, requiring further investigations: i) its enzymatic breakdown (Rankin & Fowler, 2020), as NAAA (the primary enzyme responsible for PEA hydrolysis) is expressed in HCT116 cells; ii) HCT116 cells can activate biological pathways that can counteract the antiproliferative effects of um-PEA. According to previous studies documenting the inhibitory effects of PEA on several types of cancer cells, including melanoma, neuroblastoma, and breast cancer cells, we demonstrated that um-PEA exhibited selective inhibitory effects on cell proliferation in two distinct colon cancer cell lines, HCT116 and Caco-2, without affecting healthy cell proliferation (HCEC) (De Petrocellis et al., 2002; Hamtiaux et al., 2011; Hamtiaux et al., 2012). Among shreds of evidence, previous authors already demonstrated a PEA inhibitory effect on Caco-2 cell growth, with a maximum effect greater than what was observed in our studies (G. Esposito et al., 2014). Further research will clarify this discrepancy. Using the PEA main targets' selective antagonist (Petrosino & Di Marzo, 2017), we detected that the um-PEA mechanism of antiproliferative action is at least partially mediated by PPAR-α and GPR55. Subsequently, this research addressed to PEA effect on cancer cell cycle progression. As a result, um-PEA treatment showed a twofold action: colon cancer cell cycle arrest in G2/M as well as reduction of S phase cell percentage. Since the cyclin B1/CDK1 complex is a key checkpoint regulating G2/M transition, we further investigated this scenario (Malumbres & Barbacid, 2005). Um-PEA can modulate the cyclin B1/CDK1 complex functionality, impacting the tumor cell cycle.

To provide a more detailed understanding of um-PEA's mechanism, we also evaluated whether um-PEA could affect the mTOR pathway, a well-known signaling supporting cancer hallmark, including cell proliferation (Wiese et al., 2023). Based on our data, we proved that um-PEA antiproliferative action is not mediated by the mTOR pathway, since no changes were observed. While our data do not align with the findings of Sarnelli et al. (2016) regarding Caco-2 cells, they are consistent with existing literature that demonstrates the independence of the mTOR pathway in colorectal cancer about the activation of PPAR-α and GPR55, which are the primary targets of our study. As alteration in the G2/M checkpoint has been a well-established DNA-inducing damage factor (Yam, Lim, & Surana, 2022), we also verified the um-PEA effect in this context. Our findings suggest that um-PEA treatment induces DNA damage, providing evidence for the connection between the G2/M cell cycle arrest and the DNA damage caused by PEA. One of the main features of cancer cells is cell migration (Friedl & Wolf, 2003) *via* several mechanisms, enhancing tumor progression (F. Wu et al., 2021). Due to the above findings, we investigated um-PEA's ability to impact CRC cell migration. As a result, HCT116 and Caco-2 cell migration was reduced by um-PEA treatment *via* MMP2, a member of a matrix metalloproteinases family, and TIMP1, the tissue inhibitor matrix metalloproteinase 1, reduction (Dantas et al., 2023; Peng, Zhang, Liu, & Chen, 2023). Lastly, we wonder whether um-PEA could exert anti-cancer properties, representing a druggable target, also in an in vivo model of CRC induced by AOM injection. AOM is a well-known chemical-induced model of CRC that accurately replicates the morphological characteristics of human colorectal cancer (Neufert et al., 2021). By performing quantitative analysis only, um-PEA showed a chemopreventive effect, being able to significantly reduce histopathological hallmarks of CRC, ACF, and tumor number formation, and showing a trend in reducing the number of polyps. The chemopreventive effects of um-PEA could be related to its ability to attenuate in vivo colonic inflammation a well-known risk factor for the development of colon cancer (Borrelli et al., 2015; G. Esposito et al., 2014; Terzic et al., 2010).

Part II: NAAA expression is altered in CRC human biopsies and its pharmacological modulation reduces cancer growth

By employing a multi-faceted approach encompassing both in vivo and in vitro experiments, as well as analysis of human colorectal biopsies, we shed light on the critical role of NAAA in colon carcinogenesis. First, we characterized NAAA's role in vivo by using AM9053, a potent and selective NAAA inhibitor, in two different models of CRC. As corroborated by xenograft model data, NAAA pharmacological modulation demonstrated efficacy in suppressing tumor

growth, and development by increasing selectively OEA, findings underscore the potential therapeutic value of NAAA inhibition in CRC management. Further exploration of the molecular mechanisms underlying NAAA's impact on CRC proliferation unveils intriguing insights. Ki-67 staining, a widely utilized marker for tumor cell proliferation, demonstrated a substantial reduction in proliferative cells upon treatment with AM9053. Interestingly, while AM9053 does not alter the expression of proteins involved in canonical proliferative pathways such as pAKT, ERK1/2, and pS6, it exerts a profound antiproliferative effect, hinting at novel mechanisms of action. Furthermore, AM9053 treatment was able to reduce the number of tumors in the AOM model of CRC. Moreover, we collected tumor secretomes from xenograft mice, to treat or not them with AM9053 and evaluate any changes in crucial protein expression regulating tumor growth. As shown by the data, the secretome derived from CRC xenograft tumors led to a decrease in NAAA expression in CRC cells. Additionally, tumor secretomes from mice treated with AM9053 showed a significant reduction in the expression of EGF family members, which are essential regulators of tumor cell proliferation (Yarden & Sliwkowski, 2001). Further investigation will be required to elucidate the main component of the tumor secretome responsible for the observed effect. Collectively, our findings highlighted the critical role of NAAA in CRC progression. We also addressed our study to in vitro evaluations to further characterize NAAA's action in CRC, by using two different CRC cell lines (i.e., HCT116 and Caco-2). Our observations, coupled with previous findings in bladder cancer cells (Vago, Bettiga, Salonia, Ciuffreda, & Ottria, 2017), highlight the potential role of NAAA inhibition in mitigating tumor metastasis, without impacting healthy cells, a critical aspect of CRC management. provide mechanistic insights into AM9053's antiproliferative effects, we extended our study by conducting pharmacological studies in the presence of main targets-specific antagonists (PPAR-α, TRPV1, and CB receptors) of the principle NAAA substrates (PEA, OEA, and anandamide) (Alexander et al., 2021).These antagonists were incubated with AM9053. The findings of our study indicate that the ability of AM9053 to inhibit cell proliferation in colorectal cancer cells was reduced when PPAR-α or TRPV1 antagonists were used. This suggests that the antiproliferative effects of NAAA inhibition are achieved by increasing the levels of AEs and subsequently activating two specific molecular targets, PPAR-α and TRPV1 receptors. Collectively, AM9053 acts as an indirect agonist on these receptors. To further evaluate the antiproliferative effect of inhibiting NAAA, we also examined whether AM9053 could influence cell cycle progression. Notably, NAAA modulation results in S-phase cell cycle arrest in CRC, accompanied by a simultaneous drop in the proportion of cells in the G0/G1 phase and downregulation of cyclin A2 and CDK2 expression. Furthermore, we noted

that the AM9053 reduced the migration rate of both CRC cell lines, without involving PPAR-α and TRPV1 modulation. By genetically silencing NAAA expression in the HCT116 adenocarcinoma cell line, we provided additional evidence of NAAA's role in the antiproliferative effects of AM9053. We found not only that siNAAA-HCT116 cells exhibited a decreased rate of cell proliferation, but also that AM9053 didn't impact siNAAA-HCT116 cells, supporting the role of NAAA in the effects of AM9053 on CRC cell proliferation and the specificity of the inhibitor for this enzyme at the tested concentration. Significantly, siNAAA-HCT116 cells similarly displayed the S-phase cell cycle arrest observed in AM9053-treated cells, accompanied by a concomitant decrease in cyclin A2 expression. Our study extends beyond in vitro and in vivo investigations to explore the clinical relevance of NAAA in CRC. NAAA levels were further analyzed in human specimens obtained from CRC patients, revealing a striking downregulation of NAAA expression in tumor tissues compared to adjacent healthy tissues. Concurrently, we noticed a marked increase in NAAA primary substrates, PEA, OEA, and AEA levels, suggesting an adaptive response to tumor growth.

Part III: NAAA pharmacological modulation improves intestinal fibrosis via IL-23 signaling

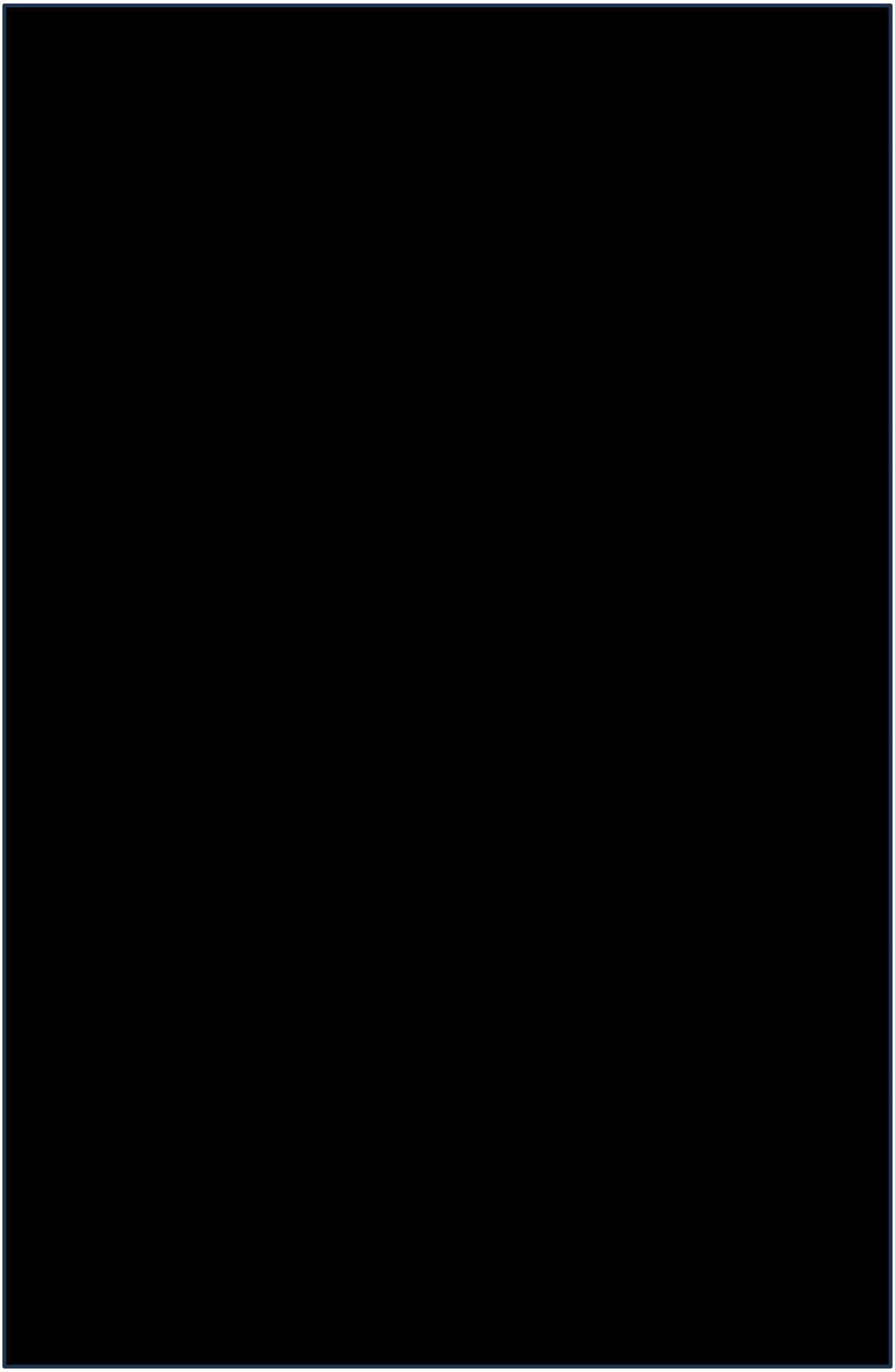

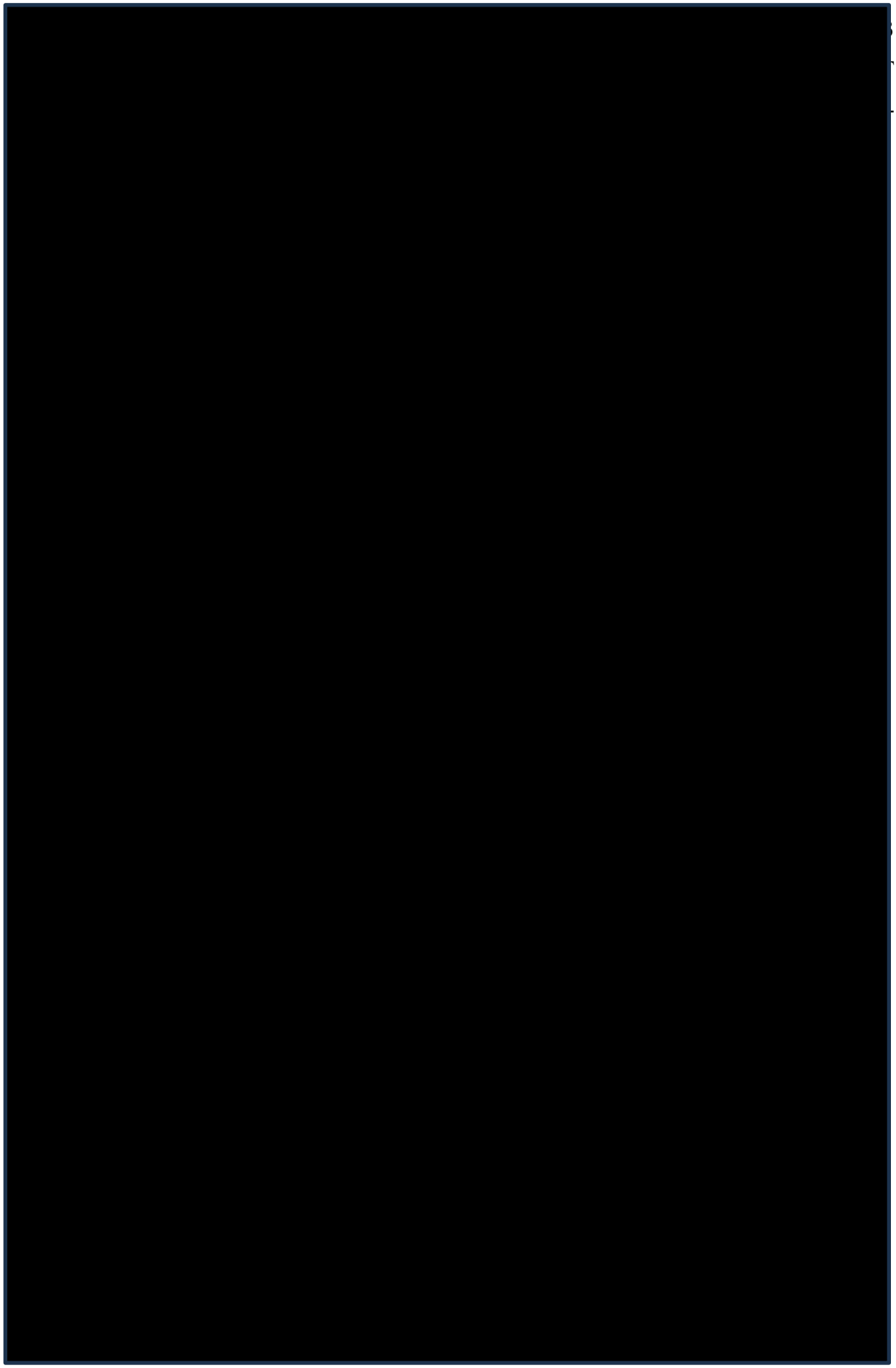

Conclusions

Given the complexity of intestinal disorders, substantial research is necessary to effectively tackle the challenges they present to the global health system. Growing evidence suggests the potential beneficial effect of nutraceuticals (i.e., functional food, food supplements, and herbal plants) as natural bioactive that gaining an increasing role in the treatment of various chronic intestinal diseases, including IBD and CRC. Here we highlighted the role of PEA and its main degradative enzyme (NAAA) in two different, but crucially connected, intestinal diseases: CRC and intestinal fibrosis.

In summary, we have shown that:

- In the context of CRC, PEA is a very promising natural compound, capable of exerting both in vitro (influencing cell proliferation, migration, and inducing cell cycle arrest) and in vivo (by reducing the number of preneoplastic lesions (i.e., ACF) and tumors) beneficial effects. Moreover, PEA's central degradative enzyme modulation (NAAA) by AM9053 showed a helpful outcome by reducing tumor growth and cell proliferation in vitro and induced cell cycle arrest in vivo. Interestingly, in a more translational view, NAAA was found to be downregulated in human CRC tissues, potentially limiting cancer expansion.
- In the context of intestinal inflammation, NAAA pharmacological inhibition with AM9053, showed its favourable outcome to modulate both TNBS-induced gut fibrosis by ameliorating survival rate, inflammation, collagen deposition, fibrosis-related gene expression, and impacting immune response and in vitro inflammation by strongly perturbing IL-23 signalling pathway. Remarkably, in fibrotic CD patients, NAAA expression was dysregulated with a consequential reduction of its primary substrates, suggesting its predictive role.

Overall, our findings provide new insights into role of a nutraceutical compound and its modulation at endogenous level in colon carcinogenesis and intestinal fibrosis pointing to a novel future pharmacological strategy for these intestinal disorder's approaches.

References

Abotchie, P. N., Vernon, S. W., & Du, X. L. (2012). Gender differences in colorectal cancer incidence in the United States, 1975-2006. *J Womens Health (Larchmt), 21*(4), 393-400. doi:10.1089/jwh.2011.2992

Alexander, S. P., Christopoulos, A., Davenport, A. P., Kelly, E., Mathie, A., Peters, J. A., . . . Ye, R. D. (2021). THE CONCISE GUIDE TO PHARMACOLOGY 2021/22: G protein-coupled receptors. *Br J Pharmacol, 178 Suppl 1*, S27-S156. doi:10.1111/bph.15538

Alhouayek, M., Bottemanne, P., Subramanian, K. V., Lambert, D. M., Makriyannis, A., Cani, P. D., & Muccioli, G. G. (2015). N-Acylethanolamine-hydrolyzing acid amidase inhibition increases colon N-palmitoylethanolamine levels and counteracts murine colitis. *FASEB J, 29*(2), 650-661. doi:10.1096/fj.14-255208

Ammendola, R., Parisi, M., Esposito, G., & Cattaneo, F. (2021). Pro-Resolving FPR2 Agonists Regulate NADPH Oxidase-Dependent Phosphorylation of HSP27, OSR1, and MARCKS and Activation of the Respective Upstream Kinases. *Antioxidants (Basel), 10*(1). doi:10.3390/antiox10010134

Ananthakrishnan, A. N., Kaplan, G. G., & Ng, S. C. (2020). Changing Global Epidemiology of Inflammatory Bowel Diseases: Sustaining Health Care Delivery Into the 21st Century. *Clin Gastroenterol Hepatol, 18*(6), 1252-1260. doi:10.1016/j.cgh.2020.01.028

Ban, Q. Y., Liu, M., Ding, N., Chen, Y., Lin, Q., Zha, J. M., & He, W. Q. (2022). Nutraceuticals for the Treatment of IBD: Current Progress and Future Directions. *Front Nutr, 9*, 794169. doi:10.3389/fnut.2022.794169

Bandiera, T., Ponzano, S., & Piomelli, D. (2014). Advances in the discovery of N-acylethanolamine acid amidase inhibitors. *Pharmacol Res, 86*, 11-17. doi:10.1016/j.phrs.2014.04.011

Batkai, S., Pacher, P., Osei-Hyiaman, D., Radaeva, S., Liu, J., Harvey-White, J., . . . Kunos, G. (2004). Endocannabinoids acting at cannabinoid-1 receptors regulate cardiovascular function in hypertension. *Circulation, 110*(14), 1996-2002. doi:10.1161/01.CIR.0000143230.23252.D2

Becker, C., Fantini, M. C., Wirtz, S., Nikolaev, A., Kiesslich, R., Lehr, H. A., . . . Neurath, M. F. (2005). In vivo imaging of colitis and colon cancer development in mice using high resolution chromoendoscopy. *Gut, 54*(7), 950-954. doi:10.1136/gut.2004.061283

Benson, A. B., Venook, A. P., Al-Hawary, M. M., Arain, M. A., Chen, Y. J., Ciombor, K. K., . . . Gurski, L. A. (2021). Colon Cancer, Version 2.2021, NCCN Clinical Practice Guidelines in Oncology. *J Natl Compr Canc Netw, 19*(3), 329-359. doi:10.6004/jnccn.2021.0012

Bhatt, A. P., Redinbo, M. R., & Bultman, S. J. (2017). The role of the microbiome in cancer development and therapy. *CA Cancer J Clin, 67*(4), 326-344. doi:10.3322/caac.21398

Bonezzi, F. T., Sasso, O., Pontis, S., Realini, N., Romeo, E., Ponzano, S., . . . Piomelli, D. (2016). An Important Role for N-Acylethanolamine Acid Amidase in the Complete Freund's Adjuvant Rat Model of Arthritis. *J Pharmacol Exp Ther, 356*(3), 656-663. doi:10.1124/jpet.115.230516

Borrelli, F., Romano, B., Petrosino, S., Pagano, E., Capasso, R., Coppola, D., . . . Izzo, A. A. (2015). Palmitoylethanolamide, a naturally occurring lipid, is an orally effective intestinal anti-inflammatory agent. *Br J Pharmacol, 172*(1), 142-158. doi:10.1111/bph.12907

Bottemanne, P., Guillemot-Legris, O., Paquot, A., Masquelier, J., Malamas, M., Makriyannis, A., . . . Muccioli, G. G. (2021). N-Acylethanolamine-Hydrolyzing Acid Amidase Inhibition, but Not Fatty Acid Amide Hydrolase Inhibition, Prevents the Development

of Experimental Autoimmune Encephalomyelitis in Mice. *Neurotherapeutics, 18*(3), 1815-1833. doi:10.1007/s13311-021-01074-x

Bottemanne, P., Muccioli, G. G., & Alhouayek, M. (2018). N-acylethanolamine hydrolyzing acid amidase inhibition: tools and potential therapeutic opportunities. *Drug Discov Today, 23*(8), 1520-1529. doi:10.1016/j.drudis.2018.03.007

Breynaert, C., de Bruyn, M., Arijs, I., Cremer, J., Martens, E., Van Lommel, L., . . . Van Assche, G. (2016). Genetic Deletion of Tissue Inhibitor of Metalloproteinase-1/TIMP-1 Alters Inflammation and Attenuates Fibrosis in Dextran Sodium Sulphate-induced Murine Models of Colitis. *J Crohns Colitis, 10*(11), 1336-1350. doi:10.1093/ecco-jcc/jjw101

Buranaamnuay, K. (2021). The MTT assay application to measure the viability of spermatozoa: A variety of the assay protocols. *Open Vet J, 11*(2), 251-269. doi:10.5455/OVJ.2021.v11.i2.9

Burke, J. P., Cunningham, M. F., Sweeney, C., Docherty, N. G., & O'Connell, P. R. (2011). N-cadherin is overexpressed in Crohn's stricture fibroblasts and promotes intestinal fibroblast migration. *Inflamm Bowel Dis, 17*(8), 1665-1673. doi:10.1002/ibd.21543

Cabral-Pacheco, G. A., Garza-Veloz, I., Castruita-De la Rosa, C., Ramirez-Acuna, J. M., Perez-Romero, B. A., Guerrero-Rodriguez, J. F., . . . Martinez-Fierro, M. L. (2020). The Roles of Matrix Metalloproteinases and Their Inhibitors in Human Diseases. *Int J Mol Sci, 21*(24). doi:10.3390/ijms21249739

Cassotta, M., Cianciosi, D., De Giuseppe, R., Navarro-Hortal, M. D., Armas Diaz, Y., Forbes-Hernández, T. Y., Pifarre, K. T., Pascual Barrera, A. E., Grosso, G., Xiao, J., Battino, M., & Giampieri, F. (2023). Possible role of nutrition in the prevention of inflammatory bowel disease-related colorectal cancer: A focus on human studies. Nutrition (Burbank, Los Angeles County, Calif.), 110, 111980. https://doi.org/10.1016/j.nut.2023.111980

Chalkidi, N., Paraskeva, C., & Koliaraki, V. (2022). Fibroblasts in intestinal homeostasis, damage, and repair. *Front Immunol, 13*, 924866. doi:10.3389/fimmu.2022.924866

Chao, H. M., Wang, T. W., Chern, E., & Hsu, S. H. (2022). Regulatory RNAs, microRNA, long-non coding RNA and circular RNA roles in colorectal cancer stem cells. World journal of gastrointestinal oncology, 14(4), 748–764. https://doi.org/10.4251/wjgo.v14.i4.748

Chey W. D. (2013). The role of food in the functional gastrointestinal disorders: introduction to a manuscript series. The American journal of gastroenterology, 108(5), 694–697. https://doi.org/10.1038/ajg.2013.62

Cho, S. K., Bekaii-Saab, T., Kavati, A., Babajanyan, S., Hocum, B., & Barzi, A. (2022). Value-Based Analysis of Therapies in Refractory Metastatic Colorectal Cancer in US. *Clin Colorectal Cancer, 21*(4), 277-284. doi:10.1016/j.clcc.2022.09.003

Chung, S. C., Hammarsten, P., Josefsson, A., Stattin, P., Granfors, T., Egevad, L., . . . Fowler, C. J. (2009). A high cannabinoid CB(1) receptor immunoreactivity is associated with disease severity and outcome in prostate cancer. *Eur J Cancer, 45*(1), 174-182. doi:10.1016/j.ejca.2008.10.010

Correia-Sa, I. B., Carvalho, C. M., Serrao, P. V., Machado, V. A., Carvalho, S. O., Marques, M., & Vieira-Coelho, M. A. (2021). AM251, a cannabinoid receptor 1 antagonist, prevents human fibroblasts differentiation and collagen deposition induced by TGF-beta - An in vitro study. *Eur J Pharmacol, 892*, 173738. doi:10.1016/j.ejphar.2020.173738

Corsello, A., Pugliese, D., Gasbarrini, A., & Armuzzi, A. (2020). Diet and Nutrients in Gastrointestinal Chronic Diseases. Nutrients, 12(9), 2693. https://doi.org/10.3390/nu12092693

Couch, D. G., Tasker, C., Theophilidou, E., Lund, J. N., & O'Sullivan, S. E. (2017). Cannabidiol and palmitoylethanolamide are anti-inflammatory in the acutely inflamed human colon. *Clin Sci (Lond), 131*(21), 2611-2626. doi:10.1042/CS20171288

Cravatt, B. F., Demarest, K., Patricelli, M. P., Bracey, M. H., Giang, D. K., Martin, B. R., & Lichtman, A. H. (2001). Supersensitivity to anandamide and enhanced endogenous cannabinoid signaling in mice lacking fatty acid amide hydrolase. *Proc Natl Acad Sci U S A, 98*(16), 9371-9376. doi:10.1073/pnas.161191698

D'Alessio, S., Ungaro, F., Noviello, D., Lovisa, S., Peyrin-Biroulet, L., & Danese, S. (2022). Revisiting fibrosis in inflammatory bowel disease: the gut thickens. *Nat Rev Gastroenterol Hepatol, 19*(3), 169-184. doi:10.1038/s41575-021-00543-0

Danesi, F., & Ferguson, L. R. (2017). Could Pomegranate Juice Help in the Control of Inflammatory Diseases? *Nutrients, 9*(9). doi:10.3390/nu9090958

Dantas, E., Murthy, A., Ahmed, T., Ahmed, M., Ramsamooj, S., Hurd, M. A., . . . Goncalves, M. D. (2023). TIMP1 is an early biomarker for detection and prognosis of lung cancer. *Clin Transl Med, 13*(10), e1391. doi:10.1002/ctm2.1391

De Conno, B., Pesce, M., Chiurazzi, M., Andreozzi, M., Rurgo, S., Corpetti, C., Seguella, L., Del Re, A., Palenca, I., Esposito, G., & Sarnelli, G. (2022). Nutraceuticals and Diet Supplements in Crohn's Disease: A General Overview of the Most Promising Approaches in the Clinic. Foods (Basel, Switzerland), 11(7), 1044. https://doi.org/10.3390/foods11071044

De Petrocellis, L., Bisogno, T., Ligresti, A., Bifulco, M., Melck, D., & Di Marzo, V. (2002). Effect on cancer cell proliferation of palmitoylethanolamide, a fatty acid amide interacting with both the cannabinoid and vanilloid signalling systems. *Fundam Clin Pharmacol, 16*(4), 297-302. doi:10.1046/j.1472-8206.2002.00094.x

Desai, D., & Dhoble, P. (2024). Rapidly changing epidemiology of inflammatory bowel disease: Time to gear up for the challenge before it is too late. *Indian J Gastroenterol, 43*(1), 15-17. doi:10.1007/s12664-023-01453-6

Devane, W. A., Hanus, L., Breuer, A., Pertwee, R. G., Stevenson, L. A., Griffin, G., . . . Mechoulam, R. (1992). Isolation and structure of a brain constituent that binds to the cannabinoid receptor. *Science, 258*(5090), 1946-1949. doi:10.1126/science.1470919

Di Marzo, V., & Piscitelli, F. (2015). The Endocannabinoid System and its Modulation by Phytocannabinoids. *Neurotherapeutics, 12*(4), 692-698. doi:10.1007/s13311-015-0374-6

Dick, M. K., Miao, J. H., & Limaiem, F. (2024). Histology, Fibroblast. In *StatPearls*. Treasure Island (FL) ineligible companies. Disclosure: Julia Miao declares no relevant financial relationships with ineligible companies. Disclosure: Faten Limaiem declares no relevant financial relationships with ineligible companies.

Dmochowska, N., Tieu, W., Keller, M. D., Hollis, C. A., Campaniello, M. A., Mavrangelos, C., . . . Hughes, P. A. (2020). (89)Zr-pro-MMP-9 F(ab')(2) detects colitis induced intestinal and kidney fibrosis. *Sci Rep, 10*(1), 20372. doi:10.1038/s41598-020-77390-7

Du, F., Li, Y., Zhang, W., Kale, S. P., McFerrin, H., Davenport, I., . . . Zhang, Q. J. (2016). Highly and moderately aggressive mouse ovarian cancer cell lines exhibit differential gene expression. *Tumor Biol, 37*(8), 11147-11162. doi:10.1007/s13277-015-4518-4

Eberlein, B., Eicke, C., Reinhardt, H. W., & Ring, J. (2008). Adjuvant treatment of atopic eczema: assessment of an emollient containing N-palmitoylethanolamine (ATOPA study). *J Eur Acad Dermatol Venereol, 22*(1), 73-82. doi:10.1111/j.1468-3083.2007.02351.x

Edge, S. B., & Compton, C. C. (2010). The American Joint Committee on Cancer: the 7th edition of the AJCC cancer staging manual and the future of TNM. *Ann Surg Oncol, 17*(6), 1471-1474. doi:10.1245/s10434-010-0985-4

Edwards, B. K., Ward, E., Kohler, B. A., Eheman, C., Zauber, A. G., Anderson, R. N., . . . Ries, L. A. (2010). Annual report to the nation on the status of cancer, 1975-2006, featuring colorectal cancer trends and impact of interventions (risk factors, screening, and treatment) to reduce future rates. *Cancer, 116*(3), 544-573. doi:10.1002/cncr.24760

Esposito, E., & Cuzzocrea, S. (2013). Palmitoylethanolamide is a new possible pharmacological treatment for the inflammation associated with trauma. *Mini Rev Med Chem, 13*(2), 237-255.

Esposito, G., Capoccia, E., Turco, F., Palumbo, I., Lu, J., Steardo, A., . . . Steardo, L. (2014). Palmitoylethanolamide improves colon inflammation through an enteric glia/toll like receptor 4-dependent PPAR-alpha activation. *Gut, 63*(8), 1300-1312. doi:10.1136/gutjnl-2013-305005

Fraguas-Sanchez, A. I., Martin-Sabroso, C., & Torres-Suarez, A. I. (2018). Insights into the effects of the endocannabinoid system in cancer: a review. *Br J Pharmacol, 175*(13), 2566-2580. doi:10.1111/bph.14331

Friedl, P., & Wolf, K. (2003). Tumor-cell invasion and migration: diversity and escape mechanisms. *Nat Rev Cancer, 3*(5), 362-374. doi:10.1038/nrc1075

Friedrich, M., Pohin, M., & Powrie, F. (2019). Cytokine Networks in the Pathophysiology of Inflammatory Bowel Disease. *Immunity, 50*(4), 992-1006. doi:10.1016/j.immuni.2019.03.017

Frolkis, A., Dieleman, L. A., Barkema, H. W., Panaccione, R., Ghosh, S., Fedorak, R. N., . . . Alberta, I. B. D. C. (2013). Environment and the inflammatory bowel diseases. *Can J Gastroenterol, 27*(3), e18-24. doi:10.1155/2013/102859

Gaffen, S. L., Jain, R., Garg, A. V., & Cua, D. J. (2014). The IL-23-IL-17 immune axis: from mechanisms to therapeutic testing. *Nat Rev Immunol, 14*(9), 585-600. doi:10.1038/nri3707

Gagliardi, A., Molinaro, R., Fresta, M., Duranti, A., & Cosco, D. (2022). alpha-Acylamino-beta-lactone N-Acylethanolamine-hydrolyzing Acid Amidase Inhibitors Encapsulated in PLGA Nanoparticles: Improvement of the Physical Stability and Protection of Human Cells from Hydrogen Peroxide-Induced Oxidative Stress. *Antioxidants (Basel), 11*(4). doi:10.3390/antiox11040686

Gamallat, Y., Meyiah, A., Kuugbee, E. D., Hago, A. M., Chiwala, G., Awadasseid, A., . . . Xin, Y. (2016). Lactobacillus rhamnosus induced epithelial cell apoptosis, ameliorates inflammation and prevents colon cancer development in an animal model. *Biomed Pharmacother, 83*, 536-541. doi:10.1016/j.biopha.2016.07.001

Gao, L. Q., Xu, J., & Chen, S. D. (2020). In Silico Screening of Potential Chinese Herbal Medicine Against COVID-19 by Targeting SARS-CoV-2 3CLpro and Angiotensin Converting Enzyme II Using Molecular

Geng, Z., Chen, M., Yu, Q., Guo, S., Chen, T., & Liu, D. (2023). Histone Modification of Colorectal Cancer by Natural Products. Pharmaceuticals (Basel, Switzerland), 16(8), 1095. https://doi.org/10.3390/ph16081095 Docking. *Chin J Integr Med, 26*(7), 527-532. doi:10.1007/s11655-020-3476-x

Gieseck, R. L., 3rd, Wilson, M. S., & Wynn, T. A. (2018). Type 2 immunity in tissue repair and fibrosis. *Nat Rev Immunol, 18*(1), 62-76. doi:10.1038/nri.2017.90

Glocker, E., & Grimbacher, B. (2012). Inflammatory bowel disease: is it a primary immunodeficiency? *Cell Mol Life Sci, 69*(1), 41-48. doi:10.1007/s00018-011-0837-9

Gobbi, G., Bambico, F. R., Mangieri, R., Bortolato, M., Campolongo, P., Solinas, M., . . . Piomelli, D. (2005). Antidepressant-like activity and modulation of brain monoaminergic transmission by blockade of anandamide hydrolysis. *Proc Natl Acad Sci U S A, 102*(51), 18620-18625. doi:10.1073/pnas.0509591102

Gouveia-Figueira, S., & Nording, M. L. (2014). Development and validation of a sensitive UPLC-ESI-MS/MS method for the simultaneous quantification of 15 endocannabinoids and related compounds in milk and other biofluids. *Anal Chem, 86*(2), 1186-1195. doi:10.1021/ac403352e

Guo, S., Zhao, W., Zhang, W., Li, S., Teng, G., & Liu, L. (2023). Vitamin D Promotes Ferroptosis in Colorectal Cancer Stem Cells via SLC7A11 Downregulation. Oxidative medicine and cellular longevity, 2023, 4772134. https://doi.org/10.1155/2023/4772134

Gupta, S., Bharti, B., Ahnen, D. J., Buchanan, D. D., Cheng, I. C., Cotterchio, M., . . . Martinez, M. E. (2020). Potential impact of family history-based screening guidelines on the detection of early-onset colorectal cancer. *Cancer, 126*(13), 3013-3020. doi:10.1002/cncr.32851

Gustavsson, B., Carlsson, G., Machover, D., Petrelli, N., Roth, A., Schmoll, H. J., . . . Gibson, F. (2015). A review of the evolution of systemic chemotherapy in the management of colorectal cancer. *Clin Colorectal Cancer, 14*(1), 1-10. doi:10.1016/j.clcc.2014.11.002

Hamtiaux, L., Hansoulle, L., Dauguet, N., Muccioli, G. G., Gallez, B., & Lambert, D. M. (2011). Increasing antiproliferative properties of endocannabinoids in N1E-115 neuroblastoma cells through inhibition of their metabolism. *PLoS One, 6*(10), e26823. doi:10.1371/journal.pone.0026823

Hamtiaux, L., Masquelier, J., Muccioli, G. G., Bouzin, C., Feron, O., Gallez, B., & Lambert, D. M. (2012). The association of N-palmitoylethanolamine with the FAAH inhibitor URB597 impairs melanoma growth through a supra-additive action. *BMC Cancer, 12*, 92. doi:10.1186/1471-2407-12-92

Heichman, K. A., & Roberts, J. M. (1994). Rules to replicate by. *Cell, 79*(4), 557-562. doi:10.1016/0092-8674(94)90541-x

Ho, W. S., Barrett, D. A., & Randall, M. D. (2008). 'Entourage' effects of N-palmitoylethanolamide and N-oleoylethanolamide on vasorelaxation to anandamide occur through TRPV1 receptors. *Br J Pharmacol, 155*(6), 837-846. doi:10.1038/bjp.2008.324

Hossain, M. S., Karuniawati, H., Jairoun, A. A., Urbi, Z., Ooi, J., John, A., . . . Hadi, M. A. (2022). Colorectal Cancer: A Review of Carcinogenesis, Global Epidemiology, Current Challenges, Risk Factors, Preventive and Treatment Strategies. *Cancers (Basel), 14*(7). doi:10.3390/cancers14071732

Huang, D., Shen, J., Zhai, L., Chen, H., Fei, J., Zhu, X., & Zhou, J. (2021). Insights Into the Prognostic Value and Immunological Role of NAAA in Pan-Cancer. *Front Immunol, 12*, 812713. doi:10.3389/fimmu.2021.812713

Iannotti, F. A., Di Marzo, V., & Petrosino, S. (2016). Endocannabinoids and endocannabinoid-related mediators: Targets, metabolism and role in neurological disorders. *Prog Lipid Res, 62*, 107-128. doi:10.1016/j.plipres.2016.02.002

Izzo, A. A., Aviello, G., Petrosino, S., Orlando, P., Marsicano, G., Lutz, B., . . . Endocannabinoid Research, G. (2008). Increased endocannabinoid levels reduce the development of precancerous lesions in the mouse colon. *J Mol Med (Berl), 86*(1), 89-98. doi:10.1007/s00109-007-0248-4

Islam, M. R., Akash, S., Rahman, M. M., Nowrin, F. T., Akter, T., Shohag, S., Rauf, A., Aljohani, A. S. M., & Simal-Gandara, J. (2022). Colon cancer and colorectal cancer: Prevention and treatment by potential natural products. Chemico-biological interactions, 368, 110170. https://doi.org/10.1016/j.cbi.2022.110170

Jayasinghe, M., Karunanayake, V., Mohtashim, A., Caldera, D., Mendis, P., Prathiraja, O., Rashidi, F., & Damianos, J. A. (2024). The Role of Diet in the Management of Irritable Bowel Syndrome: A Comprehensive Review. Cureus, 16(2), e54244. https://doi.org/10.7759/cureus.54244

Ji, Q., Liu, X., Fu, X., Zhang, L., Sui, H., Zhou, L., Sun, J., Cai, J., Qin, J., Ren, J., & Li, Q. (2013). Resveratrol inhibits invasion and metastasis of colorectal cancer cells via MALAT1 mediated Wnt/β-catenin signal pathway. PloS one, 8(11), e78700. https://doi.org/10.1371/journal.pone.0078700

Jiang, H. Y., Zhang, X., Yu, Z. H., Zhang, Z., Deng, M., Zhao, J. H., & Ruan, B. (2018). Altered gut microbiota profile in patients with generalized anxiety disorder. *J Psychiatr Res, 104*, 130-136. doi:10.1016/j.jpsychires.2018.07.007

Kalluri, R., & Weinberg, R. A. (2009). The basics of epithelial-mesenchymal transition. *J Clin Invest, 119*(6), 1420-1428. doi:10.1172/JCI39104

Kaplan, G. G., & Ng, S. C. (2017). Understanding and Preventing the Global Increase of Inflammatory Bowel Disease. *Gastroenterology, 152*(2), 313-321 e312. doi:10.1053/j.gastro.2016.10.020

Karamanos, N. K., Theocharis, A. D., Piperigkou, Z., Manou, D., Passi, A., Skandalis, S. S., . . . Onisto, M. (2021). A guide to the composition and functions of the extracellular matrix. *FEBS J, 288*(24), 6850-6912. doi:10.1111/febs.15776

Kathuria, S., Gaetani, S., Fegley, D., Valino, F., Duranti, A., Tontini, A., . . . Piomelli, D. (2003). Modulation of anxiety through blockade of anandamide hydrolysis. *Nat Med, 9*(1), 76-81. doi:10.1038/nm803

Kaulmann, A., & Bohn, T. (2016). Bioactivity of Polyphenols: Preventive and Adjuvant Strategies toward Reducing Inflammatory Bowel Diseases-Promises, Perspectives, and Pitfalls. *Oxid Med Cell Longev, 2016*, 9346470. doi:10.1155/2016/9346470

Khan, I., Ullah, N., Zha, L., Bai, Y., Khan, A., Zhao, T., . . . Zhang, C. (2019). Alteration of Gut Microbiota in Inflammatory Bowel Disease (IBD): Cause or Consequence? IBD Treatment Targeting the Gut Microbiome. *Pathogens, 8*(3). doi:10.3390/pathogens8030126

Knowles, S. R., Graff, L. A., Wilding, H., Hewitt, C., Keefer, L., & Mikocka-Walus, A. (2018). Quality of Life in Inflammatory Bowel Disease: A Systematic Review and Meta-analyses-Part I. *Inflamm Bowel Dis, 24*(4), 742-751. doi:10.1093/ibd/izx100

Kofla-Dlubacz, A., Pytrus, T., Akutko, K., Sputa-Grzegrzolka, P., Piotrowska, A., & Dziegiel, P. (2022). Etiology of IBD-Is It Still a Mystery? *Int J Mol Sci, 23*(20). doi:10.3390/ijms232012445

Koliaraki, V., Prados, A., Armaka, M., & Kollias, G. (2020). The mesenchymal context in inflammation, immunity and cancer. *Nat Immunol, 21*(9), 974-982. doi:10.1038/s41590-020-0741-2

Kvakova, M., Kamlarova, A., Stofilova, J., Benetinova, V., & Bertkova, I. (2022). Probiotics and postbiotics in colorectal cancer: Prevention and complementary therapy. World journal of gastroenterology, 28(27), 3370–3382. https://doi.org/10.3748/wjg.v28.i27.3370

Kuppusamy, P., Yusoff, M. M., Maniam, G. P., Ichwan, S. J., Soundharrajan, I., & Govindan, N. (2014). Nutraceuticals as potential therapeutic agents for colon cancer: a review. *Acta Pharm Sin B, 4*(3), 173-181. doi:10.1016/j.apsb.2014.04.002

Lam, P. M., Marczylo, T. H., & Konje, J. C. (2010). Simultaneous measurement of three N-acylethanolamides in human bio-matrices using ultra performance liquid chromatography-tandem mass spectrometry. *Anal Bioanal Chem, 398*(5), 2089-2097. doi:10.1007/s00216-010-4103-z

Latella, G., & Viscido, A. (2020). Controversial Contribution of Th17/IL-17 Toward the Immune Response in Intestinal Fibrosis. *Dig Dis Sci, 65*(5), 1299-1306. doi:10.1007/s10620-020-06161-1

Lawrance, I. C., Wu, F., Leite, A. Z., Willis, J., West, G. A., Fiocchi, C., & Chakravarti, S. (2003). A murine model of chronic inflammation-induced intestinal fibrosis down-regulated by antisense NF-kappa B. *Gastroenterology, 125*(6), 1750-1761. doi:10.1053/j.gastro.2003.08.027

Leeb, S. N., Vogl, D., Falk, W., Scholmerich, J., Rogler, G., & Gelbmann, C. M. (2002). Regulation of migration of human colonic myofibroblasts. *Growth Factors, 20*(2), 81-91. doi:10.1080/08977190290031941

Liu, X., Xin, Z., & Wang, K. (2023). Patient-derived xenograft model in colorectal cancer basic and translational research. *Animal Model Exp Med, 6*(1), 26-40. doi:10.1002/ame2.12299

Liu, Y., Chen, J., Sethi, A., Li, Q. K., Chen, L., Collins, B., . . . Aebersold, R. (2014). Glycoproteomic analysis of prostate cancer tissues by SWATH mass spectrometry discovers N-acylethanolamine acid amidase and protein tyrosine kinase 7 as signatures for tumor aggressiveness. *Mol Cell Proteomics, 13*(7), 1753-1768. doi:10.1074/mcp.M114.038273

Lovisa, S., Genovese, G., & Danese, S. (2019). Role of Epithelial-to-Mesenchymal Transition in Inflammatory Bowel Disease. *J Crohns Colitis, 13*(5), 659-668. doi:10.1093/ecco-jcc/jjy201

Lu, R., Neff, N. F., Quake, S. R., & Weissman, I. L. (2011). Tracking single hematopoietic stem cells in vivo using high-throughput sequencing in conjunction with viral genetic barcoding. *Nat Biotechnol, 29*(10), 928-933. doi:10.1038/nbt.1977

Luebeck, E. G., & Moolgavkar, S. H. (2002). Multistage carcinogenesis and the incidence of colorectal cancer. *Proc Natl Acad Sci U S A, 99*(23), 15095-15100. doi:10.1073/pnas.222118199

Maccarrone, M., Bab, I., Biro, T., Cabral, G. A., Dey, S. K., Di Marzo, V., . . . Zimmer, A. (2015). Endocannabinoid signaling at the periphery: 50 years after THC. *Trends Pharmacol Sci, 36*(5), 277-296. doi:10.1016/j.tips.2015.02.008

Malamas, M. S., Farah, S. I., Lamani, M., Pelekoudas, D. N., Perry, N. T., Rajarshi, G., . . . Makriyannis, A. (2020). Design and synthesis of cyanamides as potent and selective N-acylethanolamine acid amidase inhibitors. *Bioorg Med Chem, 28*(1), 115195. doi:10.1016/j.bmc.2019.115195

Malumbres, M., & Barbacid, M. (2005). Mammalian cyclin-dependent kinases. *Trends Biochem Sci, 30*(11), 630-641. doi:10.1016/j.tibs.2005.09.005

Marino, P., Pepe, G., Basilicata, M. G., Vestuto, V., Marzocco, S., Autore, G., Procino, A., Gomez-Monterrey, I. M., Manfra, M., & Campiglia, P. (2023). Potential Role of Natural Antioxidant Products in Oncological Diseases. Antioxidants (Basel, Switzerland), 12(3), 704. https://doi.org/10.3390/antiox12030704

McDowell, C., Farooq, U., & Haseeb, M. (2024). Inflammatory Bowel Disease. In *StatPearls*. Treasure Island (FL) with ineligible companies. Disclosure: Umer Farooq declares no relevant financial relationships with ineligible companies. Disclosure: Muhammad Haseeb declares no relevant financial relationships with ineligible companies.

Medina Pabon, M. A., & Babiker, H. M. (2024). A Review of Hereditary Colorectal Cancers. In *StatPearls*. Treasure Island (FL) ineligible companies. Disclosure: Hani Babiker declares no relevant financial relationships with ineligible companies.

Mijan, M. A., & Lim, B. O. (2018). Diets, functional foods, and nutraceuticals as alternative therapies for inflammatory bowel disease: Present status and future trends. *World J Gastroenterol, 24*(25), 2673-2685. doi:10.3748/wjg.v24.i25.2673

Mock, E. D., Gagestein, B., & van der Stelt, M. (2023). Anandamide and other N-acylethanolamines: A class of signaling lipids with therapeutic opportunities. *Prog Lipid Res, 89*, 101194. doi:10.1016/j.plipres.2022.101194

Molodecky, N. A., Soon, I. S., Rabi, D. M., Ghali, W. A., Ferris, M., Chernoff, G., . . . Kaplan, G. G. (2012). Increasing incidence and prevalence of the inflammatory bowel diseases with time, based on systematic review. *Gastroenterology, 142*(1), 46-54 e42; quiz e30. doi:10.1053/j.gastro.2011.10.001

Morgan, E., Arnold, M., Gini, A., Lorenzoni, V., Cabasag, C. J., Laversanne, M., . . . Bray, F. (2023). Global burden of colorectal cancer in 2020 and 2040: incidence and mortality estimates from GLOBOCAN. *Gut, 72*(2), 338-344. doi:10.1136/gutjnl-2022-327736

Neufert, C., Becker, C., & Neurath, M. F. (2007). An inducible mouse model of colon carcinogenesis for the analysis of sporadic and inflammation-driven tumor progression. *Nat Protoc, 2*(8), 1998-2004. doi:10.1038/nprot.2007.279

Neufert, C., Heichler, C., Brabletz, T., Scheibe, K., Boonsanay, V., Greten, F. R., & Neurath, M. F. (2021). Inducible mouse models of colon cancer for the analysis of sporadic and inflammation-driven tumor progression and lymph node metastasis. *Nat Protoc, 16*(1), 61-85. doi:10.1038/s41596-020-00412-1

Neurath, M. F. (2019). Targeting immune cell circuits and trafficking in inflammatory bowel disease. *Nat Immunol, 20*(8), 970-979. doi:10.1038/s41590-019-0415-0

Ng, S. C., Shi, H. Y., Hamidi, N., Underwood, F. E., Tang, W., Benchimol, E. I., . . . Kaplan, G. G. (2017). Worldwide incidence and prevalence of inflammatory bowel disease in the 21st century: a systematic review of population-based studies. *Lancet, 390*(10114), 2769-2778. doi:10.1016/s0140-6736(17)32448-0

O'Sullivan, D. E., Sutherland, R. L., Town, S., Chow, K., Fan, J., Forbes, N., . . . Brenner, D. R. (2022). Risk Factors for Early-Onset Colorectal Cancer: A Systematic Review and Meta-analysis. *Clin Gastroenterol Hepatol, 20*(6), 1229-1240 e1225. doi:10.1016/j.cgh.2021.01.037

Ohara, M., Ohnishi, S., Hosono, H., Yamamoto, K., Fu, Q., Maehara, O., . . . Sakamoto, N. (2018). Palmitoylethanolamide Ameliorates Carbon Tetrachloride-Induced Liver Fibrosis in Rats. *Front Pharmacol, 9*, 709. doi:10.3389/fphar.2018.00709

Ojo, O. A., Adeyemo, T. R., Rotimi, D., Batiha, G. E., Mostafa-Hedeab, G., Iyobhebhe, M. E., Elebiyo, T. C., Atunwa, B., Ojo, A. B., Lima, C. M. G., & Conte-Junior, C. A. (2022). Anticancer Properties of Curcumin Against Colorectal Cancer: A Review. Frontiers in oncology, 12, 881641. https://doi.org/10.3389/fonc.2022.881641

Okamoto, Y., Morishita, J., Tsuboi, K., Tonai, T., & Ueda, N. (2004). Molecular characterization of a phospholipase D generating anandamide and its congeners. *J Biol Chem, 279*(7), 5298-5305. doi:10.1074/jbc.M306642200

Pacher, P., Batkai, S., & Kunos, G. (2006). The endocannabinoid system as an emerging target of pharmacotherapy. *Pharmacol Rev, 58*(3), 389-462. doi:10.1124/pr.58.3.2

Pagano, E., Borrelli, F., Orlando, P., Romano, B., Monti, M., Morbidelli, L., . . . Izzo, A. A. (2017). Pharmacological inhibition of MAGL attenuates experimental colon carcinogenesis. *Pharmacol Res, 119*, 227-236. doi:10.1016/j.phrs.2017.02.002

Park, S. J., Yoon, B. H., Kim, S. K., & Kim, S. Y. (2019). GENT2: an updated gene expression database for normal and tumor tissues. *BMC Med Genomics, 12*(Suppl 5), 101. doi:10.1186/s12920-019-0514-7

Patel, S. G., Karlitz, J. J., Yen, T., Lieu, C. H., & Boland, C. R. (2022). The rising tide of early-onset colorectal cancer: a comprehensive review of epidemiology, clinical features, biology, risk factors, prevention, and early detection. *Lancet Gastroenterol Hepatol, 7*(3), 262-274. doi:10.1016/S2468-1253(21)00426-X

Peng, K., Zhang, Y., Liu, D., & Chen, J. (2023). MMP2 is a immunotherapy related biomarker and correlated with cancer-associated fibroblasts infiltrate in melanoma. *Cancer Cell Int, 23*(1), 26. doi:10.1186/s12935-023-02862-5

Petrosino, S., & Di Marzo, V. (2017). The pharmacology of palmitoylethanolamide and first data on the therapeutic efficacy of some of its new formulations. *Br J Pharmacol, 174*(11), 1349-1365. doi:10.1111/bph.13580

Petrosino, S., Schiano Moriello, A., Verde, R., Allara, M., Imperatore, R., Ligresti, A., . . . Di Marzo, V. (2019). Palmitoylethanolamide counteracts substance P-induced mast cell activation in vitro by stimulating diacylglycerol lipase activity. *J Neuroinflammation, 16*(1), 274. doi:10.1186/s12974-019-1671-5

Piomelli, D., Scalvini, L., Fotio, Y., Lodola, A., Spadoni, G., Tarzia, G., & Mor, M. (2020). N-Acylethanolamine Acid Amidase (NAAA): Structure, Function, and Inhibition. *J Med Chem, 63*(14), 7475-7490. doi:10.1021/acs.jmedchem.0c00191

Pontis, S., Ribeiro, A., Sasso, O., & Piomelli, D. (2016). Macrophage-derived lipid agonists of PPAR-alpha as intrinsic controllers of inflammation. *Crit Rev Biochem Mol Biol, 51*(1), 7-14. doi:10.3109/10409238.2015.1092944

Rankin, L., & Fowler, C. J. (2020). The Basal Pharmacology of Palmitoylethanolamide. *Int J Mol Sci, 21*(21). doi:10.3390/ijms21217942

Raucci, F., Saviano, A., Casillo, G. M., Guerra-Rodriguez, M., Mansour, A. A., Piccolo, M., . . . Maione, F. (2022). IL-17-induced inflammation modulates the mPGES-1/PPAR-gamma pathway in monocytes/macrophages. *Br J Pharmacol, 179*(9), 1857-1873. doi:10.1111/bph.15413

Ribeiro, A., Pontis, S., Mengatto, L., Armirotti, A., Chiurchiu, V., Capurro, V., . . . Piomelli, D. (2015). A Potent Systemically Active N-Acylethanolamine Acid Amidase Inhibitor that Suppresses Inflammation and Human Macrophage Activation. *ACS Chem Biol, 10*(8), 1838-1846. doi:10.1021/acschembio.5b00114

Rieder, F., Kessler, S. P., West, G. A., Bhilocha, S., de la Motte, C., Sadler, T. M., . . . Fiocchi, C. (2011). Inflammation-induced endothelial-to-mesenchymal transition: a novel mechanism of intestinal fibrosis. *Am J Pathol, 179*(5), 2660-2673. doi:10.1016/j.ajpath.2011.07.042

Romano, B., Borrelli, F., Pagano, E., Cascio, M. G., Pertwee, R. G., & Izzo, A. A. (2014). Inhibition of colon carcinogenesis by a standardized Cannabis sativa extract with high content of cannabidiol. *Phytomedicine, 21*(5), 631-639. doi:10.1016/j.phymed.2013.11.006

Rossi, M., Mirbagheri, S., Keshavarzian, A., & Bishehsari, F. (2018). Nutraceuticals in colorectal cancer: A mechanistic approach. *Eur J Pharmacol, 833*, 396-402. doi:10.1016/j.ejphar.2018.06.027

Roviezzo, F., Rossi, A., Caiazzo, E., Orlando, P., Riemma, M. A., Iacono, V. M., . . . Izzo, A. A. (2017). Palmitoylethanolamide Supplementation during Sensitization Prevents Airway Allergic Symptoms in the Mouse. *Front Pharmacol, 8*, 857. doi:10.3389/fphar.2017.00857

Sakura, Y., Tsuboi, K., Uyama, T., Zhang, X., Taoka, R., Sugimoto, M., . . . Ueda, N. (2016). A quantitative study on splice variants of N-acylethanolamine acid amidase in human prostate cancer cells and other cells. *Biochim Biophys Acta, 1861*(12 Pt A), 1951-1958. doi:10.1016/j.bbalip.2016.09.018

Santacroce, G., Lenti, M. V., & Di Sabatino, A. (2022). Therapeutic Targeting of Intestinal Fibrosis in Crohn's Disease. *Cells, 11*(3). doi:10.3390/cells11030429

Santini, A., Tenore, G. C., & Novellino, E. (2017). Nutraceuticals: A paradigm of proactive medicine. *Eur J Pharm Sci, 96*, 53-61. doi:10.1016/j.ejps.2016.09.003

Sarnelli, G., Gigli, S., Capoccia, E., Iuvone, T., Cirillo, C., Seguella, L., . . . Esposito, G. (2016). Palmitoylethanolamide Exerts Antiproliferative Effect and Downregulates VEGF Signaling in Caco-2 Human Colon Carcinoma Cell Line Through a Selective PPAR-alpha-Dependent Inhibition of Akt/mTOR Pathway. *Phytother Res, 30*(6), 963-970. doi:10.1002/ptr.5601

Sgroi, S., Romeo, E., Fruscia, P. D., Porceddu, P. F., Russo, D., Realini, N., . . . Reggiani, A. (2021). Inhibition of N-acylethanolamine-hydrolyzing acid amidase reduces T cell infiltration in a mouse model of multiple sclerosis. *Pharmacol Res, 172*, 105816. doi:10.1016/j.phrs.2021.105816

Shehzad, A., Lee, J., & Lee, Y. S. (2013). Curcumin in various cancers. *Biofactors, 39*(1), 56-68. doi:10.1002/biof.1068

Siegel, R. L., Miller, K. D., Fuchs, H. E., & Jemal, A. (2022). Cancer statistics, 2022. *CA Cancer J Clin, 72*(1), 7-33. doi:10.3322/caac.21708

Simon, K. (2016). Colorectal cancer development and advances in screening. *Clin Interv Aging, 11*, 967-976. doi:10.2147/CIA.S109285

Stock, K., Kumar, J., Synowitz, M., Petrosino, S., Imperatore, R., Smith, E. S., . . . Glass, R. (2012). Neural precursor cells induce cell death of high-grade astrocytomas through stimulation of TRPV1. *Nat Med, 18*(8), 1232-1238. doi:10.1038/nm.2827

Su, A. I., Wiltshire, T., Batalov, S., Lapp, H., Ching, K. A., Block, D., . . . Hogenesch, J. B. (2004). A gene atlas of the mouse and human protein-encoding transcriptomes. *Proc Natl Acad Sci U S A, 101*(16), 6062-6067. doi:10.1073/pnas.0400782101

Su, L. J., Zhang, J. H., Gomez, H., Murugan, R., Hong, X., Xu, D., . . . Peng, Z. Y. (2019). Reactive Oxygen Species-Induced Lipid Peroxidation in Apoptosis, Autophagy, and Ferroptosis. *Oxid Med Cell Longev, 2019*, 5080843. doi:10.1155/2019/5080843

Sun, K. H., Chang, Y., Reed, N. I., & Sheppard, D. (2016). alpha-Smooth muscle actin is an inconsistent marker of fibroblasts responsible for force-dependent TGFbeta activation or collagen production across multiple models of organ fibrosis. *Am J Physiol Lung Cell Mol Physiol, 310*(9), L824-836. doi:10.1152/ajplung.00350.2015

Talbott, H. E., Mascharak, S., Griffin, M., Wan, D. C., & Longaker, M. T. (2022). Wound healing, fibroblast heterogeneity, and fibrosis. *Cell Stem Cell, 29*(8), 1161-1180. doi:10.1016/j.stem.2022.07.006

Terzic, J., Grivennikov, S., Karin, E., & Karin, M. (2010). Inflammation and colon cancer. *Gastroenterology, 138*(6), 2101-2114 e2105. doi:10.1053/j.gastro.2010.01.058

Testa, U., Pelosi, E., & Castelli, G. (2018). Colorectal cancer: genetic abnormalities, tumor progression, tumor heterogeneity, clonal evolution and tumor-initiating cells. *Med Sci (Basel), 6*(2). doi:10.3390/medsci6020031

Tsuboi, K., Sun, Y. X., Okamoto, Y., Araki, N., Tonai, T., & Ueda, N. (2005). Molecular characterization of N-acylethanolamine-hydrolyzing acid amidase, a novel member of the choloylglycine hydrolase family with structural and functional similarity to acid ceramidase. *J Biol Chem, 280*(12), 11082-11092. doi:10.1074/jbc.M413473200

Tsuboi, K., Uyama, T., Okamoto, Y., & Ueda, N. (2018). Endocannabinoids and related N-acylethanolamines: biological activities and metabolism. *Inflamm Regen, 38*, 28. doi:10.1186/s41232-018-0086-5

Uehara, H., Nakagawa, T., Katsuno, T., Sato, T., Isono, A., Noguchi, Y., & Saito, Y. (2010). Emergence of fibrocytes showing morphological changes in the inflamed colonic mucosa. *Dig Dis Sci, 55*(2), 253-260. doi:10.1007/s10620-009-0730-7

Vago, R., Bettiga, A., Salonia, A., Ciuffreda, P., & Ottria, R. (2017). Development of new inhibitors for N-acylethanolamine-hydrolyzing acid amidase as promising tool against bladder cancer. *Bioorg Med Chem, 25*(3), 1242-1249. doi:10.1016/j.bmc.2016.12.042

Valdoz, J. C., Franks, N. A., Cribbs, C. G., Jacobs, D. J., Dodson, E. L., Knight, C. J., . . . Van Ry, P. M. (2022). Soluble ECM promotes organotypic formation in lung alveolar model. *Biomaterials, 283*, 121464. doi:10.1016/j.biomaterials.2022.121464

Vellecco, V., Saviano, A., Raucci, F., Casillo, G. M., Mansour, A. A., Panza, E., . . . Maione, F. (2023). Interleukin-17 (IL-17) triggers systemic inflammation, peripheral vascular dysfunction, and related prothrombotic state in a mouse model of Alzheimer's disease. *Pharmacol Res, 187*, 106595. doi:10.1016/j.phrs.2022.106595

Venables, B. J., Waggoner, C. A., & Chapman, K. D. (2005). N-acylethanolamines in seeds of selected legumes. *Phytochemistry, 66*(16), 1913-1918. doi:10.1016/j.phytochem.2005.06.014

Vipperla, K., & O'Keefe, S. J. (2016). Diet, microbiota, and dysbiosis: a 'recipe' for colorectal cancer. *Food Funct, 7*(4), 1731-1740. doi:10.1039/c5fo01276g

Wagner, S., Beger, N. T., Matschos, S., Szymanski, A., Przybylla, R., Burtin, F., . . . Mullins, C. S. (2021). Tumor-Derived Cell Lines and Their Potential for Therapy Prediction in Patients with Metastatic Colorectal Cancer. *Cancers (Basel), 13*(18). doi:10.3390/cancers13184717

Wang, J., Zhao, L. Y., Uyama, T., Tsuboi, K., Wu, X. X., Kakehi, Y., & Ueda, N. (2008). Expression and secretion of N-acylethanolamine-hydrolysing acid amidase in human prostate cancer cells. *J Biochem, 144*(5), 685-690. doi:10.1093/jb/mvn122

Wang, Y., Huang, B., Jin, T., Ocansey, D. K. W., Jiang, J., & Mao, F. (2022). Intestinal Fibrosis in Inflammatory Bowel Disease and the Prospects of Mesenchymal Stem Cell Therapy. *Front Immunol, 13*, 835005. doi:10.3389/fimmu.2022.835005

Wark, G., Samocha-Bonet, D., Ghaly, S., & Danta, M. (2020). The Role of Diet in the Pathogenesis and Management of Inflammatory Bowel Disease: A Review. Nutrients, 13(1), 135. https://doi.org/10.3390/nu13010135

Wiese, W., Barczuk, J., Racinska, O., Siwecka, N., Rozpedek-Kaminska, W., Slupianek, A., . . . Majsterek, I. (2023). PI3K/Akt/mTOR Signaling Pathway in Blood Malignancies-New Therapeutic Possibilities. *Cancers (Basel), 15*(21). doi:10.3390/cancers15215297

Wijmenga, C. (2005). Expressing the differences between Crohn disease and ulcerative colitis. *PLoS Med, 2*(8), e230; quiz e304. doi:10.1371/journal.pmed.0020230

Williams, C. M., & Kirkham, T. C. (1999). Anandamide induces overeating: mediation by central cannabinoid (CB1) receptors. *Psychopharmacology (Berl), 143*(3), 315-317. doi:10.1007/s002130050953

Wirtz, S., Popp, V., Kindermann, M., Gerlach, K., Weigmann, B., Fichtner-Feigl, S., & Neurath, M. F. (2017). Chemically induced mouse models of acute and chronic intestinal inflammation. *Nat Protoc, 12*(7), 1295-1309. doi:10.1038/nprot.2017.044

Wu, F., Fan, J., He, Y., Xiong, A., Yu, J., Li, Y., . . . Zhou, C. (2021). Single-cell profiling of tumor heterogeneity and the microenvironment in advanced non-small cell lung cancer. *Nat Commun, 12*(1), 2540. doi:10.1038/s41467-021-22801-0

Wu, X., Lin, X., Tan, J., Liu, Z., He, J., Hu, F., . . . Mao, R. (2023). Cellular and Molecular Mechanisms of Intestinal Fibrosis. *Gut Liver, 17*(3), 360-374. doi:10.5009/gnl220045

Xi, Y., & Xu, P. (2021). Global colorectal cancer burden in 2020 and projections to 2040. *Transl Oncol, 14*(10), 101174. doi:10.1016/j.tranon.2021.101174

Xie, Y. H., Chen, Y. X., & Fang, J. Y. (2020). Comprehensive review of targeted therapy for colorectal cancer. *Signal Transduct Target Ther, 5*(1), 22. doi:10.1038/s41392-020-0116-z

Xue, H., Lu, B., & Lai, M. (2008). The cancer secretome: a reservoir of biomarkers. *J Transl Med, 6*, 52. doi:10.1186/1479-5876-6-52

Yam, C. Q. X., Lim, H. H., & Surana, U. (2022). DNA damage checkpoint execution and the rules of its disengagement. *Front Cell Dev Biol, 10*, 1020643. doi:10.3389/fcell.2022.1020643

Yang, J., Lim, S. Y., Ko, Y. S., Lee, H. Y., Oh, S. W., Kim, M. G., . . . Jo, S. K. (2019). Intestinal barrier disruption and dysregulated mucosal immunity contribute to kidney fibrosis in chronic kidney disease. *Nephrol Dial Transplant, 34*(3), 419-428. doi:10.1093/ndt/gfy172

Yang, L., Ji, C., Li, Y., Hu, F., Zhang, F., Zhang, H., Li, L., Ren, J., Wang, Z., & Qiu, Y. (2020). Natural Potent NAAA Inhibitor Atractylodin Counteracts LPS-Induced Microglial Activation. Frontiers in pharmacology, 11, 577319. https://doi.org/10.3389/fphar.2020.577319

Yarden, Y., & Sliwkowski, M. X. (2001). Untangling the ErbB signalling network. *Nat Rev Mol Cell Biol, 2*(2), 127-137. doi:10.1038/35052073

Zhao, L. Y., Tsuboi, K., Okamoto, Y., Nagahata, S., & Ueda, N. (2007). Proteolytic activation and glycosylation of N-acylethanolamine-hydrolyzing acid amidase, a lysosomal

enzyme involved in the endocannabinoid metabolism. *Biochim Biophys Acta, 1771*(11), 1397-1405. doi:10.1016/j.bbalip.2007.10.002